HYDROCARBON CHARACTERIZATION AND PROSPECT IDENTIFICATION OF YZ FIELD, NIGER DELTA

By

OPAWANDE, AYOMIDE ABIDEMI

18010401005

A PROJECT SUBMITTED TO THE DEPARTMENT OF GEOSCIENCES, COLLEGE OF BASIC AND APPLIED SCIENCES, IN PARTIAL FULFILMENT OF THE REQUIREMENTS FOR THE AWARD OF BACHELOR OF SCIENCE (B. Sc.) DEGREE IN GEOPHYSICS.

AUGUST, 2022

DECLARATION

I hereby declare that this project has been written by me and is a record of my own research work. It has not been presented in any previous application for a higher degree of this or any other University. All citations and sources of information are clearly acknowledged by means of reference.

……..

OPAWANDE, AYOMIDE ABIDEMI

……

Date

CERTIFICATION

I hereby certify that this research titled **HYDROCARBON CHARACTERIZATION AND PROSPECT IDENTIFICATION OF YZ FIELD, NIGER DELTA,** was prepared and submitted by OPAWANDE AYOMIDE. A with the matriculation number 18010401005 in partial fulfillment of the requirements of the Bachelor of Science in Applied Geophysics, is hereby accepted.

Mr. R.P AKINWALE _____

Project Supervisor *(Signature and date)*

DR. O.B BALOGUN _____

Head of Department *(Signature and date)*

DEDICATION

This project is dedicated to Almighty God for helping me attain a successful milestone in my life and also to my parents and siblings for their unending love and support, prayers and care towards me and the successful completion of this work.

ACKNOWLEDGEMENT

My profound gratitude goes to my wonderful and most loving parents, Mr. and Mrs. Opawande for their endless moral and financial supports.

I would like to express my sincere gratitude to my supervisor Mr. R. P. Akinwale whose constructive criticism, encouragement, mentorship and guidance have helped in keeping me on the right track during the research work, without which this research work would not have been completed. Also, to other lecturers in the Department of Geosciences Prof. E. A. Ayolabi, Prof. A. I. Olayinka, Dr. M.O Okunubi and Dr. A. Jonathan for their constant and individual support throughout my project.

I also appreciate the Head of Department, Geosciences, Dr. O.B Balogun.

I am also grateful to Mr. D. E. Ebun for the constant help and sacrifices during this research work.

Finally, to my course mates and friends who have made this journey memorable and worthwhile. God bless you all.

Table of Contents

List of Tables

List of Figures

Abbreviations

3D……Three-Dimensional

API……...American Petroleum Institute

AVO…….Amplitude Versus Offset

BW……...Bulk Water

CSEM……...Controlled Source Electro-Magnetics

DHI……...Direct Hydrocarbon Indicators

GIIP…….Gas Initially In Place

GR…….Gamma Ray

GRV……...Gross Rock Volume

ILD…….Deep Resistivity log

LWD……Logging While Drilling

MMD……..Measurements While Drilling

MT……Magneto-Tellurics

NPHI……Neutron log

NTG…….Net To Gross

RHOB……..Density log

SCF……..Standard Cubic Foot

SP…….Self Potential

STB……..Stock Tank Barrel

STOOIP…….....Stock Tank Original Oil In Place

ABSTRACT

3D seismic data interpretation and well log analysis have been carried out for hydrocarbon characterization and additional prospect identification in YZ field, in the Northern Ughelli Depobelt of Niger Delta. Recently, major focus within the Niger Delta has been tending towards the regeneration of older fields and the identification of new prospects from these old fields. To this end, indigenous companies have been involved in developing marginal fields and the search for additional prospects is pertinent in developing and expanding the profitability of these fields. The data utilized for the analysis of YZ field were 3D migrated seismic data, 6 composite well logs and check shot. The well logs were correlated in the North to South direction.

Synthetic seismogram was generated to aid mapping of the reservoir tops across the 3D seismic data coverage. Faults were delineated and mapped on the 3D seismic data by identifying abrupt terminations of seismic reflections. Seismic attributes analysis including RMS, maximum amplitude, sum of energy, sum of amplitude were extracted from the time map to enhance interpretation. From the well log correlation, five reservoirs namely Sand 1, Sand 2, Sand 3, Sand 4 and Sand 5 were identified. The pay thickness ranges from 3 to 39m across the reservoirs. The net to gross of the reservoirs ranges from 76 to 97% and effective porosity ranges from 18 to 22.2%. Petrophysical analysis have shown that the hydrocarbon type in Sand 2 is predominantly gas, Sand 4 is partly oil and gas and Sand 5 is predominantly oil. The hydrocarbon saturation ranges from 58 to 76 %. On the other hand, Sand 1 and Sand 3 has indicated no accumulation of hydrocarbon within the tested trap. It was also observed that four major growth faults are present in YZ field while other faults are either synthetic or antithetic to the major faults. Four horizons corresponding to the top of Sand 1 to 4 in the well log analysis were mapped across the 3D migrated seismic data. The structural maps from the mapped horizons, reveals structural highs and closures that are observed as fault assisted and dependent traps. Four to five additional prospects were observed across the mapped Sand reservoirs.

The attribute analysis has shown high anomalies on some of the prospects which is supportive of possible accumulation of hydrocarbon. The identified prospects were ranked partly based on type of closure (fault assisted versus fault dependent), attribute support and volume estimates. In conclusion the additional STOIIP for YZ field is 194,025,188stb and GIIP is 193,804,479scf. Therefore, YZ field can be considered viable and encouraging for further development.

Keywords: 3D seismic, Well logs, Prospect, hydrocarbon.

CHAPTER ONE

1.1 Introduction

The YZ field is located within the Niger Delta Basin, onshore Niger Delta Nigeria (Figure 1.1). Major focus in recent time, in hydrocarbon exploration has been moved towards the renewal of older fields and the identification of new prospects from these old fields (Emina et al, 2016). Recent studies in the Niger Delta, has shown that reservoirs in this basin contain a number of undiscovered hydrocarbons in the Tertiary Niger Delta (Akata-Agbada) Petroleum System is about 40.5 billion barrels of oil and 133 trillion cubic feet of gas (Michele et al, 1999). This means a large amount of hydrocarbon reserves is yet to be explored which gives room to explore for hydrocarbon perspectivity. Considering the never-ending global demand for energy, the high cost of production and the interconnected risks, identification of new prospect/renewal of older fields is much cheaper and less risky than exploring in frontier/unknown basins (Emina et al, 2016).

The major goal of hydrocarbon exploration is to establish suitable reservoir formations with commercial accumulation and therefore characterize and evaluate the reservoir very accurately in order to determine most effective way of recovering as much of the resource as possible.

Reservoir characterization is a method that involves quantitative evaluation of reservoir characteristics like facies distribution, porosity, permeability, and fluid saturations (Journel, 1995). This information is crucial for quantifying the amount of producible hydrocarbon that can be extracted from the reservoir (Schlumberger, 1989). For assessing the hydrocarbon potential of rock formations, well log data offer trustworthy downhole geological information (Asquith and Gibson, 1982). The generated information has been proven to reduce risk associated with hydrocarbon exploration (Schlumberger, 1989). Reservoir characterization technology involves the integration of all accessible subsurface data such as core data, check shot, well logs and seismic data. These data sets are a product of measurements carried out by enhanced instrumentations processed and interpreted using advanced software.

In this study, 3D migrated seismic and well logs was used to evaluate relevant reservoir petrophysical properties to characterize YZ field located onshore Niger Delta, Southern Nigeria

to prospect for further hydrocarbon accumulations within the field. The analysis determined the lithologic distribution across the field's available wells, both vertically and laterally. To identify potential fluid bearing formations, discriminate formation fluids, determine the degree of saturation of the different fluids in the reservoirs and also to delineate other prospects yet explored in this field.

1.2 Statement of Problem

Several oil companies and investors have recently began shifting focus to the rejuvenation of older field and the discerning of new prospects from these fields in order to avoid spending unnecessarily on green or frontier basins due to insufficient geological information (Emina et al, 2016).

Likewise, indigenous companies have been involved in developing marginal fields and the search for additional prospects is pertinent in developing and expanding their profitability of the fields. Detailed analysis of the field by integrating available 3D seismic and well logs will help in appraising the tested prospect and identify new prospect for field development. This will avoid the drilling of dry hydrocarbon wells due to false prospecting or just mere guess work and losing millions of dollars due to the expenses involved in drilling of hydrocarbon wells. Therefore, this thesis is aimed at carrying out adequate integration of 3D seismic and well log analysis in identifying possible hydrocarbon prospects in YZ field and appraise its viability for further development.

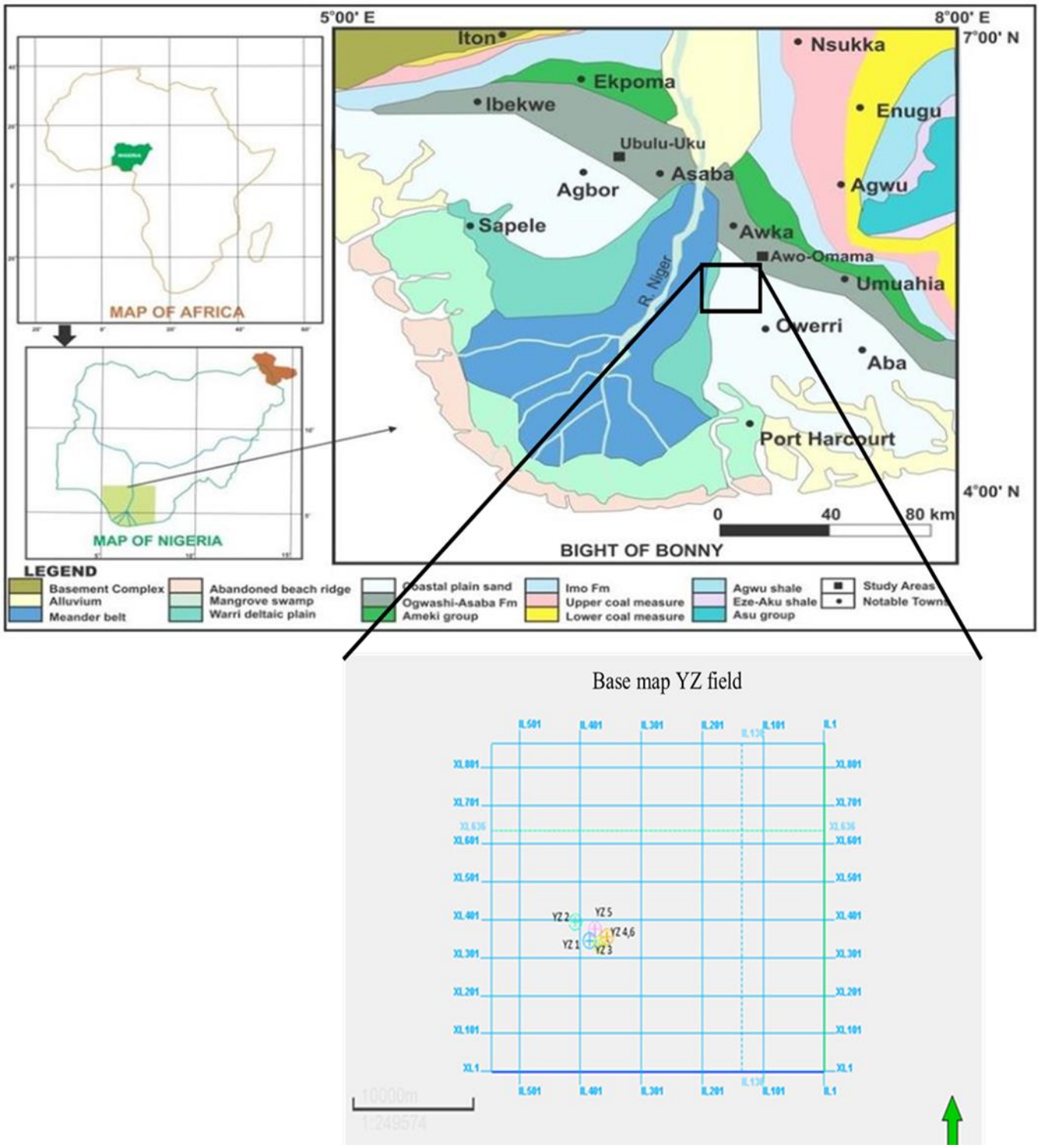

Figure 1.1: Map of Niger Delta showing the location of the study area (YZ field) modified after Nwajide, 2013.

1.3 Aim and Objectives

1.3.1 Aim

The aim of this project is to identify additional hydrocarbon prospects in YZ field by interpreting 3D migrated seismic data and well log in order to delineate additional traps for field development.

1.3.2 Objectives

The following are the objectives of this project work

i. Data loading and Quality checking
ii. Identification and correlation of reservoirs in the well logs
iii. Petrophysical analysis of reservoirs to understand the reservoir quality and hydrocarbon potential
iv. Generation of synthetic seismogram to aid seismic interpretation of identified reservoirs
v. Fault and horizon mapping to delineate reservoir geometry, identify hydrocarbon traps and additional prospects in YZ field.
vi. Volumetric estimations of hydrocarbon in place for the tested trap and additional prospects

1.4 Description of Study Area

The YZ field is located in the Northern onshore block of Niger Delta and has total area coverage of about $589.5\ km^2$. It is situated in southern Nigeria, north of the city of Port Harcourt (Figure 1.1). At the southernmost tip of the vast intracontinental Benue Trough, in southern Nigeria, on the inland edge of the Gulf of Guinea, is the Tertiary Niger Delta Basin. It is located between longitude 5 ° E and latitude 4 ° N and 7 ° N. (Figure 1.1). The Gulf of Guinea in the south, the Calabar Flank in the East, the Benin Flank in the West, the Anambra Basin and the Afikpo Syncline in the North, and older (Cretaceous) tectonic components are the boundaries of the basin (Avbovbo 1978; Ejedawe et al, 1984; Tuttle et al, 1999).

1.5 Scope of Work

This project work entails well log correlation and 3D post-stack migrated seismic data interpretation as restricted by the available data sets. The processes and results involved in the

integration of 3D seismic data with well log data to identify additional prospects in YZ field Niger Delta were carried out.

1.6 Contribution to Knowledge

Additional prospects were identified in YZ field by integrating 3D seismic with well logs. The seismic attribute analysis has shown bright amplitude anomalies on some of the prospects which is indicative of presence of hydrocarbon.

CHAPTER TWO

2.1 REVIEW OF PREVIOUS WORKS

A number of authors have worked on related research such as identifying additional prospect and hydrocarbon potential analysis of several fields in the Niger Delta Basin (Obiekezie *et al*., 2015, Asubiojo, 2016, Emina *et al*., 2016 and Olawale *et al*., 2021).

Obiekezie *et al.* (2015) evaluated the 3D structural analysis of subsurface structures and hydrocarbon trapping potential of Otu Field, Niger Delta using 3D seismic and well logs. Hydrocarbons and lithologies were initially identified with the help of deep resistivity, gamma ray, neutron and density logs. The depth and spatial distribution of lithologies were correlated across the wells in the study area. Network of faults were delineated allowing identification of growth faults which are listric in character. Three horizons, were identified and mapped to produce the structure maps. The structural maps of the tops of the reservoirs showed that the hydrocarbon structures are fault assisted anticlinal structures and they correspond to the crest of the rollover anticlines on the seismic sections. The RMS amplitude attribute extracted on the surfaces revealed bright spots on the region of the anticlinal structures which indicates that the field has economic explorable hydrocarbons accumulations

Asubiojo *et al.* (2016), examined the petrophysical properties of reservoirs with the objective of identifying the depositional environment and predicts the quality of the reservoir system at Kwe Field, Coastal Swamp Depobelt, East Niger Delta Basin. A composite log set that included the gamma ray, resistivity, density, and neutron logs from five (5) wells along with photographic data from one (1) reservoir well was used to evaluate the reservoir sand bodies. Three reservoir sands were discovered in the field by the study based on their petrophysical characteristics and architectural design. The porosity of the reservoir ranges from 26 to 27.5%, Net to Gross range of 61.4 to 70.4%, Permeability range of 91.4 to 203.99md and hydrocarbon saturation range of 70.4 to 75.03% and therefore reveals that the field contains fine-grained sand filled with hydrocarbon.

Finding marine shales (or mudstones) with these sandstones can result in the development of permeability baffles that will allow vertical flow and separate the reservoirs. As a result, these

reservoirs may accommodate various flow units. Reservoir sands are interpreted as embedded in an estuarine shoreface system using wireline log and core data, demonstrating that the Kwe area is within the marginal marine giant depositional environment.

Emina *et al.* (2016) evaluated the Olive field in the Greater Ughelli Depobelt of the Niger Delta with the aim of identifying new prospects within the field. The data used include; 3D seismic cube, four composite well logs and check shot. 3D seismic, well log and structural interpretation were carried out to calculate the hydrocarbon potentials of reservoirs. In order to identify reservoirs, determine petrophysical parameters, and find hydrocarbons, well data were employed. After the well to seismic tie, the four horizons corresponding to the chosen well tops were plotted on the 3D seismic data. From the mapped horizons, structural maps of time and depth were created.

Time and depth structural maps were established from mapped horizons. Four Hydrocarbon reservoirs range in depth from 6743 ft - 9045 ft, with shale volume (V_{sh}) ranging from 15.32% - 29.06% in volume. Total porosity ranges from 24.63% - 34.01%, while effective porosity ranges from 17.26% - 31.71%, indicating reservoirs exhibit good porosities. The Net to Gross Thickness of reservoirs ranges from 0.720 - 0.980 while the hydrocarbon saturation ranges from 70.93% - 78.86% of the gas in the given reservoirs.

Seismic interpretation shows that the field is very faulted with faults making room for hydrocarbon retention and accumulation. Four of the trapped structures have been targeted and exploited by four wells drilled at the field. Seismic amplitude attribute maps drawn from the tops of the reservoirs mapped show that the reservoirs are characterized by very high amplitudes (bright spots) in areas enclosed by the structural traps. This led to the identification of four (4) prospects within the Olive field.

Olawale *et al.* (2021), calculated the petrophysical parameters of the clastic reservoirs estimated at the AK site using well-log analyzes. This field is located along the onshore eastern coast of the Niger-Delta. Well-log analytics were used to calculate the hydrocarbon prospect of the site. The data were qualitatively and quantitatively analyzed; lithologic mapping facilitated the identification of sand layers, while fluid identification and discrimination highlighted the hydrocarbon saturated reservoir layers. To measure and describe the reservoir units, several derived characteristics including porosity, permeability, water saturation, hydrocarbon saturation,

Net to Gross (NTG), and Bulk Water (BW) were used. Four (4) sand reservoir layers, with thickness ranging from 18.3 - 106.7 m were identified from four exploration wells as hydrocarbon bearing. Reservoirs exhibited medium to high release rate (0.27 - 0.38), low to average permeability (61.6 - 685.5 mD) and significant to high hydrocarbon saturation (0.42 - 0.97).

2.2 GEOLOGIC REVIEW OF THE NIGER DELTA BASIN

Among the major hydrocarbon provinces in the world, the Niger Delta Basin is the most productive deltaic hydrocarbon province in Nigeria and the West African continental margin (Aizebeokhai et al., 2011). The Agbada Formation's sandstones and unconsolidated sands are primarily used to produce oil and gas in the Niger Delta (Tuttle et al., 1999).

The Akata, Agbada, and Benin Formations make up all of the Delta's geological structure (Figure 2.3).

Benin Formation

The Niger Delta Complex's upper alluvial coastal plain deposit is known as the Benin Formation. It spreads from the western Niger Delta across the entire region and southward past the present coastline.The Benin Formation, formed primarily of non-marine sandstone and produced in a continental fluviatile environment, is made up of coarse-grained sandstones, lignite streaks, and wood pieces with only slight intercalation of shales. Aged between the Miocene and more recent, the Benin Formation has a varied thickness that surpasses 1,820 m. (Doust and Omatsola, 1990).

In the subsurface, the age ranges from Miocene to Recent, with the subsurface in the north being of Oligocene age and getting younger as you move south There hasn't been much hydrocarbon accumulation connected to this formation (Short and Stauble, 1967).

Agbada Formation

The primary petroleum-bearing unit is the Agbada Formation, which lies beneath the Benin Formation.It was formed in paralic coastal habitats that ranged from brackish to marine fluviatile. Shale and sandstone beds were equally distributed throughout the lower Agbada Formation, but the higher part is primarily composed of sand with only a few interbeds of small shale. The predominant rock types are alternating sandstone, silt, and shale. The sandstones are unevenly sorted, slightly consolidated, rounded to sub-rounded, and the majority are unconsolidated.

Lower in the formation, the sandstones grade into shale. Eocene in the north and Pliocene in the south are the ages of the Agbada Formation. The principal hydrocarbon reservoirs for the Niger Delta oil fields are known to be the sandy portions of the formation, while the shales act as seals to keep the produced oil and gas inside the reservoir structures.

At the basin's center, the formation's thickness reaches a maximum of roughly 4500 ma.

The sandstones grade into shale in the lower part of the formation. Agbada Formation ranges in age from Eocene in the north to Pliocene in the south. The sandy parts of the formation are known to constitute the main hydrocarbon reservoirs of the delta oil fields and the shales serve as seals to constrain the generated oil and gas within the reservoir structures. The thickness of the formation reaches a maximum of about 4500 ma at the center of the basin (Short and Stauble, 1967).

Akata Formation

The lowermost unit of the Niger Delta Complex, the Akata Formation, is marine in origin and is made up primarily of thick shale sequences (possible source rock), turbidite sand (possible deep-water reservoirs), and trace amounts of clay and silt. Shale makes up the majority of it, with small amounts of sandstone and siltstone interspersed. In the middle of the delta, the structure is thought to be up to 7,000 meters thick (Doust and Omatsola, 1990). The entire delta is supported by the formation, which is normally under pressure. Both onshore in the northeast, where they are known as the Imo Shale, and offshore along the continental slope, the Akata Formation outcrops in diaper-like formations. The Akata Formation dates from the Eocene to the Recent (Short and Stauble, 1967). The Agbada sequences cover the shale of the Akata Formation, which was deposited in deep water during lowstands.

The Agbada Formation in the delta's center region is consistent with a shallow-ramp concept, with the majority of its system tracts being highstand (hydrocarbon-bearing sandstone) and transgressive (sealing shale). The Agbada Formation's faulting created structural and stratigraphic traps that served as channels for petroleum migration and collected hydrocarbons. Shale in the transgressive system tract helped to improve clay spreading in fault zones and served as a great seal above the sand. The Niger Delta Province as a whole is based on the Akata Formation. It includes stratigraphic traps associated with turbidites, rotational fault blocks inside the lower portions of the continental shelf, and growth-fault structures related to sandstone units

that contain hydrocarbons. In the deep-water region of the Niger Delta, turbidites contain channel and ponded sandstone as well as deep-water clastic fans.

Source rock

The main source rock for petroleum is found in the delta's upper Akata Formation, which is a shale facies that resembles the ocean. Additional hydrocarbon may also be produced by the lowermost Agbada formation's interbedded marine shales. Beginning in the Eocene, hydrocarbon formation in the Niger Delta region has continued to this day.

As younger deposits reached the oil window, the generation of petroleum migrated from north to south. The Agbada Formation has certain interims with high enough organic carbon levels to qualify as acceptable source rocks (Ekweozor and Okoye, 1980). However, the source-rock intervals are immature in some areas of the delta and seldom reach 10 thicknesses sufficient to establish a world-class oil province (Stacher, 1995). There are significant amounts of Akata shale located beneath the Agbada formation (Figure 2.2).

Authors (Frost, 1997; Haack et al, 2000) have proposed that beneath the east of the present Niger Delta lays oil-bearing Cretaceous rocks but no data exists on its source rock potential due to its great depth. Along the Nigerian coastline and offshore rocks and marine kerogen was reported present by Haack and others (2000). These inferences are based on oil seeps from Nigerian tar sands within the Dahomey Embayment, source-rock outcrops along the eastern margin of the delta, and geochemical data from wells. These source rocks could be contributors to hydrocarbon accumulations in the deep-water areas of the Niger Delta.

The oil window competes in the upper Akata Formation and the lower Agbada Formation in the northwest of the Niger Delta. The oil window is stratigraphically lower to the southeast, down as much as 4,000 feet from the upper Akata lower Agbada layers (Evamy *et al*, 1978). The Niger Delta's current oil-generation window is roughly 240 °F (115 °C) isotherm.

Reservoirs

Sandstone and unconsolidated sand, which are mostly found in the Agbada Formation, are used to extract hydrocarbon from the Agbada Reservoirs (Figure 2.3). Aged from the Eocene to the Pliocene, the discovered reservoir rocks are frequently layered and range in thickness from less than 15 m to more than 45 m. (Evamy *et al.*, 1978). Larger reservoirs are probably combined masses of stacked channels, according to, (Doust and Omatsola, 1990; Kulke, 1995) identified the most significant reservoir types as point bars of distributary channels and coastal barrier bars occasionally cut by sand-filled channels.

According to Edwards and Santogrossi (1990), the main Niger Delta reservoirs are Miocene sandstones with up to 40% porosity, 2 darcies permeability, and a thickness of 100 m. Growth faults exert great control over the variation in reservoir thickness; in the down-thrown block, the sandstone thickens up against the fault (Weber and Daukoru, 1975). Porosity declines as depth increases (Kulke, 1995).

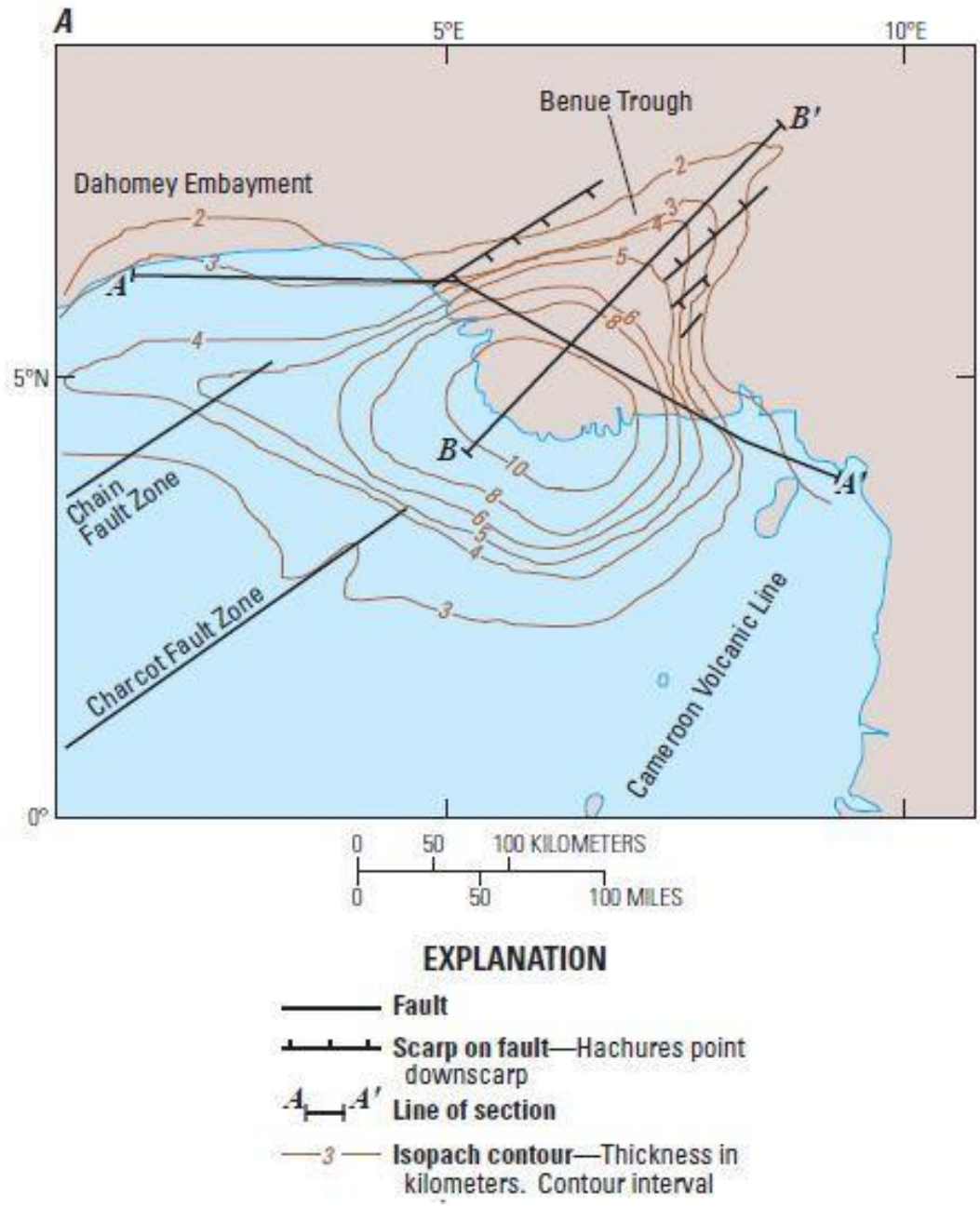

Figure 2.1: Isopach map of Niger Delta (Kaplan *et al*, 1994)

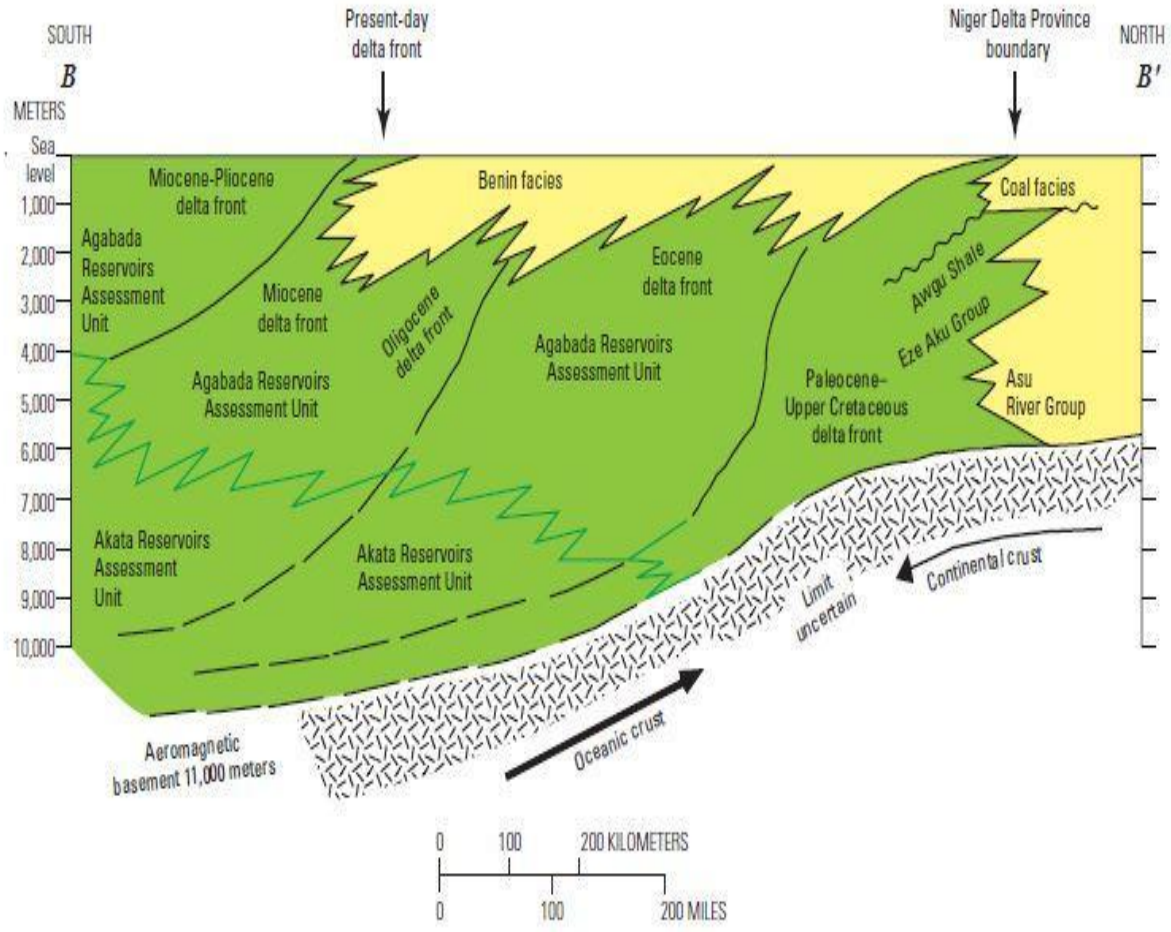

Figure 2.2: Southwest-Northeast cross section ($B - B'$) in Figure 2.1 through the Niger Delta region showing the Akata shales. Modified from Whiteman (1982).

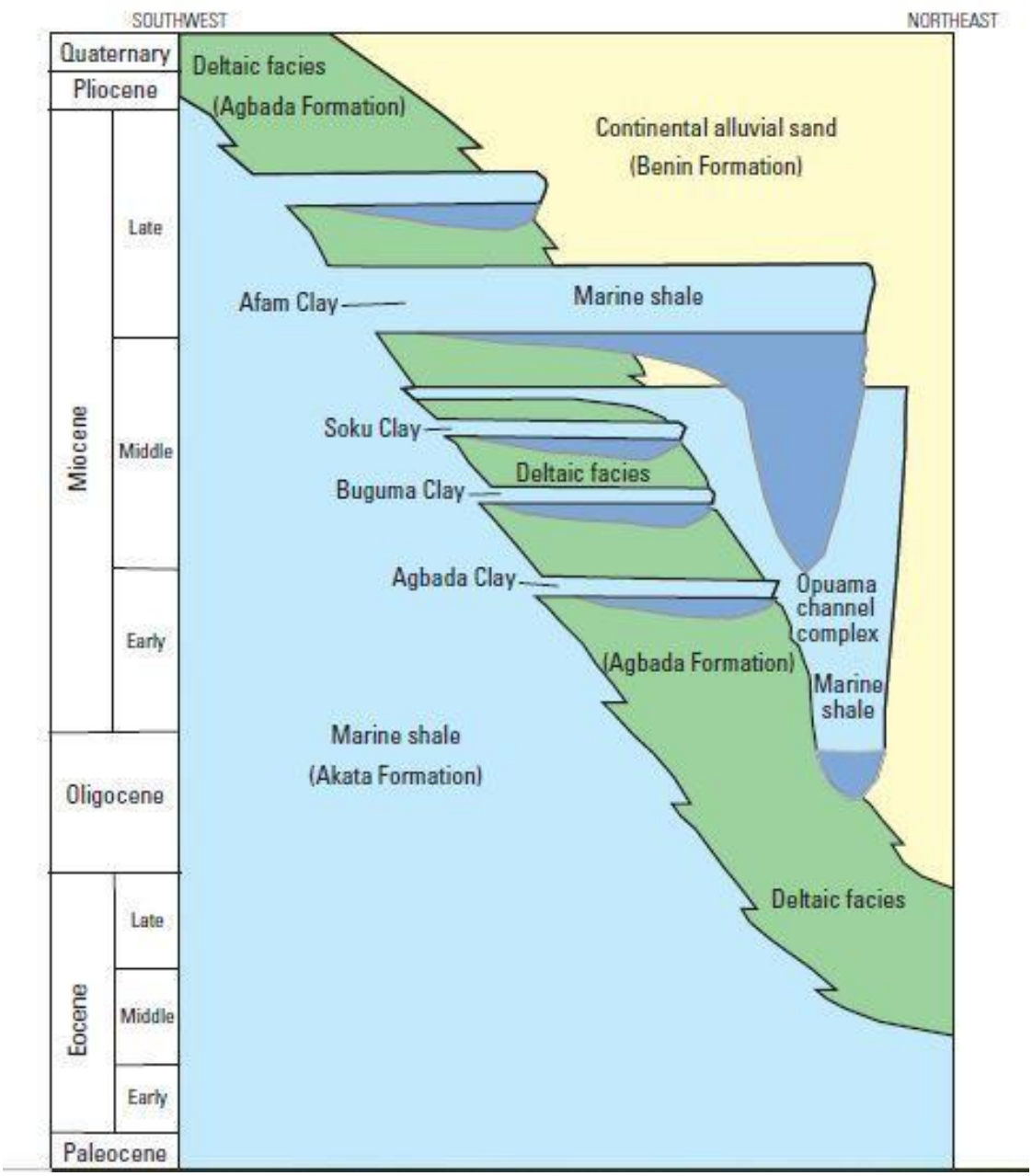

Figure 2.3: Schematic cross section of the Niger Delta, Africa Eocene Agbada formation contains deltaic sandstone reservoirs and traps. Akata formation contains Turbidite sandstone and lowstand channels, sheet sand and fans. Modified from Shannon and Naylor (1989) and Doust and Omatshola (1990).

Traps and seals

Traps in the Niger Delta are frequently structural; examples include faults and anticlinal formations. Although stratigraphic traps are frequently seen, they are typically the result of depositional phenomena, such as reefs, pinch outs, and channels, to name a few. The structural traps formed as a result of the Agbada paralic sequences' synsedimentary deformation (Evamy et al, 1978; Stacher, 1995).

Doust and Omatshola (1990) described a range of structural-trapping components, including those related to clay-filled channels, straightforward rollover structures, structures with numerous growth faults, structures with antithetic faults, and collapsed-crest structures (Figure 2.4). Structural traps are less frequent in the delta's deep offshore region.

Turbidite sands, lowstand sand bodies, and clastic fans are some of the stratigraphic principal reservoirs in Akata Reservoirs AU (Beka and Oti, 1995).

Simple rollover structure with clay filled channel

Structure with multiple growth faults

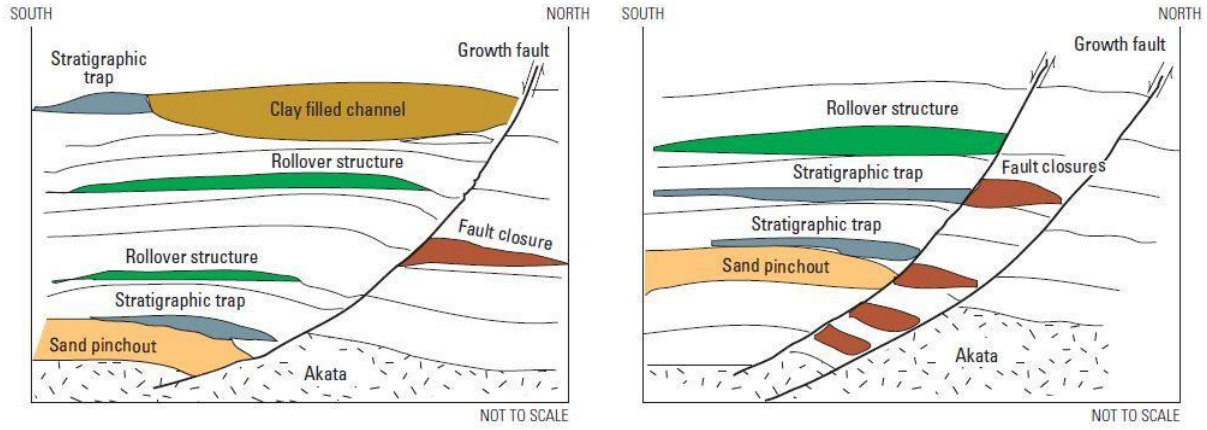

Structure with antithetic fault

Collapsed-crest structure

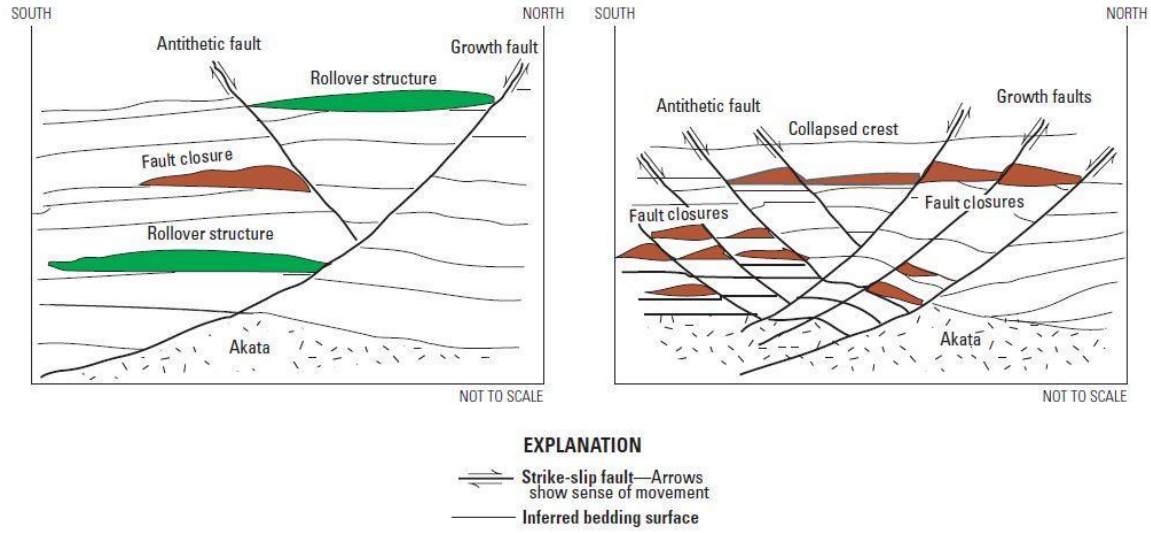

Figure 2.4: Oil field structures and associated trap types, Niger Delta, Nigeria and Cameroon Africa. Modified from Doust and Omatsola (1990) and Stacher (1995).

Depobelts

Each of the five off-lapping siliciclastic stages resulted in the deposition of the Benin, Akata, and Agbada formations in the Niger Delta. Each of the Niger Delta's five off-lapping siliciclastic sedimentation cycles resulted in the deposition of one of the three formations. These cycles (depobelts), which have widths of 30 to 60 kilometers, prograde 250 kilometers southward over oceanic crust. According to Doust and Omatshola (1990), syn-sedimentary faulting developed as a result of varying rates of subsidence and sediment delivery, and these faults extend into the Gulf of Guinea (Stacher 1995). A new depobelt was formed as a result of the interaction between supply rates and subsidence, which caused deposition to be pushed toward the sea.These facts were established by Evamy et al. in 1978 and Doust and Omatshola in 1990. Every depobelt is a discrete entity that faults and on the seaward side by significant counter-regional faults or the growing faults of the next seaward belt. There are five primary depobelts, each of which has a unique history in terms of sedimentation, deformation, and petroleum production.

They defined three depobelt provinces based on structure. The northern delta province, which overlies a very shallow basement, has rotating, regularly spaced faults that steepen as they travel toward the sea, and these faults are where the oldest growth faults are to be found.The middle delta province contains depobelts with clearly defined structures, such as progressively deeper rollover crests that travel seaward with every given growth fault. The distal delta province is the most structurally complicated in the Niger Delta due to internal gravity tectonics on the current continental slope (Figure 2.5).

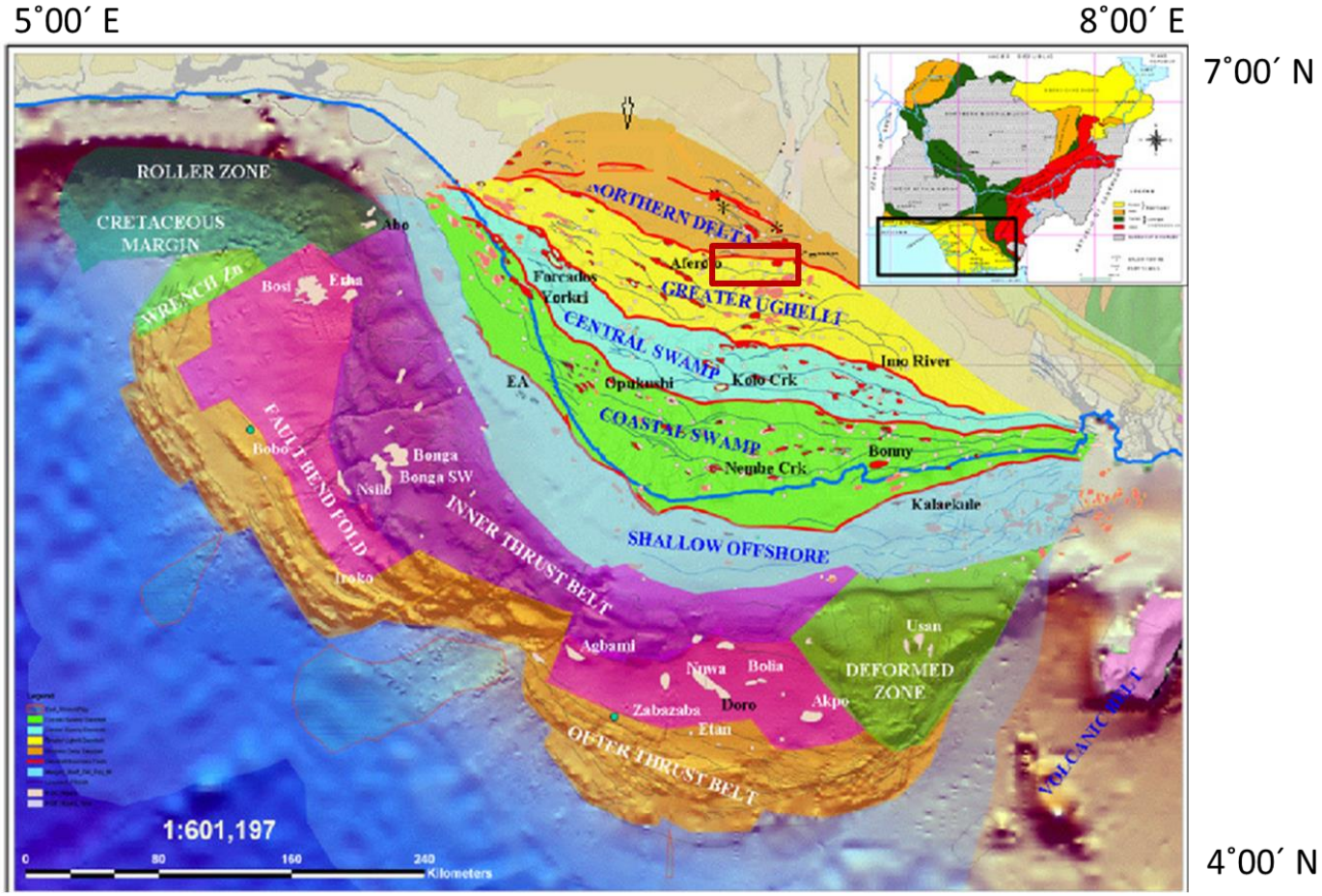

Figure 2.5: Geologic map of the Niger Delta showing the depobelts; note the study location (in red). (Modified after Ejedavwe *et al*. 2002)

2.3 BASIC THEORY OF METHODS USED

2.3.1 Borehole geophysics (Well logs)

Borehole geophysics is a branch of geophysics that deals with application of physics in studying the earth layers encountered in a borehole. The way geologists study an outcrop by dutifully taking a log of the outcrop from the base to the top to study the beds; geophysicist sends equipment that can take physical measurements such as resistivity, natural radioactivity, into a borehole to log the borehole from base to top. This equipment is adorned with sensors that transmit its measurement to the surface through connected wires, hence, the name wireline logging.

2.3.1.1 Measurements While Drilling (MWD)

With the advent of MWD tools, formation properties are being measured at the time the formation is drilled by use of special drill collars that house measuring devices. These measurement-while-drilling (MWD) tools (or logging while drilling LWD) are particularly valuable in deviated offshore wells where well bore path control is critical and where an immediate knowledge of the formation properties is vital for decision making on such matters as the choice of logging and casing points.

2.3.1.2 Open-hole logging and logging tools

The term open-hole refers to the condition of the borehole immediately after the drilling is completed or prior to casing of the borehole. There are modern equipment that can make measurements in cased holes. Open-hole logging provides a continuous record of measurement versus depth of so many formation properties. In particular, wireline logs can record formation electrical resistivity, bulk density, natural and induced radioactivity, hydrogen content, and elastic modulus.

The open-hole logging tools include:

Formation Fluid Content Indicators

i. Induction
ii. Laterolog
iii. Microfocused (micro-resistivity)
iv. Dielectric
v. Pulsed neutron
vi. Inelastic gamma

Porosity-Lithology Indicators

i. Sonic (acoustic)
ii. Density and lithologic density
iii. Neutron
iv. Natural gamma ray
v. Spectral gamma ray

Reservoir Geometry Indicators

i. Dipmeter
ii. Borehole gravimeter
iii. Ultralong spacing electric

Formation Productivity Indicators

i. Spontaneous potential (SP) log
ii. Caliper log

2.3.1.4 Gamma ray

The natural radioactivity in a formation is measured by a gamma ray tool, it responds to the presence of uranium-, potassium- and thorium-rich minerals. Minerals with low concentrations of these minerals such as quartzose sandstone will record a minimal response, but when there is a high proportion of potassium feldspar or detrital clay, glauconite, heavy minerals or mica, there is a higher response. As the clay content increases; the gamma ray response increases; the organic-rich marine shale commonly has the greatest response as it contains significant amounts of uranium-rich minerals generated by the reduction of decaying organic matter.

Generally, carbonates rocks have a low gamma ray response unless they contain notable amount of detrital clay or uranium**.** Almost all gamma radiation emitted naturally is from the radioactive potassium isotope of atomic weight 40 (40K) and by the radioactive element's uranium and thorium. The number and energies each element possess are distinctive and can be used to differentiate between them**.** This fact is used in the spectral gamma ray tool that uses selective energy windows to deconstruct the total gamma response into these separate elements.

One of the difficulties in the interpretation of the gamma ray measurements is a lack of uniqueness. There are nonradioactive clays, and there are "hot" dolomites. The use of spectral

gamma ray devices can point out anomalies such as a “hot” dolomite or other formations with some unusual excess of U, K, or Th. They permit recording the individual mass concentrations of the three radioactive components of the total gamma ray signal. Commonly the results are displayed as a total gamma ray (SGR) and a computed gamma ray (CGR), which is total gamma minus uranium.

Either type of gamma ray log may be utilized for estimating the volume of detrital clay in a reservoir, but if there is known to be a high uranium content this should not be considered when performing the exercise, and likewise if the reservoir is an arkosic sandstone with highly micaceous, significant potassium feldspar content or contains volcanic ash.

The GR device contains a detector, which measures the gamma radiation emitted close to the borehole wall (Figure 2.6). Because of the relatively small size of the counters, good resolution of formation variation is achieved and it is normally run in all tool strings as an aid to correlation. The primary calibration standard for GR tools is the American Petroleum Institute (API) test facility in Houston and logs are normally presented as API units. Older tools used a scale of micrograms of radium-equivalent per ton of formation; former Soviet Union tools continued to use this scale until the late 1990s and conversions are available for these older tools. Although largely insensitive to logging speed, the simple gamma ray tool records more ‘counts per second’ at slower speeds, improving the overall accuracy of the measurement; the spectral gamma ray is very sensitive to logging speed, however, and is normally run with density and neutron combinations. The tool response requires correction for borehole size and rugosity and the density and make-up of the drilling fluid, as these can impact on the capture of gamma rays from the formation, especially in washed out intervals or if the mud is particularly heavy. The presence of radioactive potassium chloride, KCl, as a mud additive can also affect the gamma ray response, especially where the chemical has invaded permeable intervals or has built up in the mudcake.

Applications of Gamma ray

The gamma ray log can be used to determine the volume of shale in a formation. Volume of shale can then be used to correct the apparent porosities found by the sonic, neutron, and density logs. This method of finding V_{sh} will generally yield good values in common formations. If, however, the formation is unusually radioactive, this method will not work (Cannon, 2015).

In order to determineV_{sh}, the gamma ray index (Ish) must be found from:

$$I_{sh} = \frac{GR - GR_{min}}{GR_{max} - GR_{min}}$$

$$V_{sh} = \frac{2^{GCUR \times I_{sh}} - 1}{2^{GCUR} - 1}$$

Where GCUR is Hill index, for tertiary formation, GCUR = 3.7, and for older formation is 2. V_{sh} is then found from a graph such as that shown in Figure 2.5. GR_{min} is minimum reading of GR curve, which is always found from the cleanest sand formation. GR_{shale} is found in thick shale zones near the zone of interest. This will normally be the highest reading gamma ray.

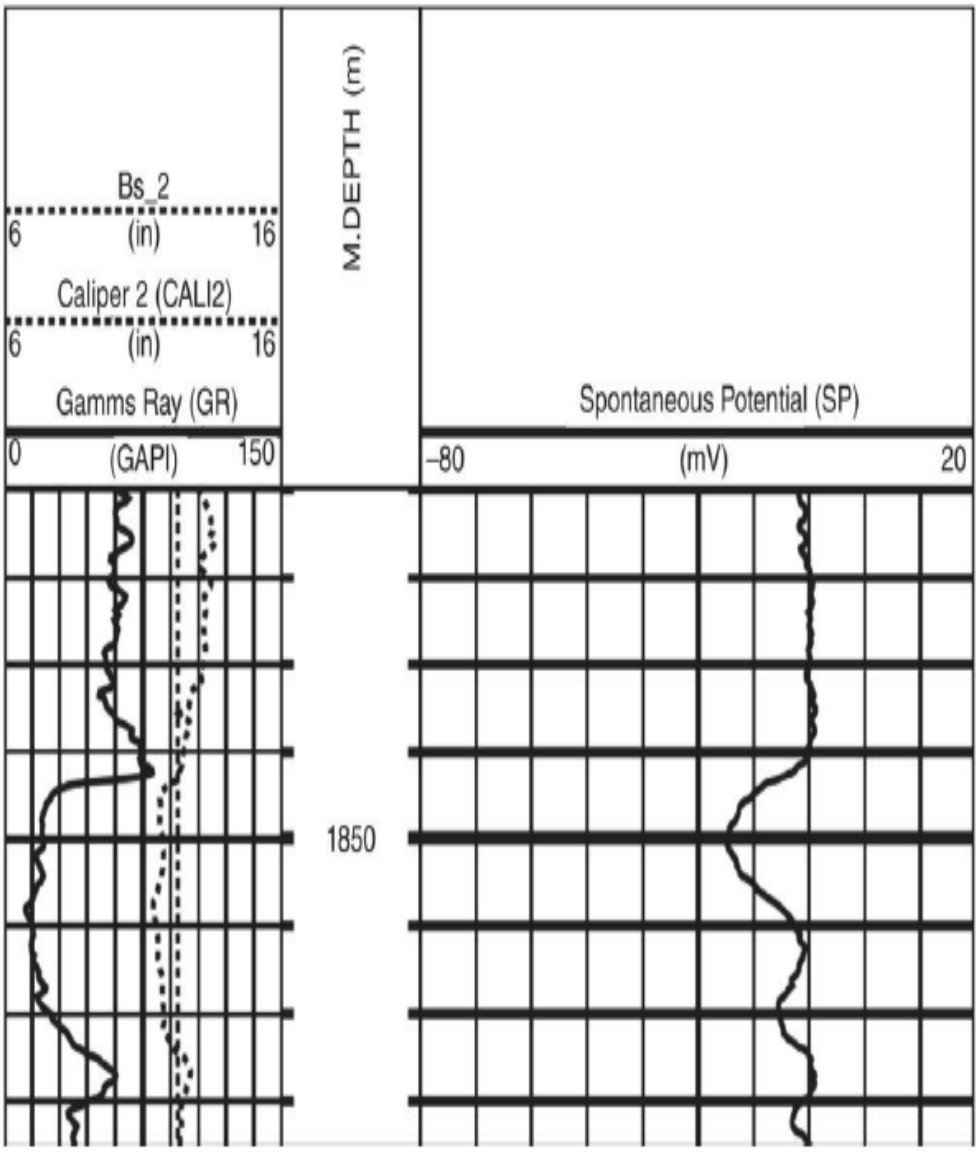

Figure 2.6: A typical gamma ray log reading (Cannon,2015)

2.3.1.5 Neutron

Neutron logs measure the hydrogen concentration in a formation, the hydrogen index (HI); the commonest source of hydrogen in the formation will be water or hydrocarbons (Figure 2.7). In shale-free rocks where the pore space is filled with water or oil, the neutron log directly measures liquid-filled porosity. Where the pores are filled with gas the concentration of hydrogen is reduced, resulting in a lower porosity reading from the tool, the so-called gas effect; there is a 'cross-over' with the density log when the neutron porosity is less than the bulk density in a porous and permeable zone. The neutron log is usually plotted across tracks 2–3 of a standard API display in conjunction with the density log; the display scale is normally 0.45 to –0.15 in limestone porosity units.

A chemical source in the tool, usually composed of americium and beryllium, continuously emits 'fast' neutrons that collide with the atomic nuclei in the formation. With each elastic collision, the neutron loses energy and eventually the neutron is absorbed by a nucleus and a gamma ray is emitted. The maximum energy loss occurs when a neutron collides with a hydrogen atom because they have similar atomic mass; thus the tool response is controlled by the formation hydrogen content, which can be directly related to the porosity for a given lithology. Neutron log responses vary depending on the type of source and the spacing between the source and detector: the effects of such variations are usually processed out, but any tool corrections should be made with full knowledge of the tool type and manufacturer. Neutron data are not measured in basic physical units, but in porosity units usually calibrated to a standard limestone or sandstone response exhibiting zero porosity. Where shale is present in the formation, the neutron log responds to the water trapped in the clay particles, resulting in an overestimation of formation porosity.

The hydrogen index (HI) is based on the number of hydrogen atoms per unit volume of rock divided by the number of hydrogen atoms per unit volume of pure water at surface conditions – a proxy measure of the porosity of a rock. If we have a tool measuring zero porosity in a pure limestone, the HI is zero because there are no hydrogen atoms in the matrix; thus we have a fixed point where HI is zero and porosity is zero. Combined with the known value for unit volume of water where porosity is unity, we are able to scale our neutron response in a porous limestone filled with water. These results, however, are affected by both hydrocarbons and excess chlorine (salt) and therefore need to be corrected.

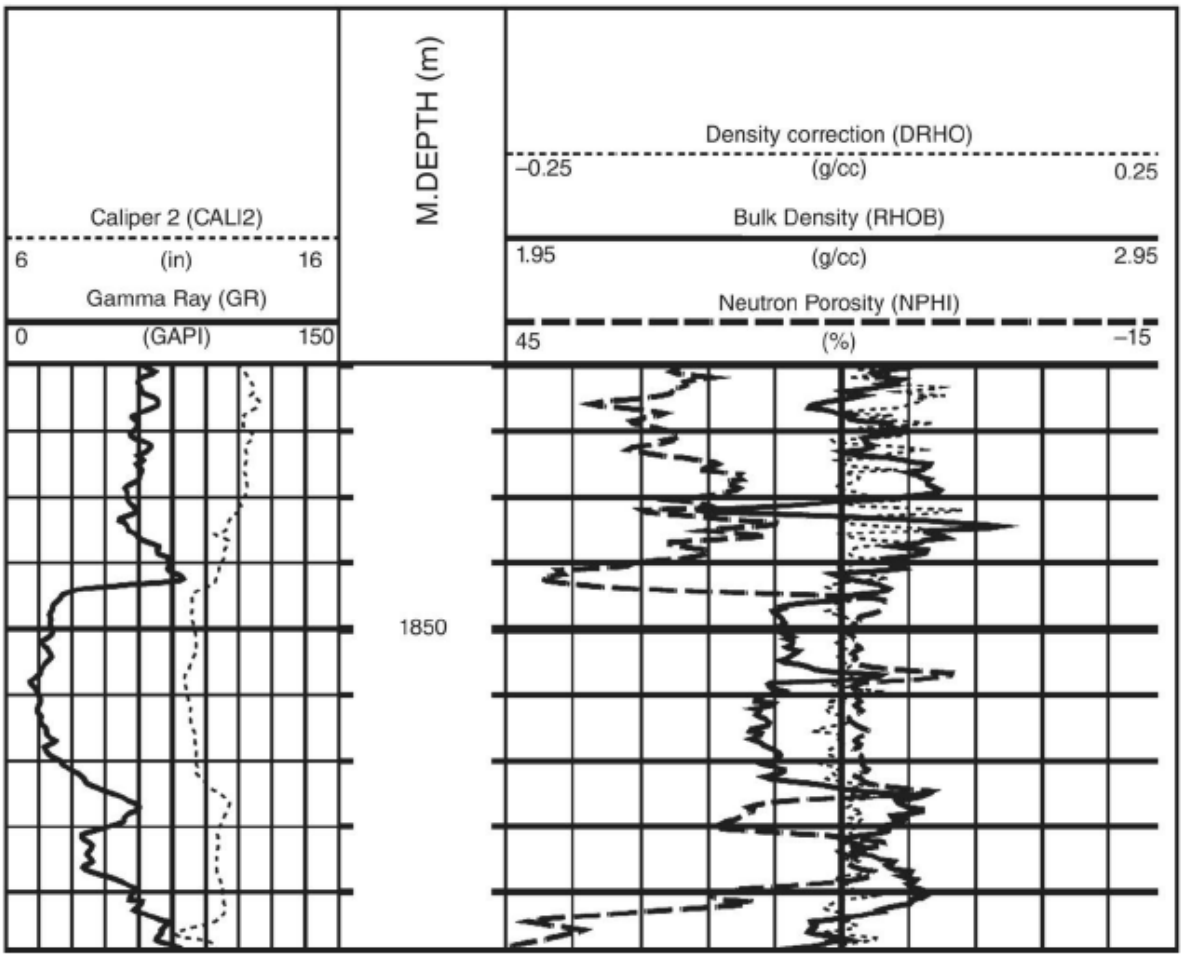

Figure 2.7: The compensated neutron porosity tool: mode of operation, application and typical display. (Cannon, 2015).

2.3.1.6 Density

The density log measures the bulk density of the formation; that is, the density of the rock plus the fluids contained in the pores. Density is measured in $g/cm^3$and is by convention given the symbol ρ (rho). The density log is usually presented across tracks 2–3 of a standard API template along with the neutron and PEF logs: the scale is usually 1.95–2.95g/cm^3. To calculate porosity from a density tool, it is necessary to know the matrix density and the density of any fluids in the pore space. The matrix or rock density is constant for a given pure lithology such as limestone or sandstone, in other words a solid with no porosity (Table 2.1).

The density tool is skid-mounted to maximize contact with the borehole wall and consists of a radioactive source, such as Cobalt (60Co) or Caesium (137Ce), which emits medium-energy gamma rays, or in more modern tools an accelerator source; tools are built with two detectors, about 50 cm from the source, to compensate for borehole rugosity. The emitted gamma rays collide with electrons in the formation and each collision results in a loss of energy from the gamma particle (Compton scattering). The scattered particles that return to the detectors in the density tool are measured in two ranges: a higher energy range affected by Compton scattering and a lower energy range governed by the photoelectric effect (PEF). The number of higher energy range particles returning to the detector is proportional to the electron density of the formation density through a constant (Tittman and Wahl, 1965). The porosity is derived from this relationship with bulk density. The combination density–PEF tool is referred to as the lithodensity (LDT) or sometimes the photodensity tool (MPD). The density tool has a relatively shallow depth of investigation (~35 cm) and as a result is held against the borehole wall (eccentred) to maximize the formation response showing the various prospects in YZ field (Cannon, 2015).

Table 2.1: Various rock types and fluids showing their density values (Cannon, 2015).

Lithology/Fluid	ρ_{matrix} or ρ_{fluid} g/cm^3	PEF (B/e)
Sandstone	2.644	1.81
Limestone	2.710	5.08
Dolomite	2.877	3.14
Gypsum	2.355	3.42
Anhydrite	2.960	5.05
Salt	2.040	4.65
Fresh water	1.0	0.36
Salt water	1.15	0.81
Oil	0.81	0.13
Barite	4.48	267

2.3.1.7 Resistivity

Resistivity logs are used primarily to distinguish water-bearing from hydrocarbon-bearing intervals, but can also indicate permeable horizons and estimate porosity. The only part of a formation able to conduct electricity is the water in the pore space or trapped by clays; the rock matrix and any hydrocarbons are normally resistive. Resistivity tools generate a current in the formation and measure the response of that formation to that current. The strength of the response varies with the salinity and volume of the formation water; more saline water gives a proportionally lower response than fresher water.

The resistivity of a porous rock depends entirely on the electrical conductivity of the formation fluid and mud filtrate, as the surrounding rock matrix acts as an electrical insulator. Drilling fluid can penetrate a permeable formation, forming a mudcake on the borehole wall and flushing the formation water away from the immediate surrounding volume, producing an annulus filled with mud filtrate; the depth of the annulus is a function of the permeability. The resistivity of the flushed or invaded zone depends on the resistivity and saturation of the mud filtrate (Rmf and Sxo) and any remaining formation water (Rt and Sw) and the porosity. When these values are known, the resistivity in the flushed zone can be corrected for invasion. The resistivity of the uninvaded formation depends on the resistivity and saturation of the formation water and the porosity, where summing together the oil, gas and water saturation is unity. Typical values of Rt vary from 0.2 to 2000-ohm m and will only be investigated by the deepest, focused resistivity tools. There are two families of resistivity tools: electrode tools (laterologs) that have electrodes set on tool pads that produce a current and measure the formation response and induction tools that use electric coils to induce a current in the formation and measure the formation conductivity. The former can only be used in boreholes filled with a water-based mud; induction logs can work in both water- and oil-based mud systems. Resistivity is measured in units of ohm m and conductance as milliohm/m. Figure 2.8 shows a resistivity log in a typical configuration.

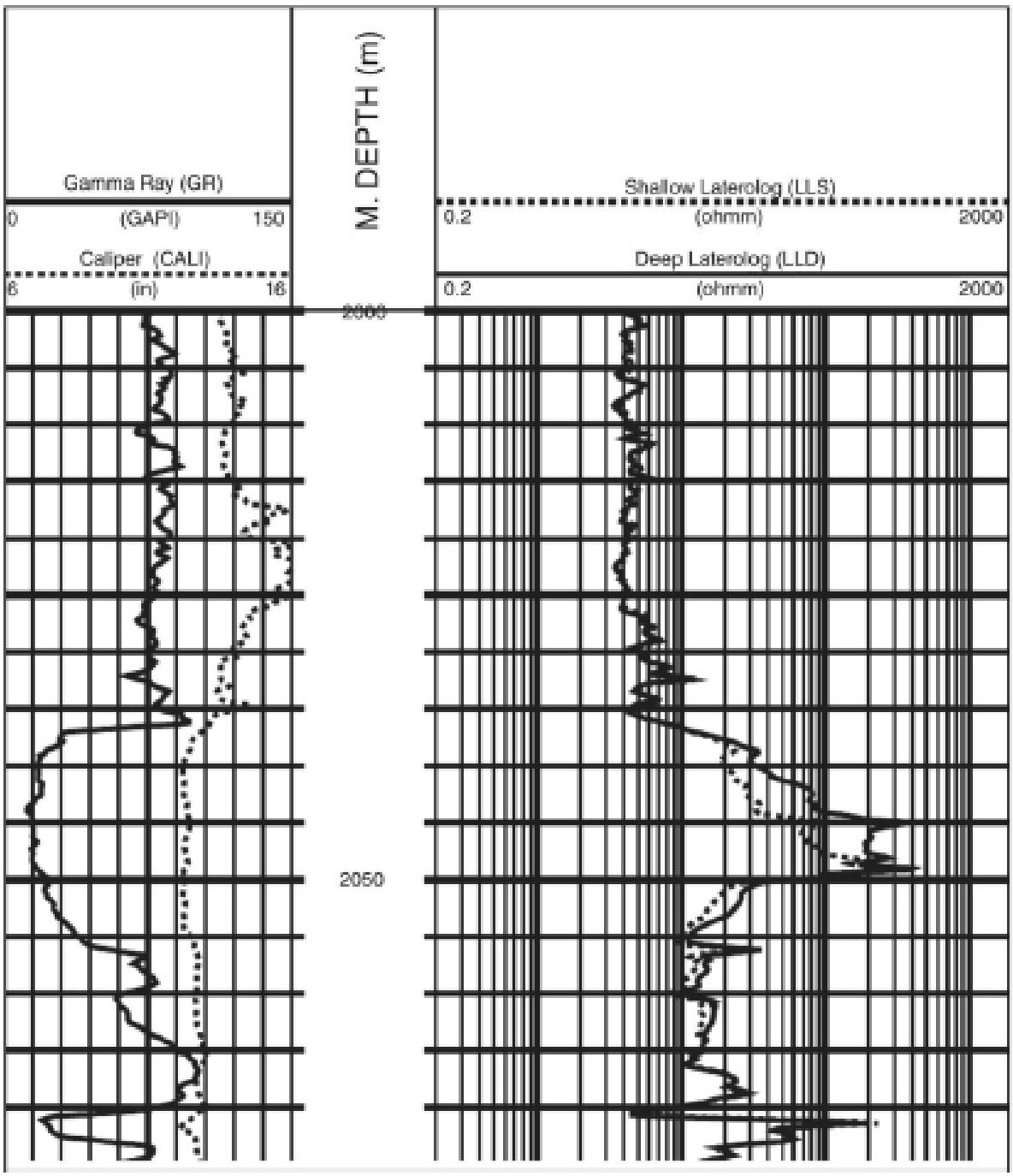

Figure 2.8: Typical resistivity log (Cannon, 2015).

2.3.1.8 Sonic

A compressional sound wave travels through the formation along the axis of the borehole wall, and the sonic log measures the interval transit time of that sound wave (Figure 2.9). Although a compressional sound wave can pass through solids, liquids, and gases, the solid provides the fastest path for the wave to go.

As a result, the sonic tool records the matrix porosity of the formation; therefore, in vuggy rocks, such as many carbonates and sandstones that have a component of secondary porosity, other methods must be used to estimate the total porosity of the formation. The sonic tool comprises one or more ultrasonic transmitters and two or more receivers positioned vertically to minimize and compensate for the effects of borehole rugosity. The interval transit and interval transit times for various -filled porosity of the formation.

The sonic log is usually presented in track 3 of a standard API display at a scale of 40 Today, the main use of the range of sonic tools is in support of seismic and geophysical interpretation, first in making a well tie between time and depth measurements for depth conversion, and second for calculating interval velocities and also for acoustic impedance studies as part of predictive rock physics experiments. (Cannon, 2015).

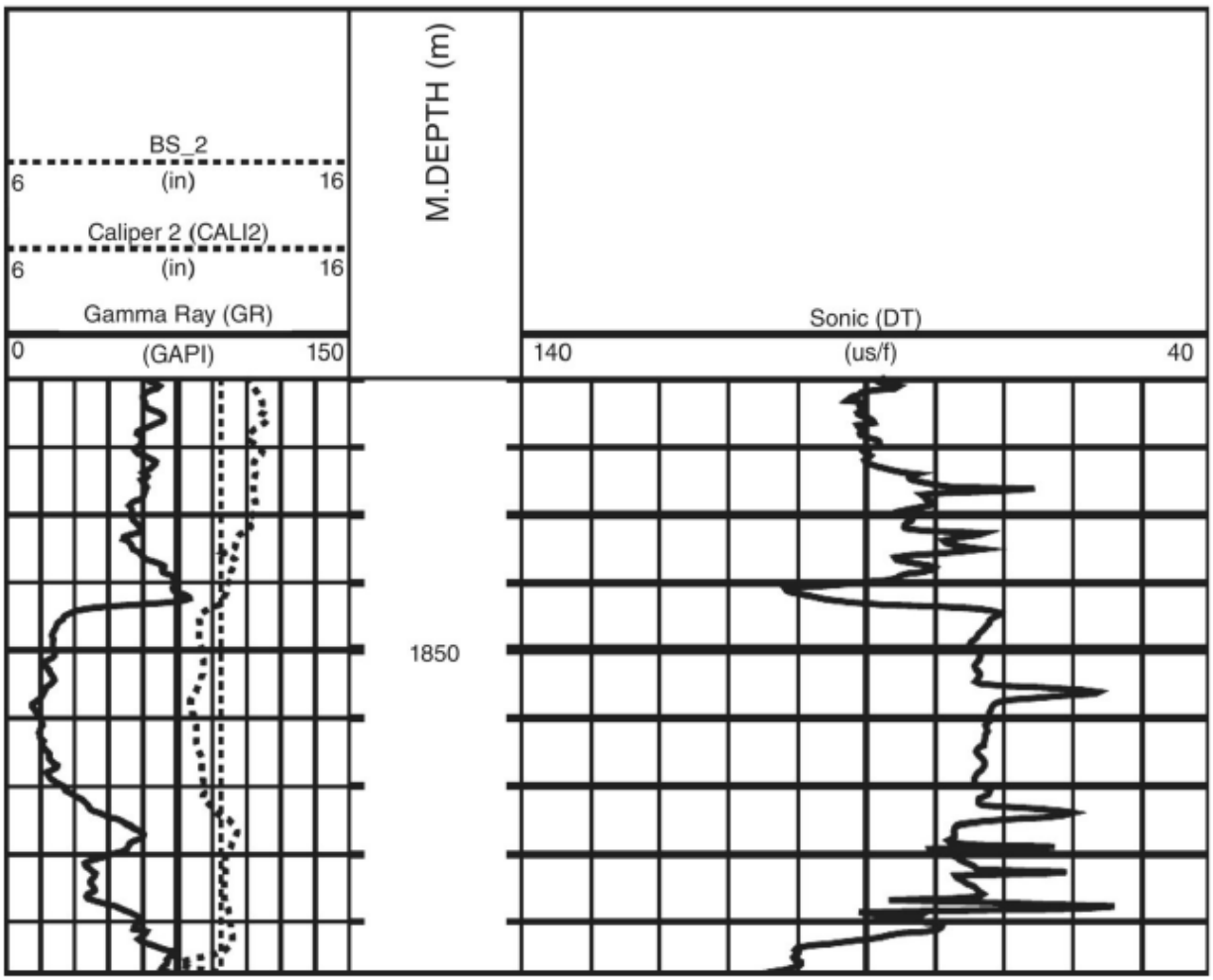

Figure 2.9: Typical sonic log (Cannon, 2015).

Table 2.2: Sonic velocities and interval transit times for different matrix type (Cannon, 2015).

Lithology/fluid	Matrix or fluid velocity (ft/s)	Δt_{matrix} or Δt_{fluid} (μs/ft)
Sandstone	18,000–19,500	55.5–51.0
Limestone	21,000–23,000	47.6
Dolomite	23,000–26,000	43.5
Anhydrite	20,000	50.0
Salt	15,000	66.7
Casing (steel)	17,500	57.0
Freshwater mud filtrate	5,280	189
Saltwater mud filtrate	5,980	185

2.3.2 BASIC THEORY OF SEISMIC REFLECTION

Seismic reflection data results from acquisition surveys carried out both onshore (on land) and offshore (in marine environments).

The seismic reflection method is, without doubt, the most used geophysical technique in the oil and gas industry, as a tool for looking for hydrocarbon reservoirs, due to its high resolution even for great depths (Gomes and Alves, 2007). Exploration seismology uses the same principles of wave propagation, mainly for compressional p-waves, which travel inside Earth's layers, produced by an artificial controlled source of energy using short source-receivers offsets. Depending on the survey target, sources and receivers acquisition geometries are previously planned to maximize the imaging capacity of the seismic method for the targets under investigation (Telford et al., 1990).

In seismic reflection data, the information about the subsurface geology, physical rock properties and layers attitude, is inferred from the reflected wave travel-time between the source and its arrival at the receivers. The two-way travel-time (TWT) is defined by the time taken for the seismic waves to travel down from the source until they meet a boundary between layers with a different seismic velocity (V), density (ρ) and acoustic impedance (Z) where they are reflected and then return to the surface. The contrast between acoustic impedance is called reflection coefficient (RC).

$$Z = \rho V$$

$$RC = \frac{Z_2 - Z_1}{Z_2 + Z_1}$$

At such interfaces, the seismic rays are partially refracted, partially transmitted and partially reflected back to the surface where they are detected by a group of receivers (Figure 2.10). The arrival of reflected seismic waves produces systematic variations from trace to trace. These variations are called seismic events, and if they are consistent in the recorded seismic data, they can probably be interpreted as real geological interfaces between layers with different reflection coefficients. Measuring the travel-time of the events allow to determine the attitude and location of the geological interfaces which gave rise to each reflection event. The interpretation process also takes into account amplitude, frequency, phase and wave shape variations. Besides trying to identify direct hydrocarbon indicators, Seismic data is most often used to identify potential structures for hydrocarbon accumulation (Telford et al., 1990; Gomes and Alves, 2007).

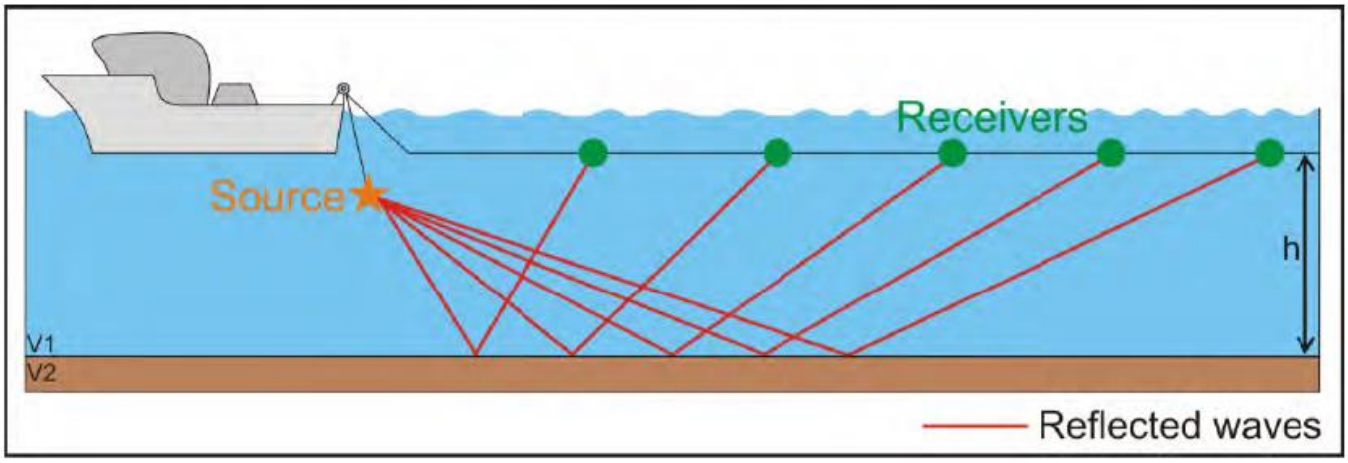

Figure 2.10: Path of the reflected seismic energy in one dimension as it travels from the source to the receivers and it is reflected from the interface between two layers with different acoustic impedance (Modified after Leonardo and Guerra, 2009).

2.3.3 SEISMIC ATTRIBUTE ANALYSIS

Oxford dictionary defined attribute as a quality ascribed to any person or thing. Richard 2008, defined Seismic Attributes as all the information obtained from seismic data, either by direct measurements or by logical or experience-based reasoning (Table 2.3).

Attributes with the most predictive results are those derived from the various seismic wavelet components. The amplitude content within the data effectively provides physical parameters about the subsurface such as acoustic impedance, reflection coefficients, velocities and absorption effects which supply structural detail or act as DHIs.

Classification of Seismic Attributes

With the increasing interest on seismic attributes and their large number and diversity it now becomes necessary to catalogue them into different classes. Many proposals have been put forward with the aim of classifying seismic attributes in a tight, strict and intuitive way, based on both the input and the expected result. Unfortunately, new attributes appear every day and algorithms of well-known attributes can be improved since sometimes they give unexpected results (Richard, 2008). The proposed classifications are constantly changing, depending on the understanding of the seismic attribute today (Taner, 2000). Table 2.4 is a summary of various seismic attributes, their concept and applicability.

Table 2.3: Many classes of attributes can be defined (Richard, 2008):

Attributes	**Comment**
Post-stack seismic	"Traditional"
Pre-stack seismic	AVO etc.
Impedances	Seismic inversion
Velocities	Imaging operations
Surfaces	Structural interpretation
CSEM, MT, Gravity, Aero-magnetic	Non-seismic attributes

Table 2.4: Some Seismic Attributes, description and applicability (Leonardo and Guerra, 2009**)**

Attribute Name	**Description**	**Applicability**
RMS Amplitude	The "root mean square" of the original amplitude within a user-defined window	Distinguish between lithological changes. High values of RMS Amplitude may indicate porous sands or sinuous channel belts. Isolated extreme values of this attribute may be a bright spot.
Instantaneous Phase	It is defined as the argument of the complex seismic trace	Enhance reflectors continuity, discontinuities, faults and pinch-outs. Is useful in stratigraphic pattern interpretation. Can be used as a DHI.
Cosine of Instantaneous Phase	It is the cosine of the instantaneous phase attribute	Improves reflectors continuity and enhance discontinuities, faults and pinch-outs. Helps the stratigraphic interpretation process. Since it is invariant with amplitude is used conjugated with the instantaneous phase attribute.
Instantaneous Frequency	It is the rate of change in time of instantaneous phase attribute	Typically used to interpret lateral and vertical changes in lithology and identify faults by absorption effects. Can also be used as a DHI, since the presence of gas often causes what so called low-frequency shadow, below the hydrocarbon reservoir.
Structural Smoothing	Fast volumetric signal processing. Apply a 3D Gaussian filter honouring, or not, the estimated bed orientation.	Reduces spatial noise within the data, improving reflectors continuity. May also enhance edges.
Variance	It computes the normalized population variance with an optional weighted vertical smoothing.	Detect edges, such as faults and discontinuities. It sharply delineates a salt body and with a short vertical window, *variance* attribute can be used to interpret depositional elements.

Iso-Frequency	It is a spectral decomposition method which uses a correlation between a user-defined cosine frequency and autocorrelation function of the original seismic data.	May indicate subtle lithologic features which are not detected in original amplitude. Can also be used to interpret depositional elements.
Relative Acoustic Impedance	It tries to estimate the natural acoustic impedance log by integrating the original seismic trace and filtering it through a Butterworth filter.	High values of relative acoustic impedance are often related with unconformity surface, sequence boundaries and discontinuities. It may also be used to detect the presence of fluids within the data.

CHAPTER THREE

3.0 METHODOLOGY

A summary of the workflow adopted in this research is presented in Figure 3.0.

3.1 DATA GATHERING (COMPOSITE WELL LOG AND 3D MIGRATED SEISMIC DATA)

The dataset used in this research is one of the datasets provided by Nigerian National Petroleum Cooperation (NNPC) and its Joint Ventures for research purposes.

The data comprises of the following:

I. 3D migrated post stack seismic data covering an area of about $589.5Km^2$. This 3D seismic is in segy format.
II. Six composite well logs (LAS format). A survey of these wells and the available logs is provided in Table 3.1.

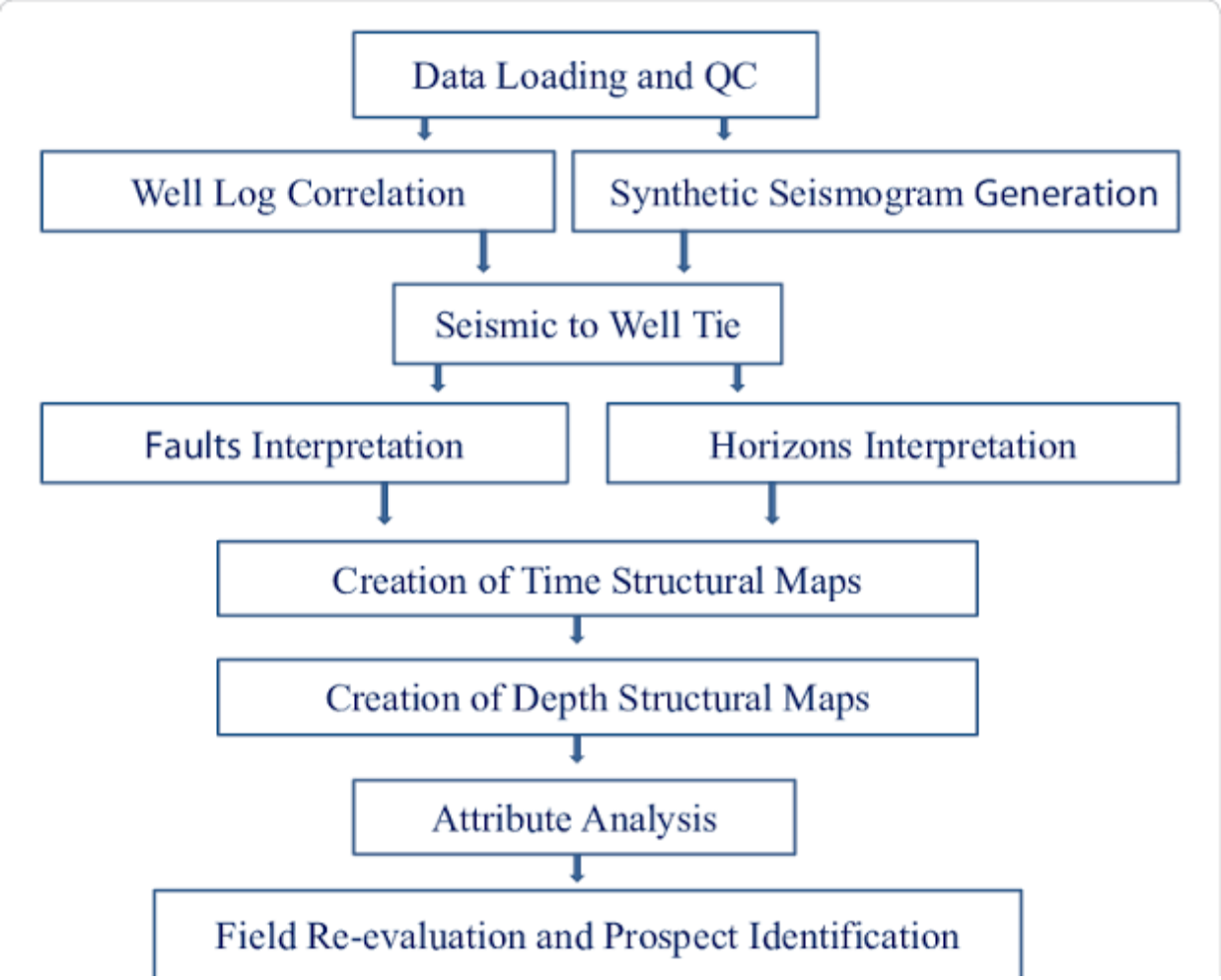

Figure 3.0: Summary of the workflow adopted for this research.

3.1.0 DATA LOADING

Well logs

The well data was first loaded into the petrel software which was in a LAS format. After the data QC was done it was discovered that only 6 wells had the complete information needed for the project. The positions of the 6 wells were uploaded into the software (Figure 3.1).

Deviations

Secondly the well deviations were loaded into the software since not all the wells encountered were straight wells. (Figure 3.2) shows how the well 6 is a side track of well 4 this was discovered after the deviation data was loaded into the software.

Check shot

The check shot data was loaded into the software so the well data could also be viewed in time and not just depth and for structural map generation. The checkshot data is the time-depth relationship data that allowed proper overlay of the borehole logs (depth domain) on the seismic data (time domain) prior to well to seismic tie (generation of the synthetic seismogram).

Seismic

The 3D seismic data (in segy) was loaded into the petrel software. The data was viewed in both 2D and 3D spaces. It can be observed that some part of the data has been muted (Figure 3.3a-b). Continuous reflections can be observed from a time window of -455.26 ms to -2214.70 ms. The faults and horizons are visibly clear within this time range. Beyond the time of -2214.70 ms chaotic reflections are observed. Generally, the seismic data is of fair to good quality. Seismic data loading was carried out so that the positions of the wells can be viewed in relation with the 3D seismic data coverage on the field. It can be observed that all the wells were drilled around the south-western region of the field (Figure 3.1a). Thus, majority of the field remained untested.

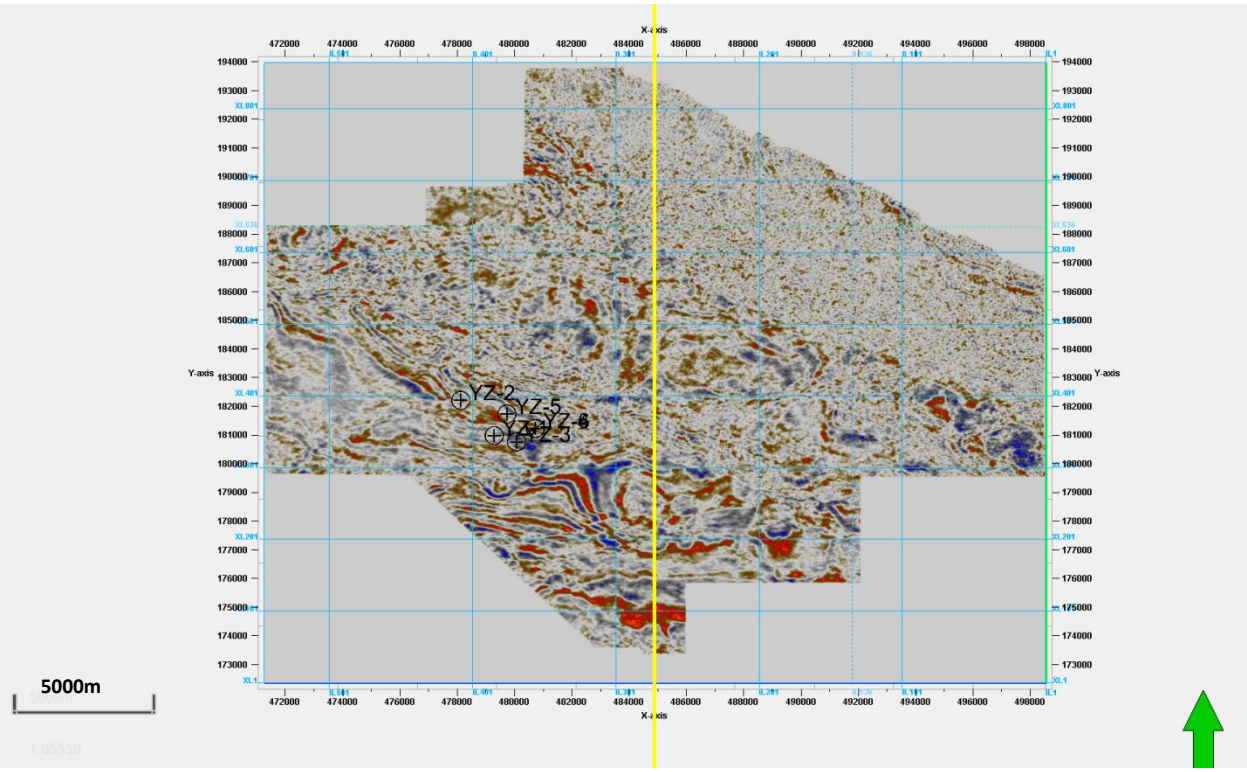

Figure 3.1: (a) Positions of the 6 wells on the 3D seismic cube from top view.

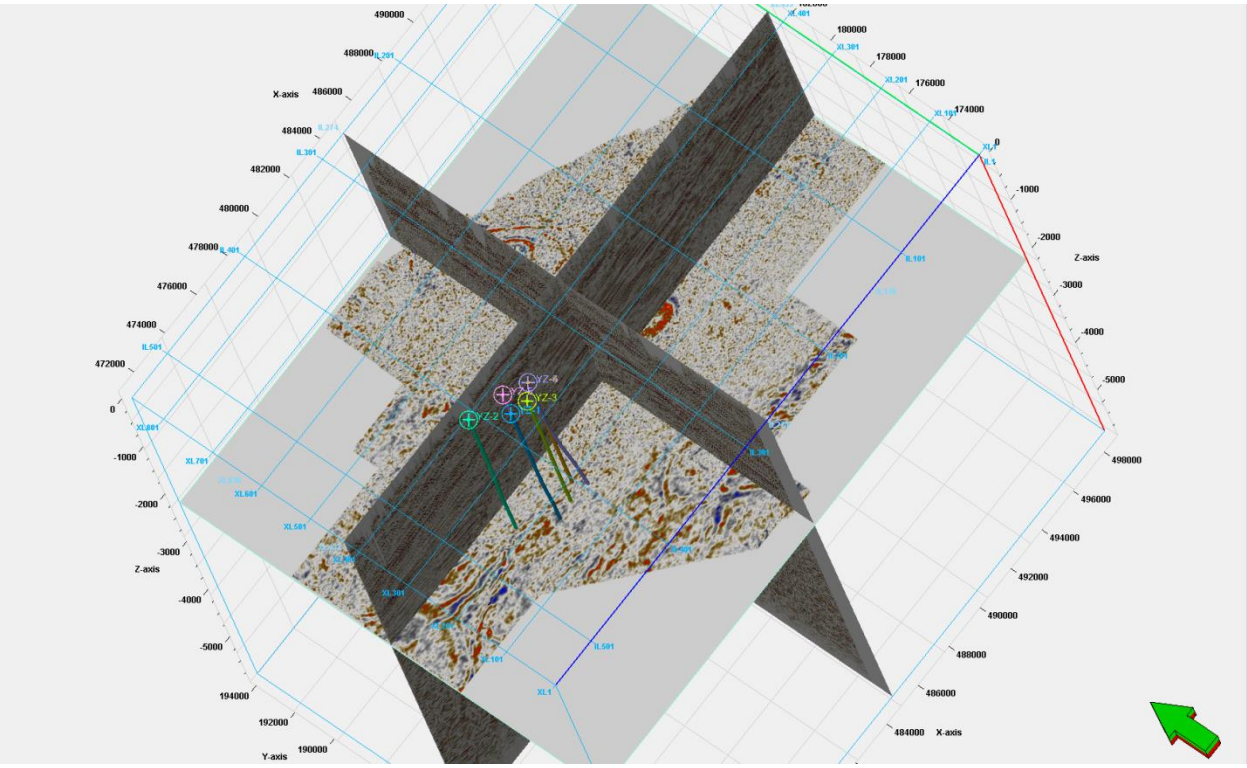

Figure 3.1 (b) Positions of the 6 wells on the 3D seismic cube from 3D view.

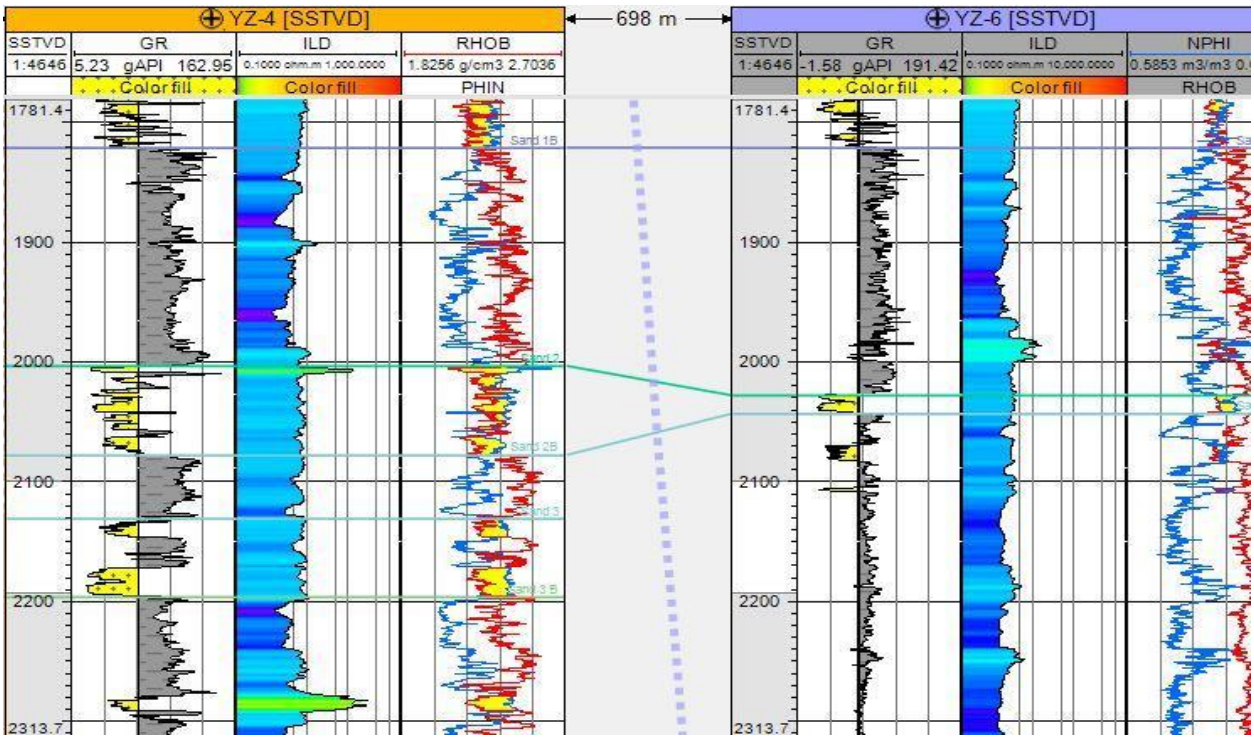

Figure 3.2: (a). Well interpretation window showing the side track of well 6 from 4.

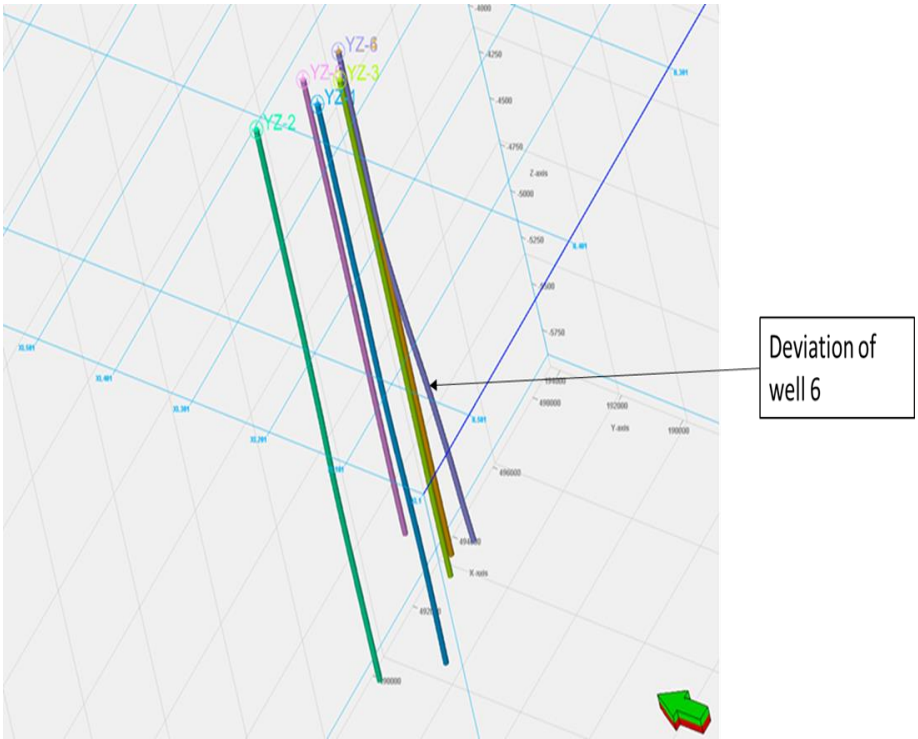

Figure 3.2 (b). 3D interpretation window showing the deviation of the wells (Note well 6).

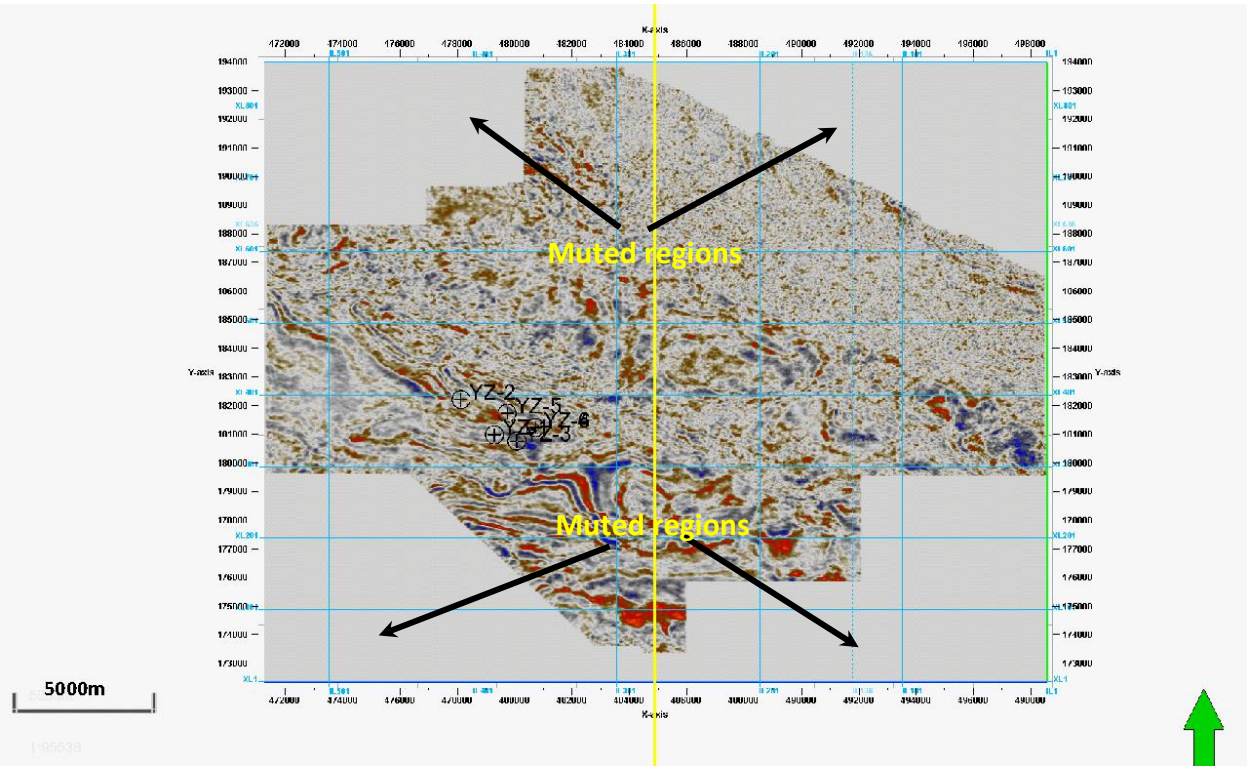

Figure 3.3: (a) Seismic data showing the muted areas from top view.

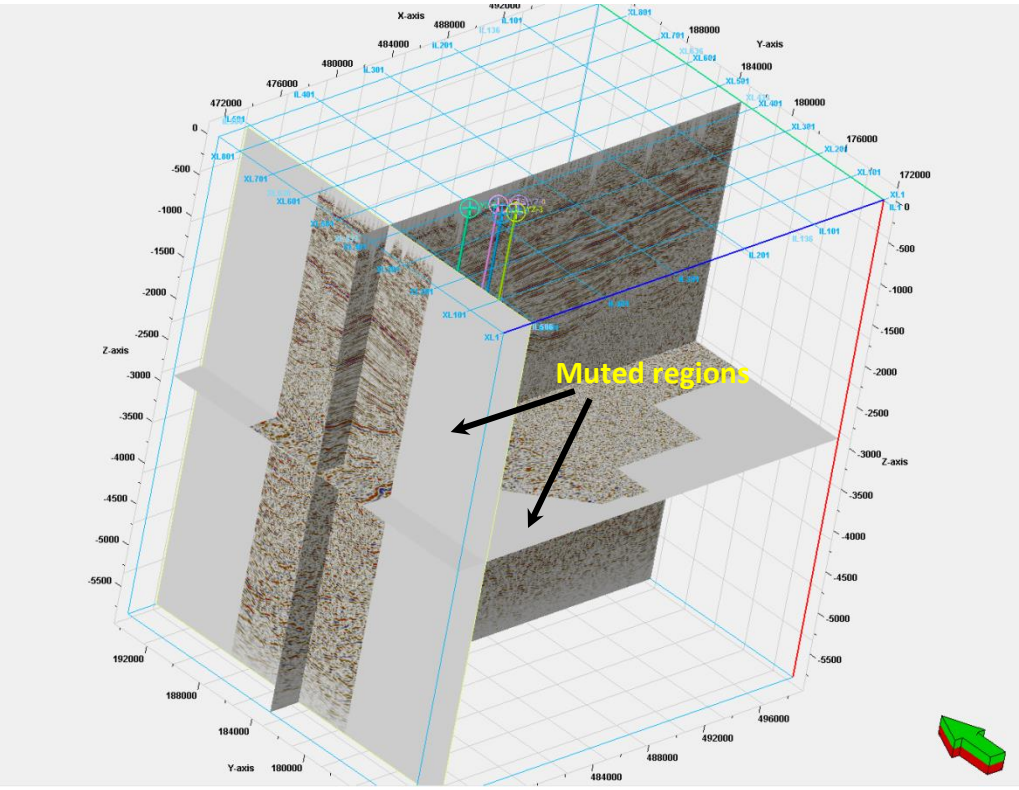

Figure 3.3 (b) Seismic data showing the muted area from side view in red.

Table 3.1: Survey containing the six wells displaying the available data logs.

	YZ 1	YZ 2	YZ 3	YZ 4	YZ 5	YZ 6
Gamma Ray	✓	✓	✓	✓	✓	✓
Resis ILD	✓	✓	✓	✓	✓	✓
Density	✓	✓	✓	✓	✓	✓
Sonic	✓	✓	✓	✓	✘	✓
Neutron	✓	✓	✓	✓	✓	✓
SP	✓	✓	✓	✓	✓	✓

3.2 WELL LOG CORRELATION AND INTERPRETATION (RESERVOIR CORRELATION AND PETROPHYSICAL ANALYSIS)

Reservoir Correlation

The well logs were arranged in a N-S direction for correlation (Figure 3.4, track 1). The hydrocarbon reservoirs were identified using combination of Resistivity and Gamma ray logs. Possible reservoirs encountered by the wells during drilling i.e., sand lithologic units were delineated using gamma ray logs. A cut off line was utilized to properly differentiate the sand from the shale units. Deflection of the gamma ray log signature to the right signifies high radioactivity was interpreted as shale while deflection of the log to the left (i.e., low radioactivity) of the cut off line was interpreted as sandstone. Having identified the reservoirs, the Net-to-gross was calculated.

Presence of Hydrocarbon

The presence of hydrocarbon in the delineated reservoir sand units was identified using deep resistivity log (Figure 3.4, track 2). Deflections to the right was interpreted as high resistivity. Hydrocarbon within the reservoirs was characterized by its high resistivity signature while low resistivity zones are characterized as saline water bearing reservoirs.

Hydrocarbon Typing (Oil or Gas)

Hydrocarbon typing was done using neutron/density log. The neutron and density logs were overlayed. The neutron log's response when the pores are filled with gas results in lower porosity estimates than the actual formation porosity. This happens because the tool processing does not take into account the fact that gas has a lower concentration of hydrogen than oil or water in a fixed pore volume. This is the 'gas effect,' which occurs in wells with a gas cap. Whereas if the formation fluid is hydrocarbon oil the density and neutron log will track side by side.

Petrophysical Estimation

Hydrocarbon saturation was calculated using equation 3.1

$$S_h = 1 - S_w. \quad (3.1)$$

Were S_h is the hydrocarbon saturation and S_w is the water saturation (see equation 3.6).

Volume of shale (V_{sh}) was calculated using the equation 3.2

$$V_{sh} = 1 - NTG\ . \quad (3.2)$$

Were NTG is the net to gross of the reservoir.

The volume of hydrocarbon oil was calculated using equation 3.3

$$STOIIP = GRV \times \frac{N}{G} \times \emptyset \times S_o \times \frac{1}{B_o}(stb) \quad (3.3)$$

The volume of hydrocarbon gas was calculated using equation 3.4

$$GIIP = GRV \times \frac{N}{G} \times \emptyset \times S_g \times \frac{1}{B_g}(scf) \quad (3.4)$$

Where $GRV = Area \times Height$

$\frac{N}{G} = Net\ To\ Gross$

$\emptyset = Porosity$

$S_g = Gas\ Saturation$

$B_g = Gas\ formation\ factor$ (0.98 *was the constant used*)

$B_o = Oil\ formation\ factor$ (1.17 *was the constant used*)

$S_o = Oil\ Saturation$

The porosity for the various reservoirs was calculated using equation 3.5

$$\emptyset = \frac{\rho_{max} - \rho_b}{\rho_{max} - \rho_f} \quad (3.5)$$

Where; ρ_{max} =Maximum density

ρ_b =Bulk density (RHOB)

ρ_f =Density of the fluid (taken as 1)

The water saturation for the reservoirs was calculated using equation 3.6

$$S_w = \sqrt[n]{\frac{a \times R_w}{\emptyset^n \times R_f}} \quad (3.6)$$

Where; $n = Saturation\ exponent$ (taken as 2)

$R_w = Formation\ water\ resistivity$ (taken as 0.8)

$R_f = Resistivity\ of\ fluid\ (ILD)$

$\emptyset = Porosity$

$a = Cementation\ exponent\ (taken\ as\ 0.81)$

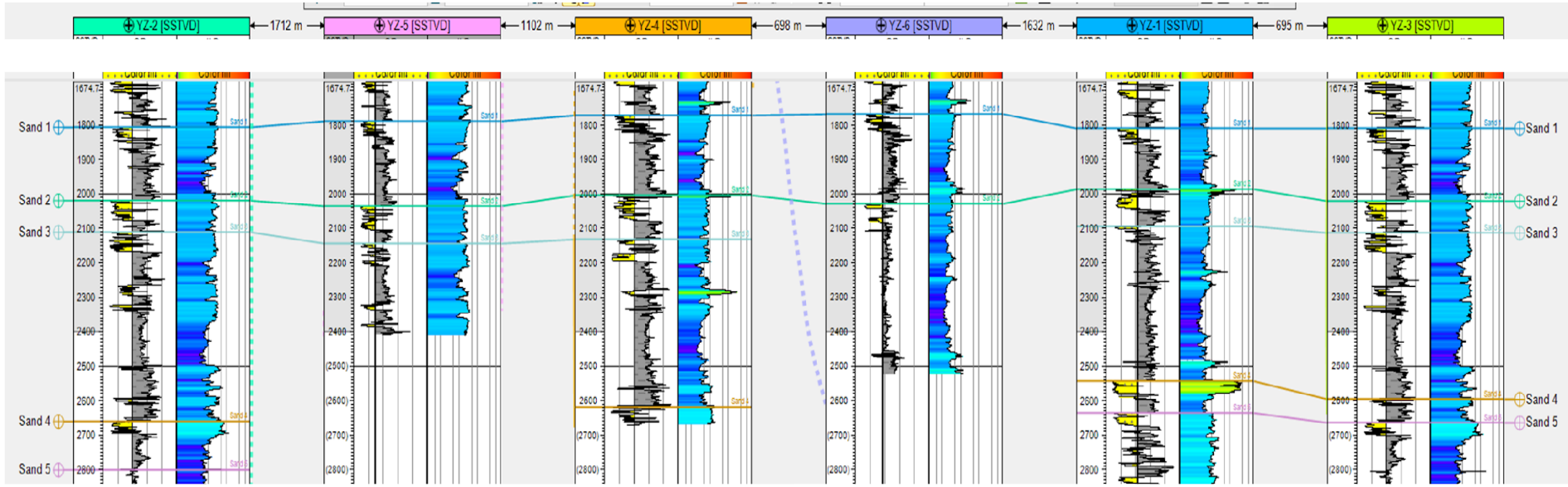

Figure 3.4: Correlation of the well logs arranged in N-S direction. Showing the identified hydrocarbon bearing formations (Sand 1 to 5).

3.3 SYNTHETIC SEISMOGRAM GENERATION

The synthetic seismogram was generated (Figure 3.5 (a-d)) by computing the reflection coefficients from the sonic and density logs (Figure 3.5a to c) of YZ well 1 using Zoepritz equation. The reflection coefficient sticks were convolved with a Ricker (zero phase) wavelet (Ricker 25Hz wavelet) to obtain the seismic "wiggle" traces. The well log which was originally in depth was converted to time using the check shot data so that the synthetic seismogram could be overlaid on the field seismic data (Figure 3.5 d). It can be observed that YZ well 1 synthetic seismogram log has a good tie; with a peak to peak and trough to trough match on the synthetic seismogram and the 3D migrated seismic data. The various reservoirs identified from the well logs was indicated on the synthetic seismogram which was mapped on the seismic data and used for the seismic horizon mapping (Figure 3.6). Continuous reflections could not be established with sand 5 which hindered the mapping of the horizon.

3.4 FAULTS INTERPRETATION

Faults were delineated using the sudden termination of seismic reflection pattern as a guide and was identified and interpreted throughout the entire seismic volume. This revealed four major growth faults which are listric in nature some of the other faults mapped are synthetic and antithetic faults (Figure 3.6).

3.5 HORIZONS INTERPRETATION

Horizons were identified from the synthetic well log. The interpreted reservoir tops on the well logs falls on the trough and was used as a guide in mapping the reservoir tops across the entire seismic coverage. The four horizons mapped are characterized by amplitude reflections which are variably low to high with above average to good continuity. Lateral continuity of horizons was terminated due to the presence of some faults and chaotic reflections which are likely due to shale diaperism (Figure 3.6).

3.6 TIME STRUCTURAL MAPS

Time structural maps (Figure 3.8 a) were developed from the horizons and faults delineated across the seismic. The contouring was derived from joining points of equal time (ms) with an interval of 25ms. Points having the same or similar time were identified having the same color and the time value each color represents is shown in the color legends in (Figure 3.8 a).

3.7 DEPTH STRUCTURAL MAPS

Depth structural maps (Figure 3.8 b) were created by simply converting the time map to depth map with the help of a velocity model generated from combining all the available check shot data. The relationship between the time (x axis), and the depth (y axis) is presented in Figure 3.7. It can be observed that a second order polynomial gave a good regression analysis of about 99.95% (Figure 3.7).

This time-depth relationship (TDR) was used in the conversion of the time maps of the mapped horizons to depth structural maps.

The contouring was produced from connecting points of equal elevation (m) with an interval spacing of 25m. Points having the same or similar depth were identified having the same color and the depth value each color represents is shown in the color legends in (Figure 3.8 b).

Quality check of the depth map generated was done by comparing with the time maps. Most structures on the time maps were preserved on the depth maps after depth conversion. Traps were identified on the depth structural maps from the closures. Most of the traps are fault dependent while some are fault assisted closures.

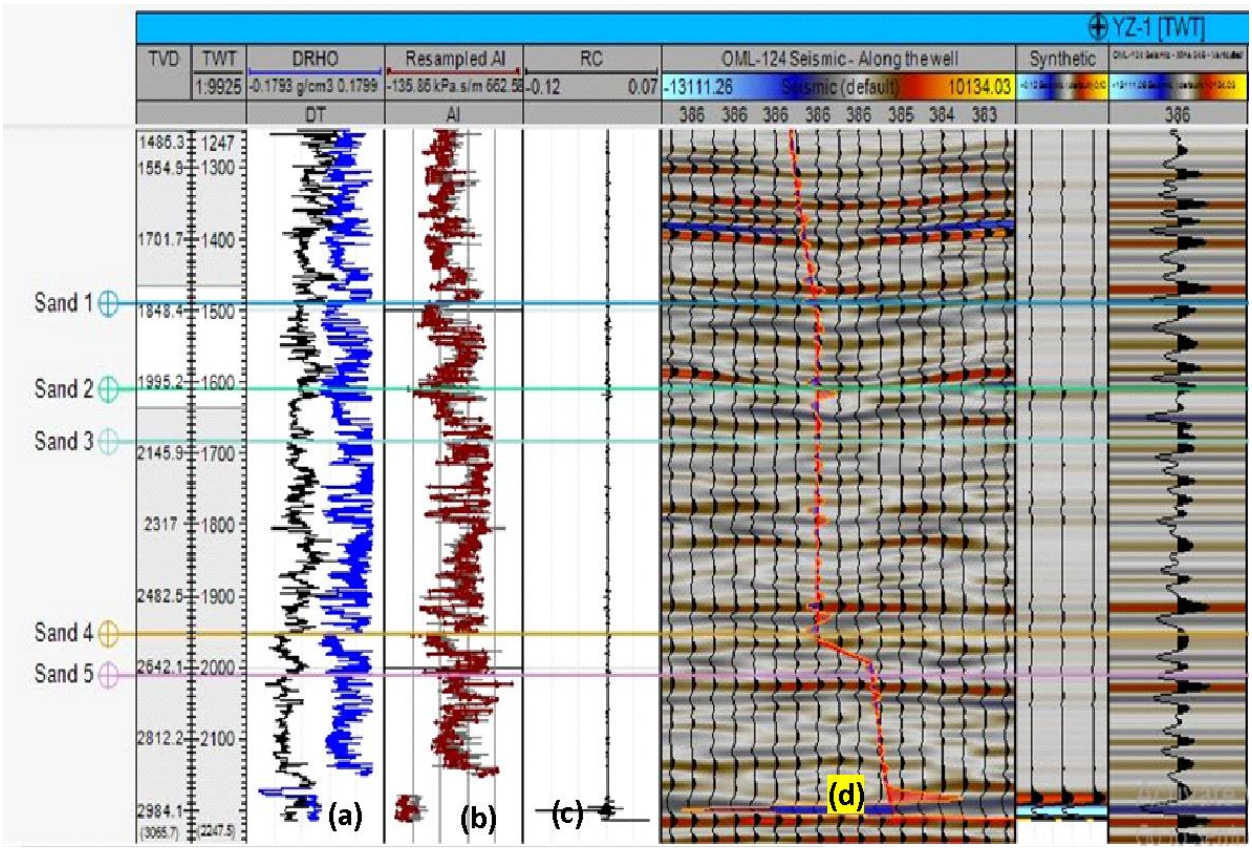

Figure 3.5 (a to d): Synthetic seismogram generated from (YZ well 1) sonic and density logs.

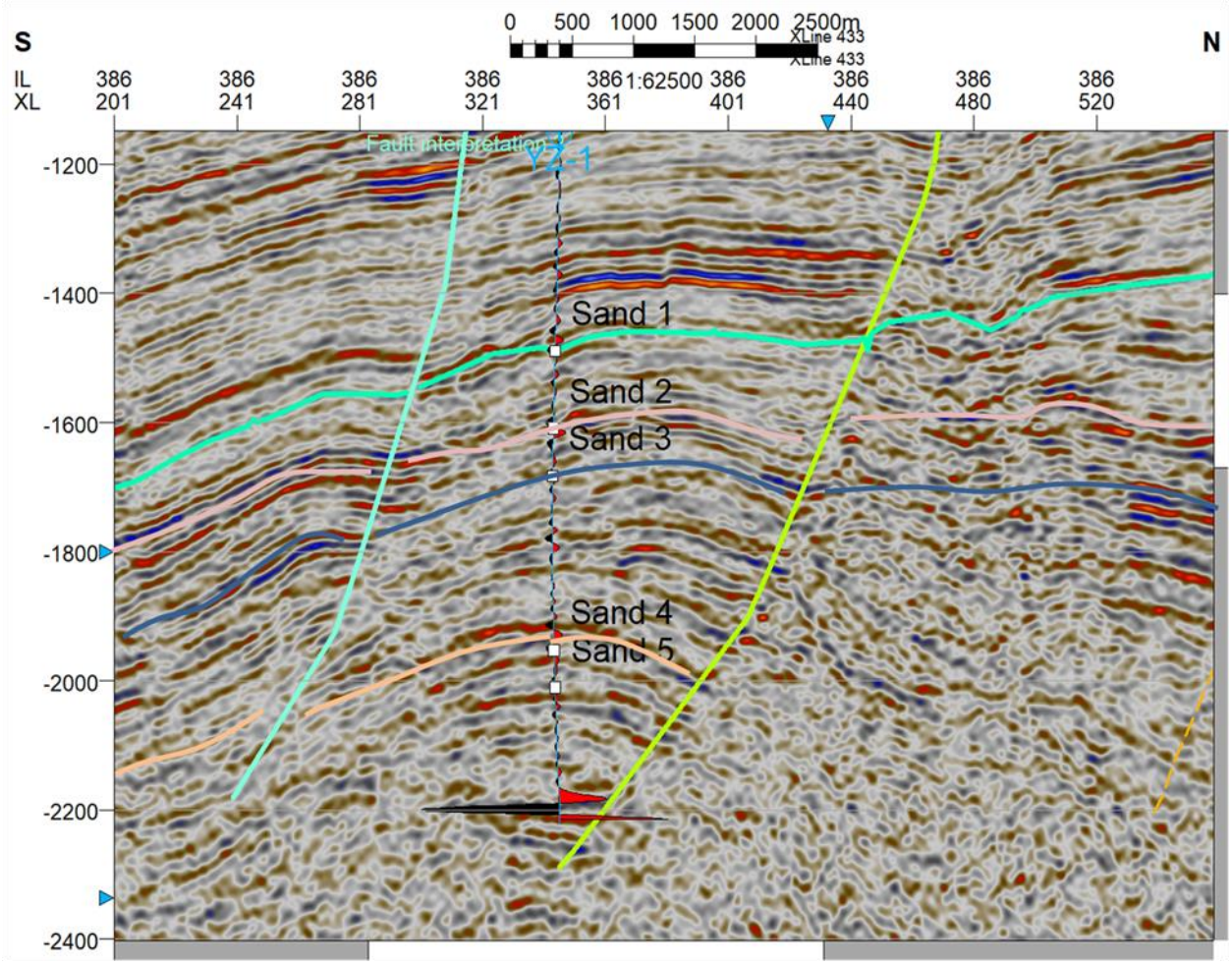

Figure 3.6: Interpretation window of inline 386 showing horizons picked on the well log showing the synthetic seismogram of YZ and the mapped well tops.

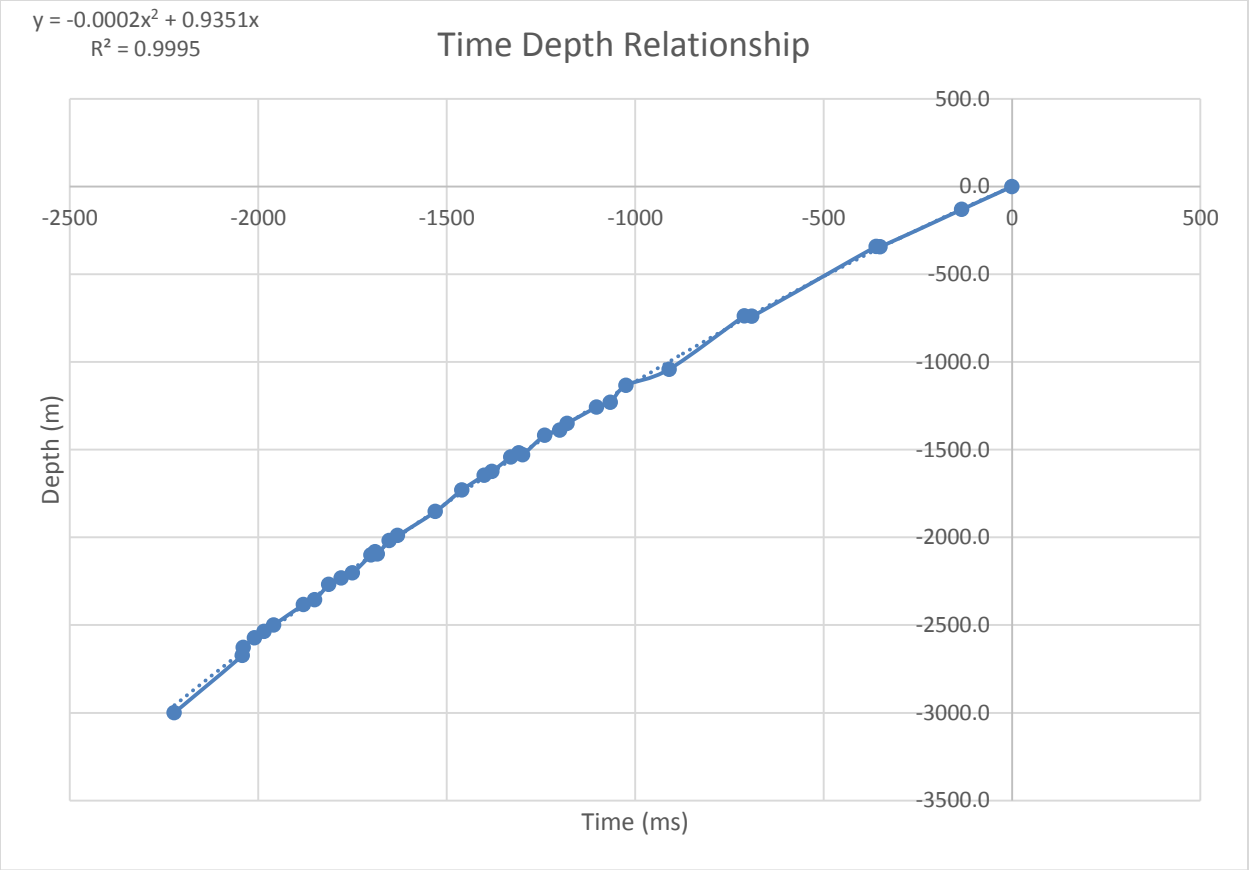

Figure 3.7: Graph showing the relationship between the time, x and the depth, y

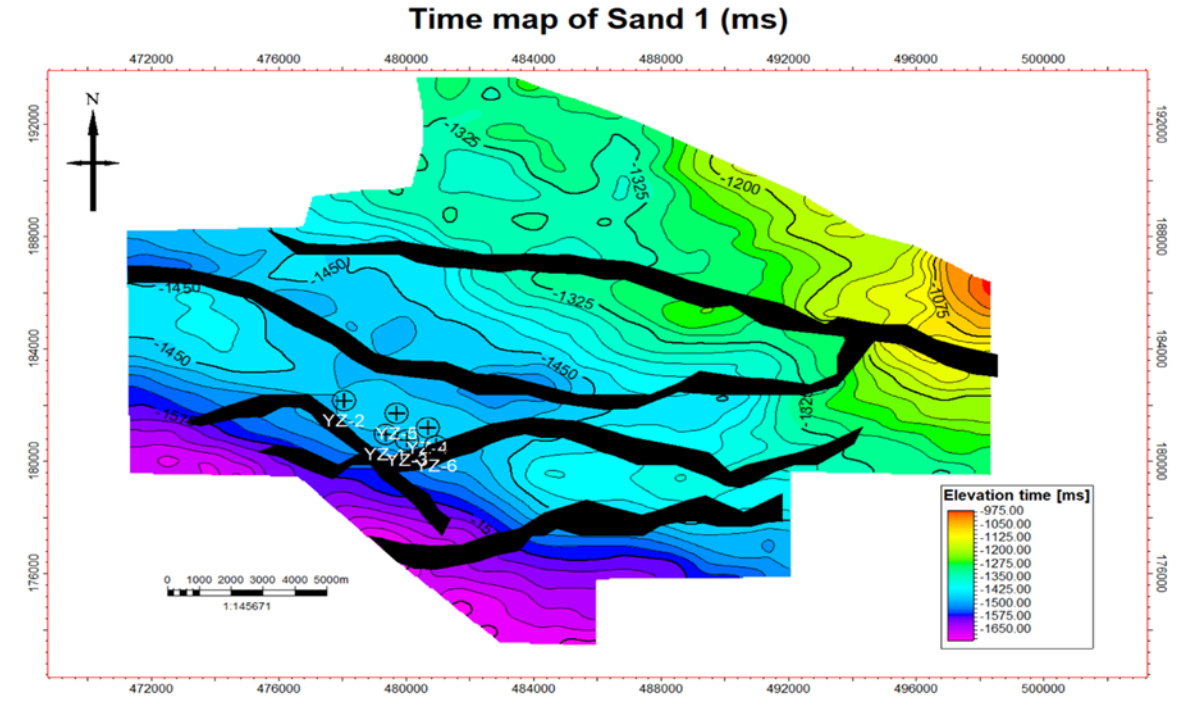

Figure 3.8a: Time map generated from sand 1.

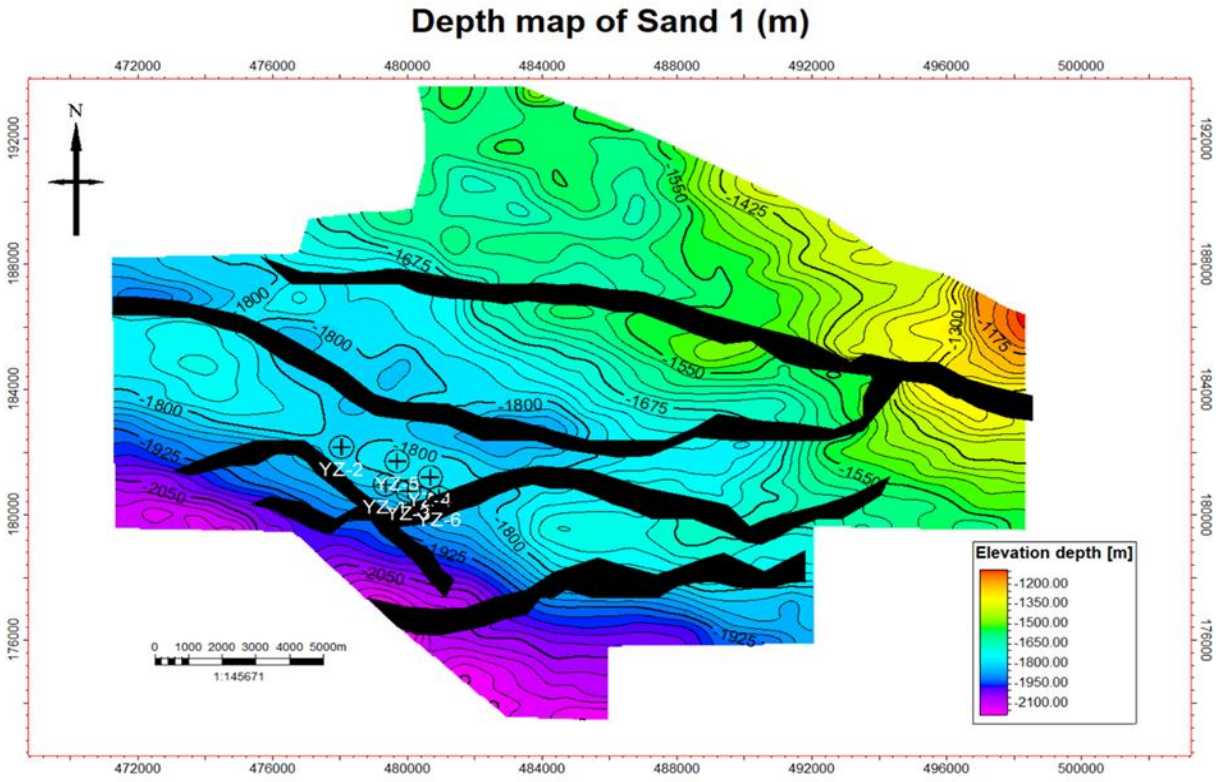

Figure 3.8b: Depth map generated from sand 1.

3.8 ATTRIBUTE ANALYSIS

Seismic attributes (RMS amplitude, sum of energy, maximum amplitude, average energy, sum of energy attribute) were extracted from the horizon/structural maps to enhance interpretation and ranking of identified prospects. Seismic attributes supported prospects were ranked higher than others as it may serve as a direct-hydrocarbon-indicator (Figure 3.9 a- 3.9 d).

3.9 FIELD RE-EVALUATION AND PROSPECT IDENTIFICATION

Hydrocarbon prospects were characterized by identifying areas with high elevation and the type of trapping configuration (four-way closure, fault assisted or fault dependent). These are regions that have not been drilled and may serve as new discoveries on YZ field.

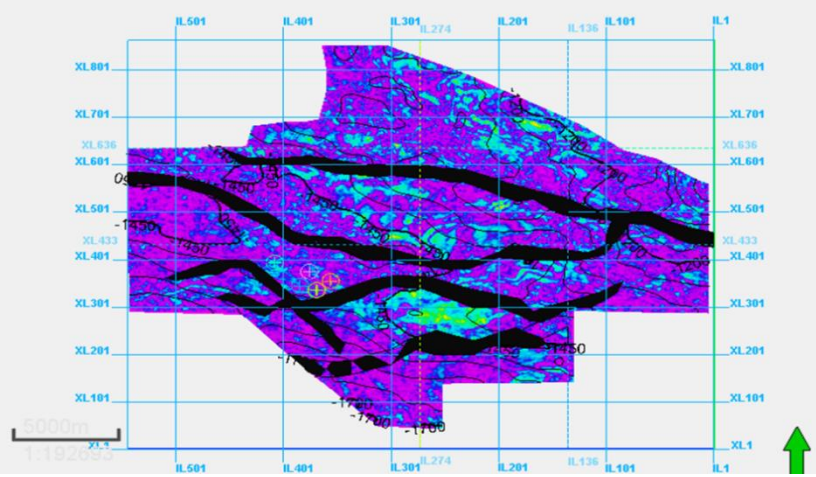

Figure 3.9a: RMS amplitude extracted from sand 1 time map

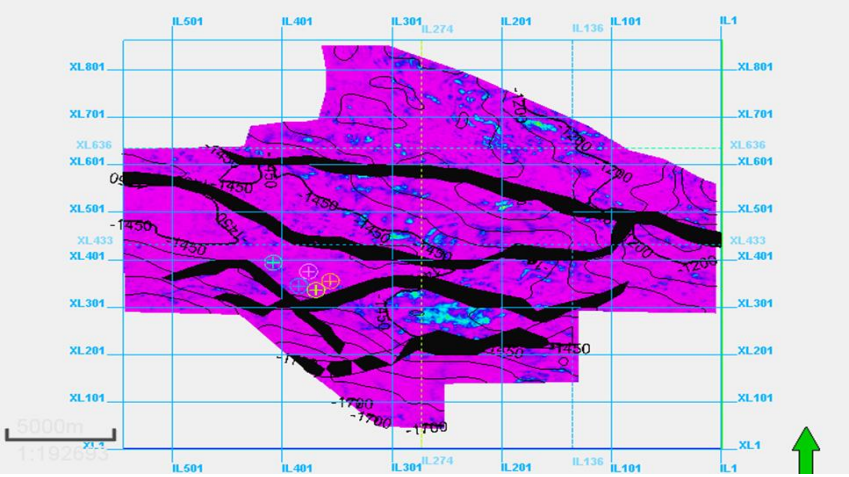

Figure 3.9b: Sum of energy amplitude extracted from sand 1 time map

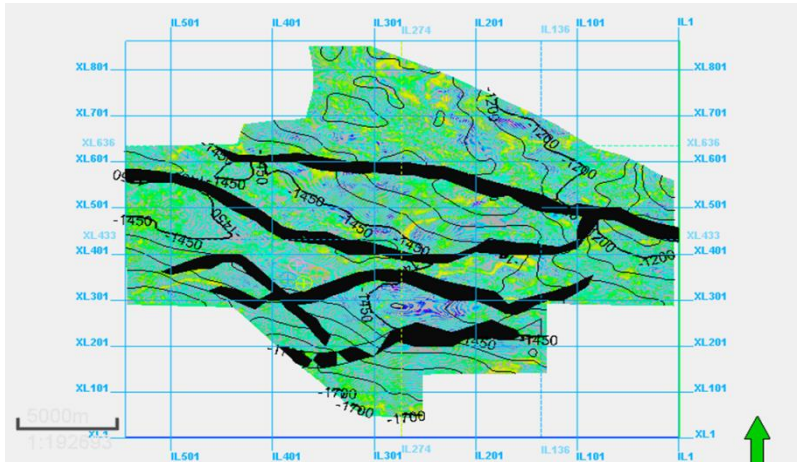

Figure 3.9c: Maximum amplitude extracted from sand 1 time map

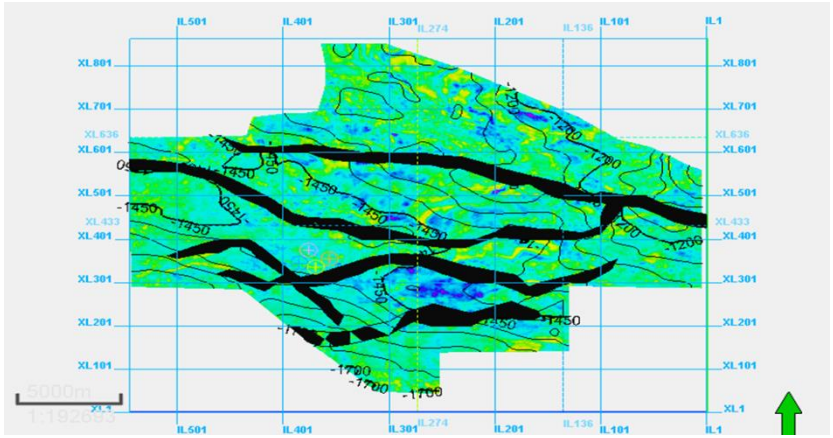

Figure 3.9d: Sum of amplitude extracted from sand 1 time map.

CHAPTER FOUR

4.0 RESULTS AND DISCUSSION

4. 1 RESULTS AND DISCUSSIONS OF THE PETROPHYSICAL EVALUATION

4.1.1 Result of petrophysical evaluation

The result of the petrophysical evaluation is summarized in Table 4.0. The result of the well log correlation including reservoir identification, hydrocarbon presence and type is presented for each of the identified reservoirs as well sections in Figures (4.1, 4.2 and 4.3).

4.1.2 Discussion of petrophysical evaluation

Five reservoirs have been identified across the available six well logs. The reservoirs are labeled Sand 1 to 5 as correlated across the wells in a North-South direction (Figure 4.0).

Sand 1: Sand 1 has a depth range of 1770m-1806m with a thickness range of 42m to 56m (Figure 4.1). The average porosity of this reservoir is about 22% and a net to gross of 80%. However, this reservoir was characterized by relatively low resistivity values (Figure 4.1, track two) which indicates no accumulation of hydrocarbon within this compartment of the reservoir on the field. Notwithstanding, this Sand was mapped on the entire 3D seismic to delineate its geometry and delineate other traps with possible hydrocarbon accumulation.

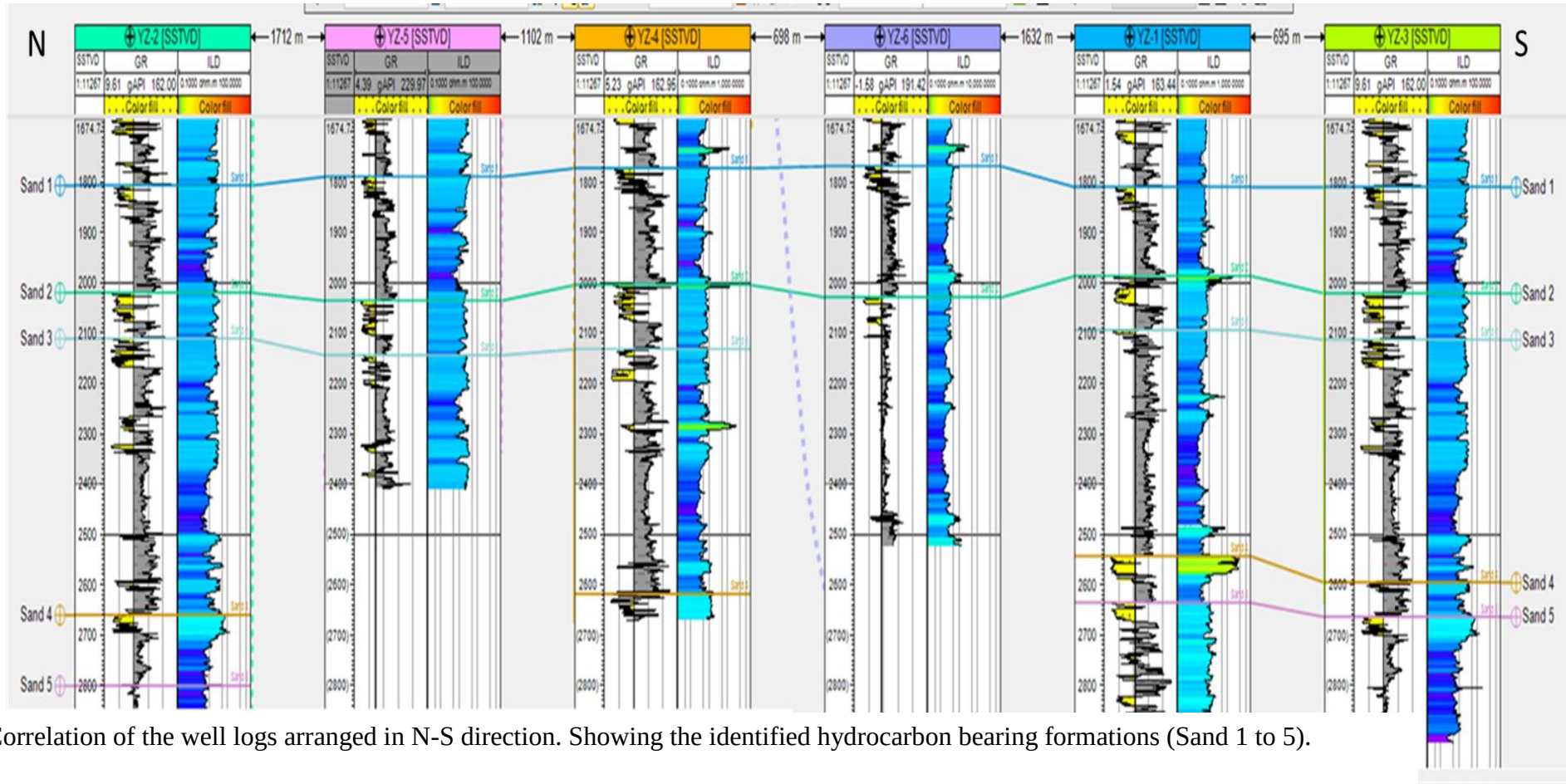

Figure 4.0: Correlation of the well logs arranged in N-S direction. Showing the identified hydrocarbon bearing formations (Sand 1 to 5).

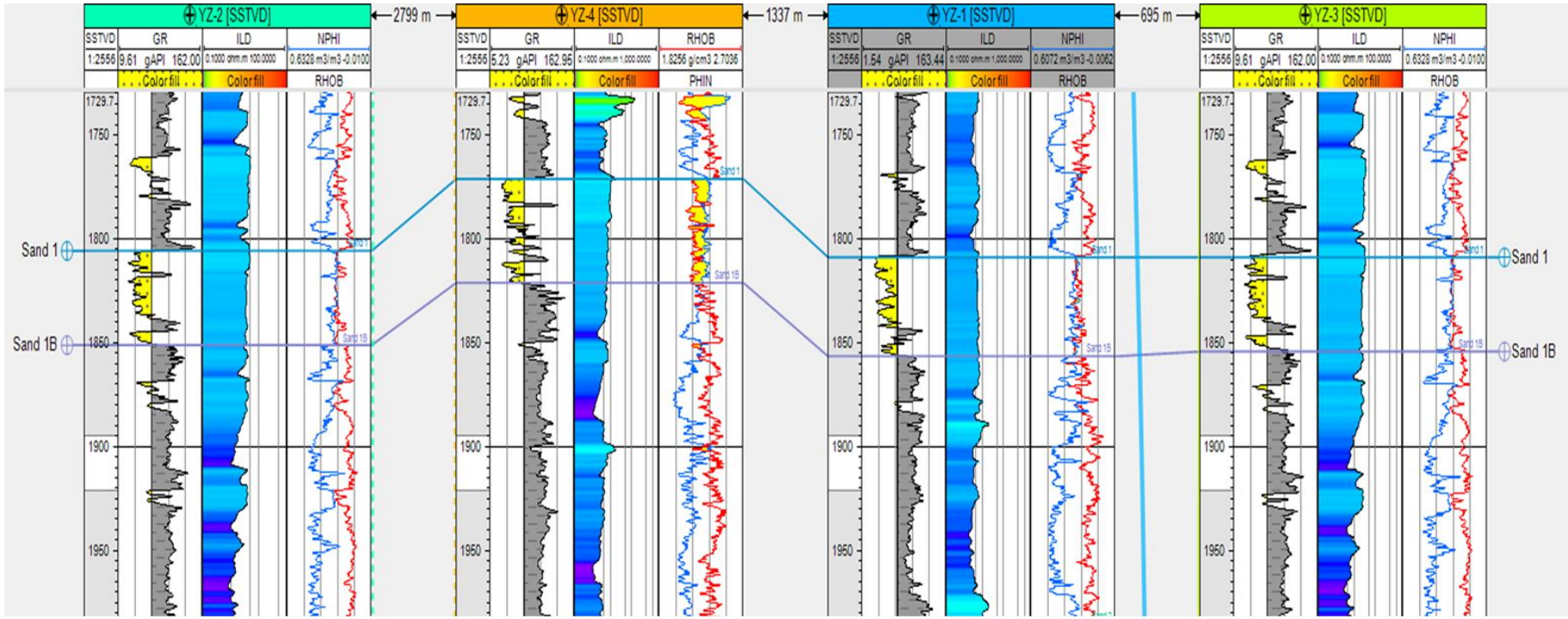

Figure 4.1: Well sections correlation for YZ sand 1 reservoir showing the top and base.

Sand 2: The result of Sand 2 is summarized in Table 4.0. This reservoir was encountered by the 6 wells in the YZ field. Sand 2 was encountered at a depth range of 1986 - 2018m with a thickness range of about 58 - 69m. An average porosity of about 18.6% and NTG of 75 % was computed for Sand 2 which portrays good reservoir properties.

Hydrocarbon presence is characterized by relatively high electrical resistivity signature on the deep resistivity log (Figure. 4.2, track 2). An overlay of the neutron (NPHI) and density (RHOB) log within this reservoir interval shows it has a 'balloon effect' which is typical behavior of hydrocarbon gas (Figure 4.2, track 3).

Sand 3 appeared in all the wells apart from well 6 this is because it is a sidetrack of well 4 (Figure 3.1). It was mapped at a depth range of 2092m-2112m with a thickness range of about 17m-65m in YZ well 1. The average porosity of this reservoir is about 20% and a net to gross of 76 %. However, it was characterized by relatively low deep resistivity values (Figure 4.2, track two) which indicates no accumulation of hydrocarbon within this compartment of the reservoir on the field.

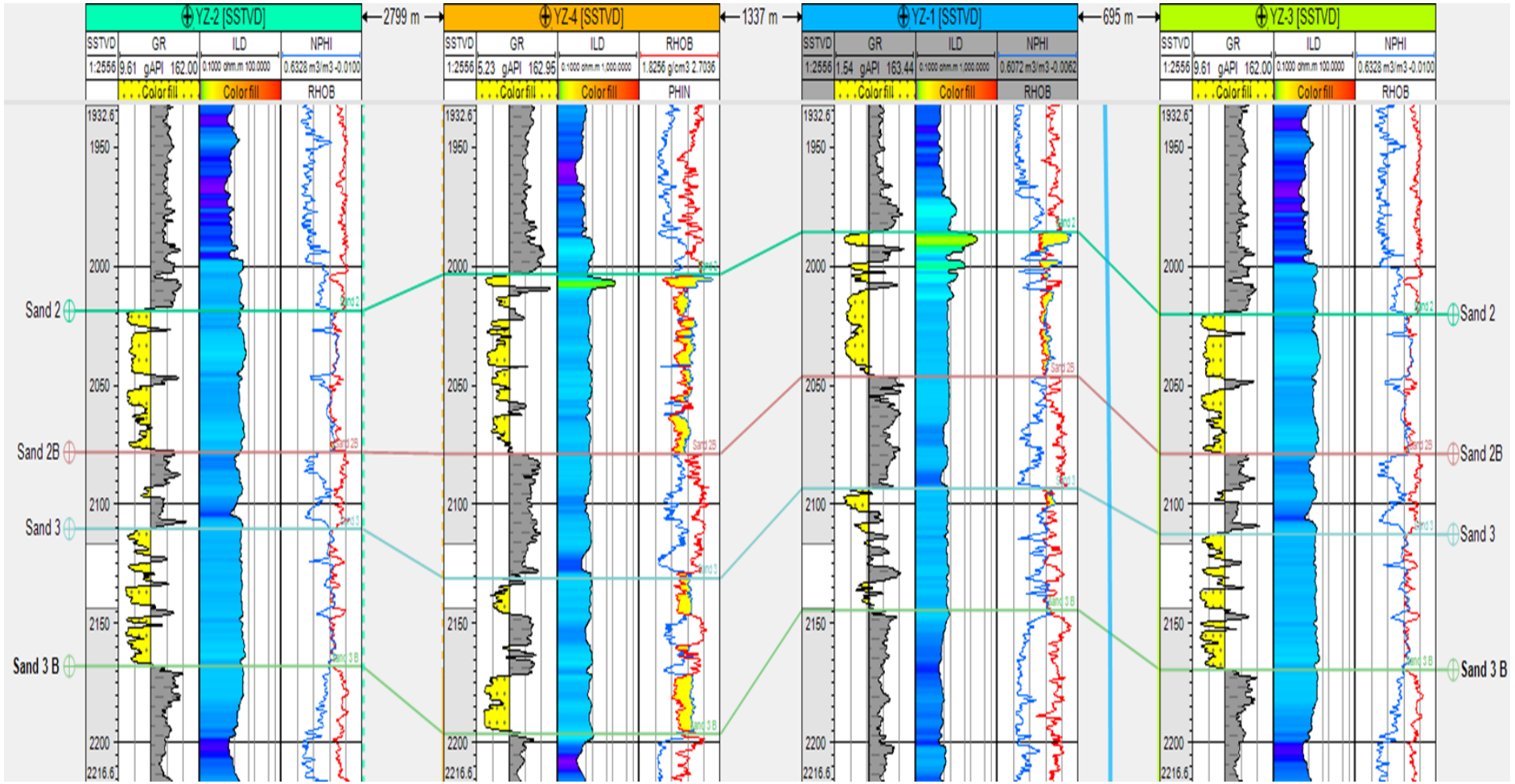

Figure 4.2: Well section correlation for YZ sand 2 and sand 3 reservoirs identifying the top and base.

Sand 4 was penetrated by wells 1, 2, 3 and 4 and it was encountered at a depth range of 2548 - 2660m with a thickness range of 37 - 43m. Sand 4 porosity ranges from 17% to 19% which is good for a hydrocarbon bearing reservoir while the NTG is about 90 % which is an excellent value for a hydrocarbon bearing reservoir this signifies the reservoir will inhibit minimum shale or clayey obstruction within the pores of the reservoir as this will increase the flow of hydrocarbon out of the reservoir. The deep resistivity log (Figure 4.3, Track 2) has indicated relatively high resistivity values within this reservoir and an Oil-Water-contact of 2572m was identified on Well 1 in this reservoir. Further analysis with an overlay of the neutron (NPHI) and density (RHOB) log (Figure 4.3, Track 3) has indicated that the hydrocarbon type is both oil and gas within this reservoir. There is a major separation on the Neutron – Density overlay ('balloon effect') which signifies gas at depth interval of 2542 to 2570 and both the density and neutron logs are tracking side by side which indicates the presence of hydrocarbon oil within depth of 2570 to 2590 (Figure 4.3, Track 3).

Sand 5 was penetrated by wells 1, 2, 3. Sand 5 was encountered at a depth range of about 2674m - 2799m with a thickness range of about 17 - 39.8m. The average porosity for sand 5 is 18% and the net to gross is about 97% which indicates very good reservoir properties. However, its deep resistivity log signature is characterized by relatively low resistivity values which indicates that there is no hydrocarbon accumulation within this reservoir (Figure 4.3, track 2). Meanwhile, this reservoir was mapped across the 3D seismic cube as hydrocarbon may be encountered within other compartments or traps on the field.

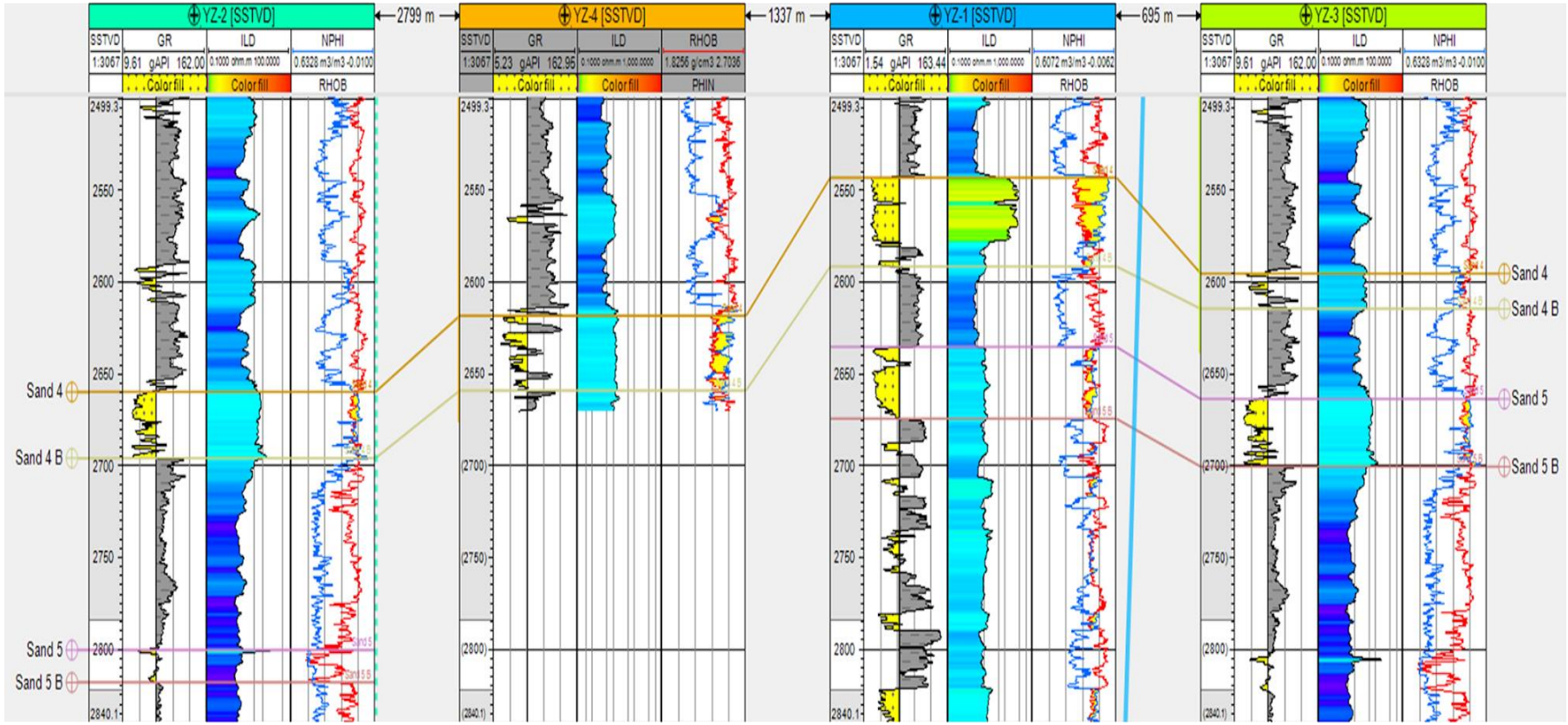

Figure 4.3: Well section correlation for YZ sand 4 and sand 5 reservoirs identifying the top and base.

Summary of Petrophysical Results

A summarized table of the petrophysical properties encountered in the four reservoirs is summarized in (Table 4.0).

Effective porosity values range from a value of about 17 to 20% which is very good and typical porosity range in the Niger Delta basin (Tertiary siliciclastic reservoirs).

NTG across the identified reservoirs ranges 76 to 90% which is within the good to excellent range. This signifies how clean the reservoir is as the lower the percentage of shale/shaliness the easier hydrocarbon fluids will improve recovery of the hydrocarbon during production.

Table 4.0: Summarized petrophysical properties of all the reservoirs

Reservoir	Interval (m)	Hydrocarbon Type	Pay thickness (m)	Net/Gross	Porosity	Hydrocarbon Saturation
Sand 1	1770 - 1806	-	39	80%	22.2%	65%
Sand 2	1986 - 2018	gas	16	78%	20.6%	66%
Sand 3	2092 - 2112	-	2.9	76%	22.1%	57%
Sand 4 gas	2542 - 2570	gas	25.5	95%	19.6%	76%
Sand 4 oil	2570 - 2590	oil	11.3	95%	18.2%	58%
Sand 5	2674 - 2799	oil	38.6	97%	18%	-

4.2 HORIZONS (TIME AND DEPTH STRUCTURAL MAPS)

The 3D view of all the reservoir surfaces (time maps) generated from the mapped horizons in YZ field is presented in Figure 4.4.

Sand 1: The time structural map is presented in Figure 4.5a and the depth structural map in Figure 4.5b. Other than the drilled trap, four prospective traps have been identified on the mapped reservoir (Figure 4.5b). The tested trap on this reservoir can be classified as a fault dependent trap. It is noteworthy that hydrocarbon accumulation was not observed on the wells drilled within this trap. The dry hole encountered may be associated to be possibility that the fault may not be sealing and might have resulted in further migration of hydrocarbon within this trap. Prospect 2 and 3 are similarly fault dependent traps and the accumulation of hydrocarbon within this reservoir is therefore dependent on the sealing or non-sealing status of the fault.

On the other hand, it can be observed that Prospect 1 and 4 are fault assisted closures and may have higher chances or possibility of hydrocarbon accumulation. The result of seismic attribute analysis carried out on this surface is presented in Figure 4.6a to d. It can be observed that Prospect 1 is attribute supported and therefore ranked the highest of the four prospects, followed by Prospect 4, 2 and 3 respectively.

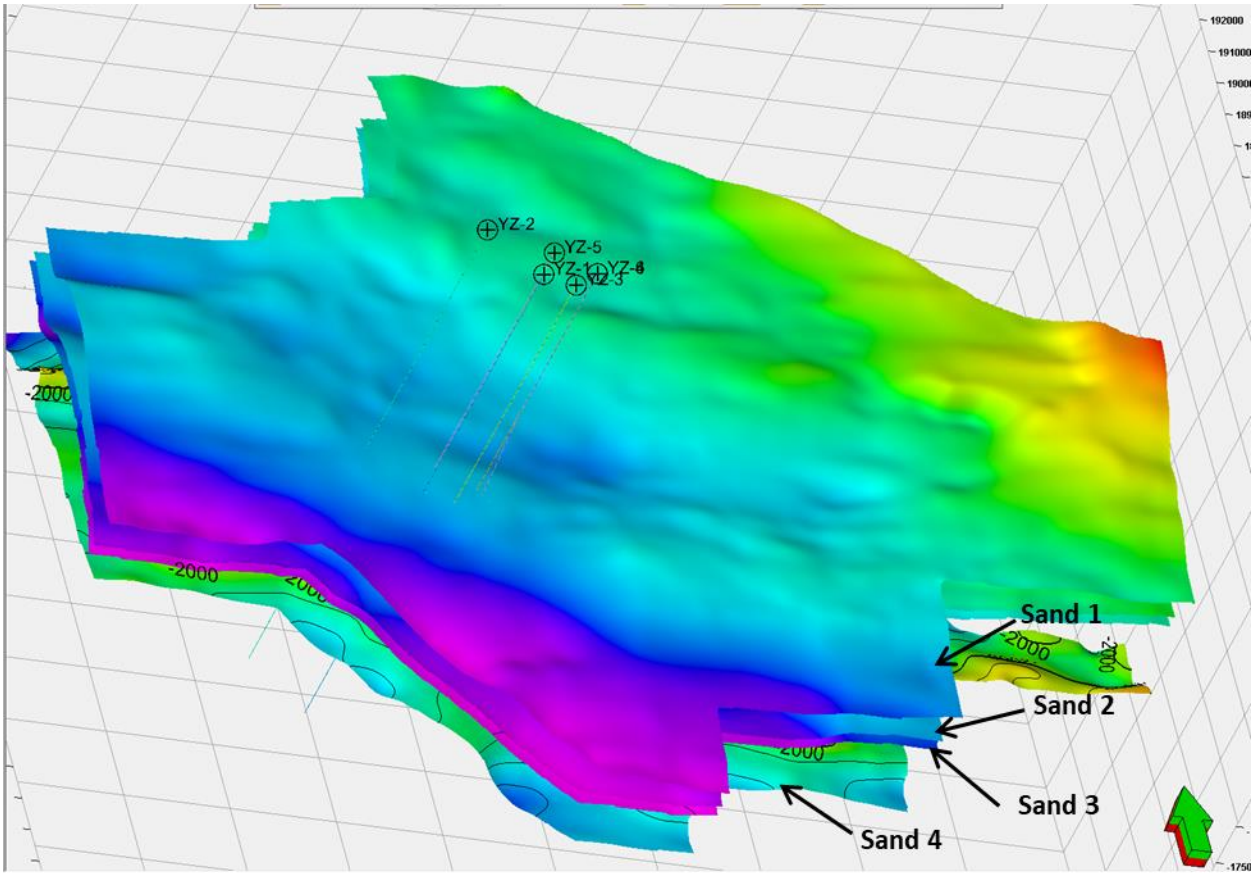

Figure 4.4: 3D view of the four horizons mapped on seismic labeled Sand 1 to 4 respectively.

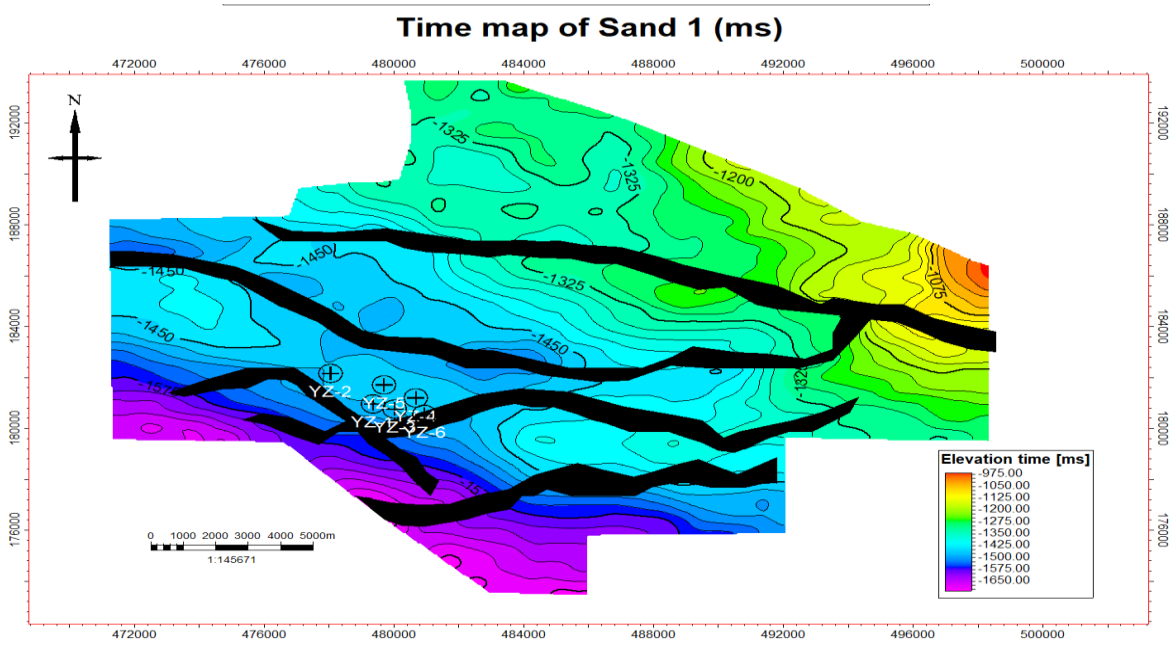

Figure 4.5a: Time structure map for sand 1.

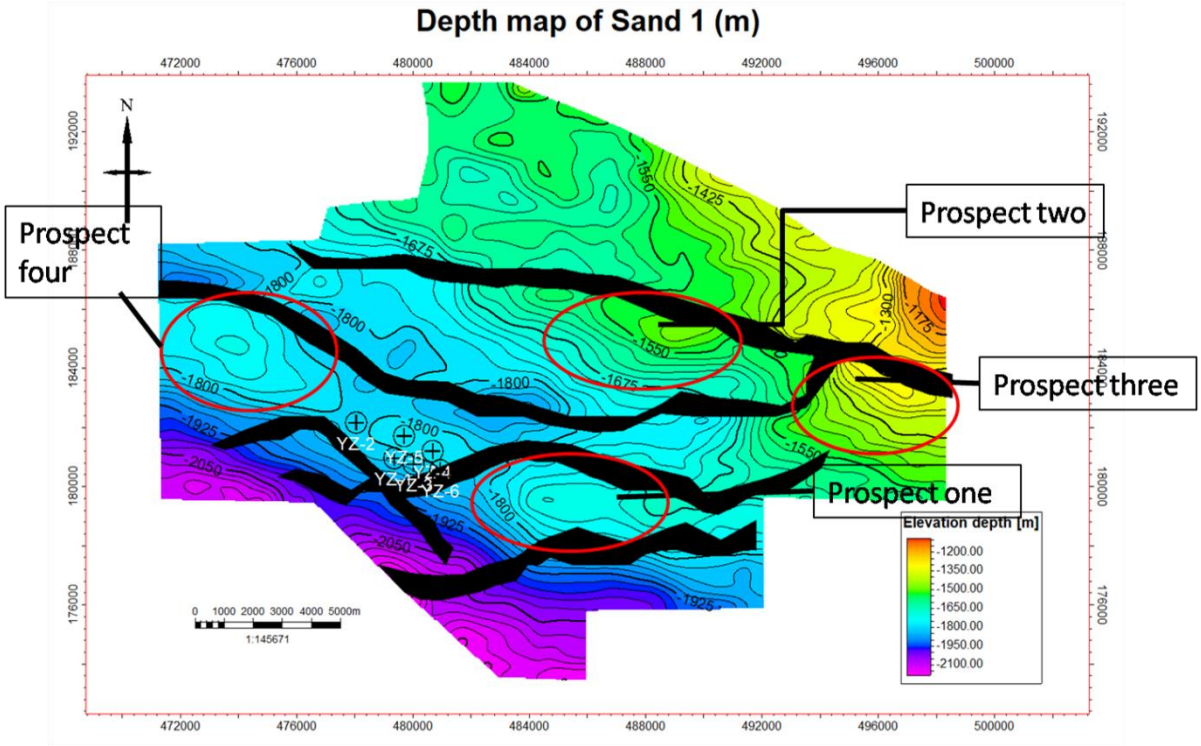

Figure 4.5a: Depth structure map for sand 1 showing the showing the various prospects in YZ field.

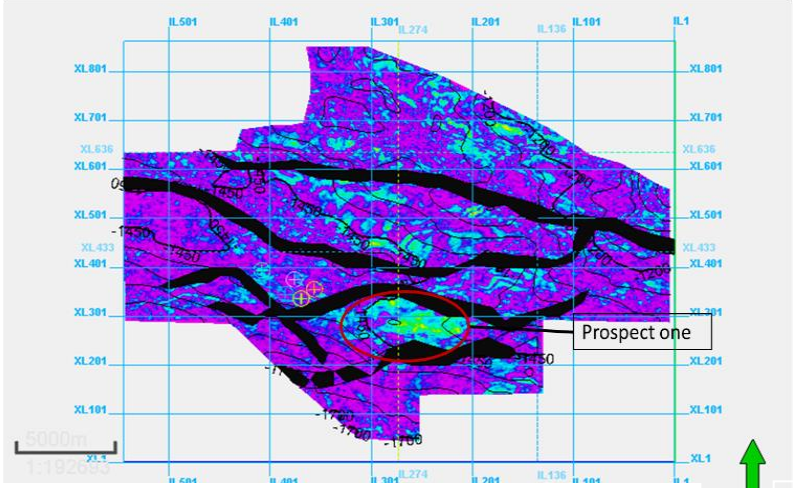

Figure 4.6a: Time map showing RMS amplitude seismic attribute on sand 1

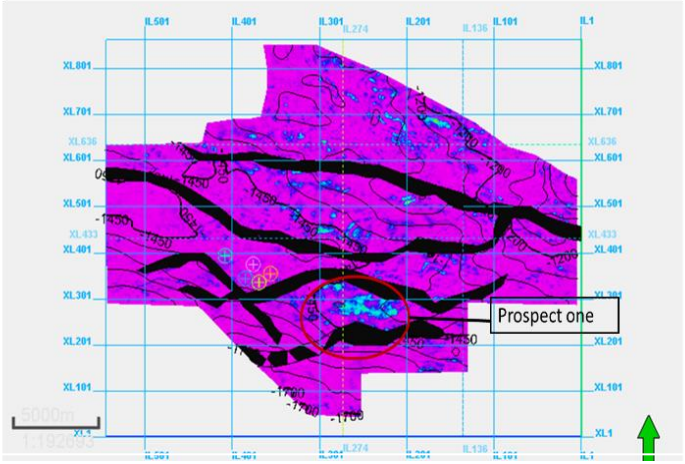

Figure 4.6b: Time map showing sum of energy attribute on sand 1.

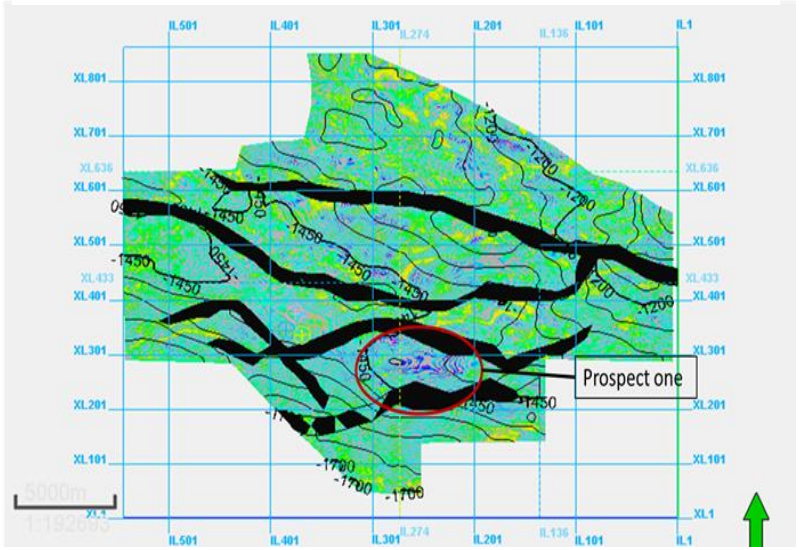

Figure 4.6c: Time map showing maximum amplitude attribute on sand 1.

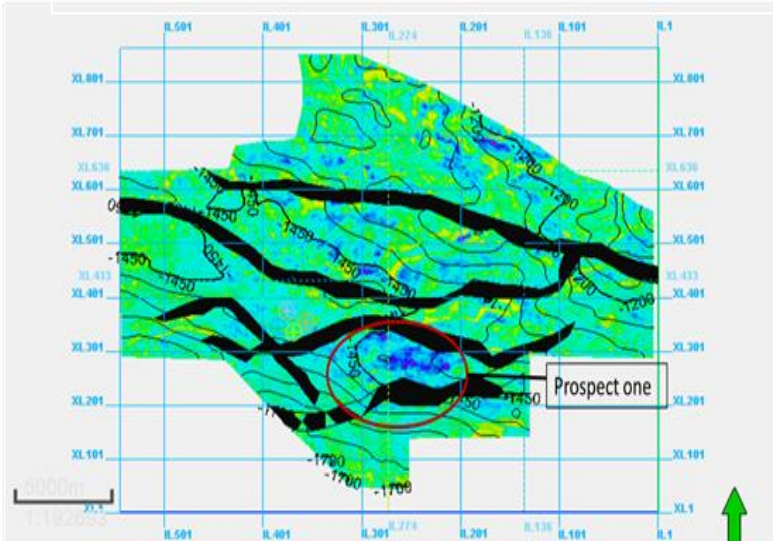

Figure 4.6d: Time map showing sum of amplitude attribute on sand 1.

Sand 2: The time structural map is presented in Figure 4.7a and the depth structural map in Figure 4.7b. Three prospective traps have been identified on the mapped reservoir (Figure 4.7b). The tested trap on this reservoir can be classified as a fault assisted trap. Similarly, Prospect 2 is a fault assisted trap while Sand 3 and 4 are fault dependent traps.

The result of seismic attribute analysis carried out on this surface is presented in Figure 4.8a to d. The seismic attribute which was extracted from sand 2 further supports the presence of hydrocarbon in the tested area of the horizon due to the relatively bright amplitude anomalies expressed by the trap (Figure 4.8a-Figure 4.8d).

However, the prospects within Sand 2 does not exhibit amplitude anomaly and may have higher risk of discovering substantial hydrocarbon accumulation (Figure 4.8a- Figure 4.8d). Prospect 1, is ranked highest because it is a fault assisted closure while prospect 3 and 2 are ranked next respectively partly due to their sizes and being fault dependent closures which are at higher risk of migration of accumulated hydrocarbon.

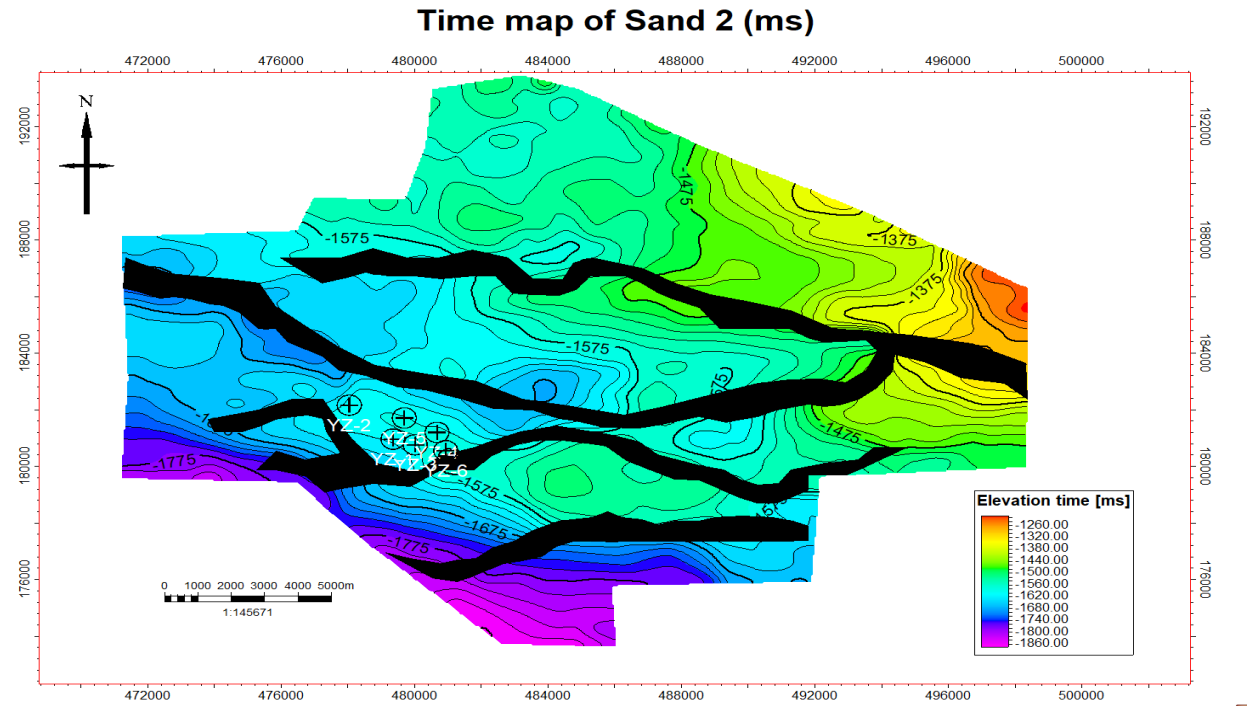

Figure 4.7a: Time structure map for sand 2.

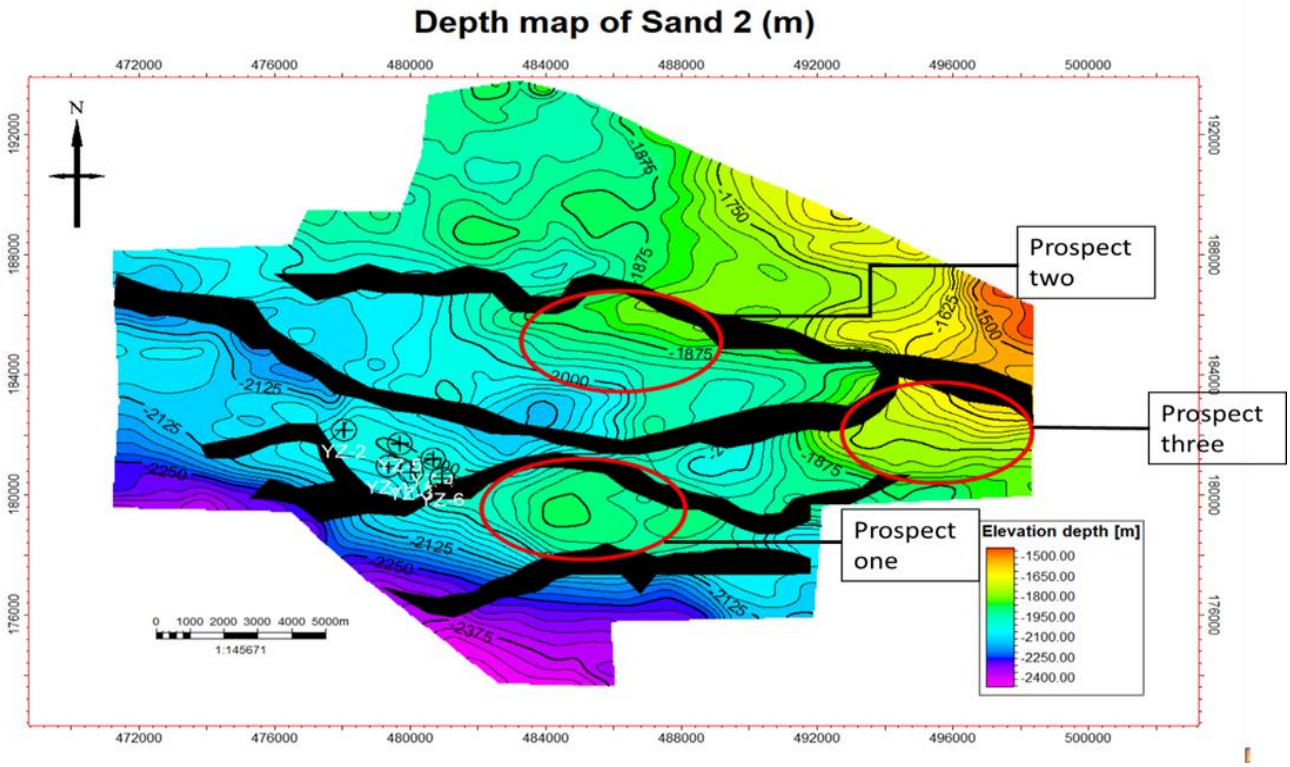

Figure 4.7b: Depth structure map for sand 2 showing the various prospects in YZ field.

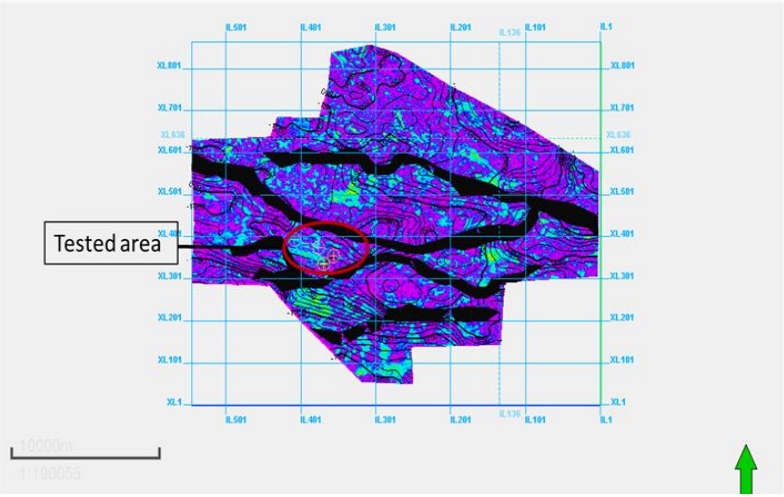

Figure 4.8a: Time map showing RMS amplitude seismic attribute on sand 2.

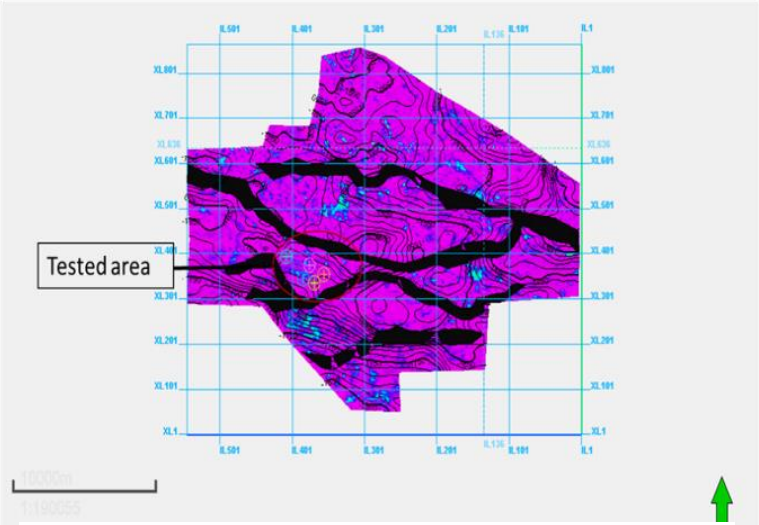

Figure 4.8b: Time map showing sum of energy attribute on sand 2.

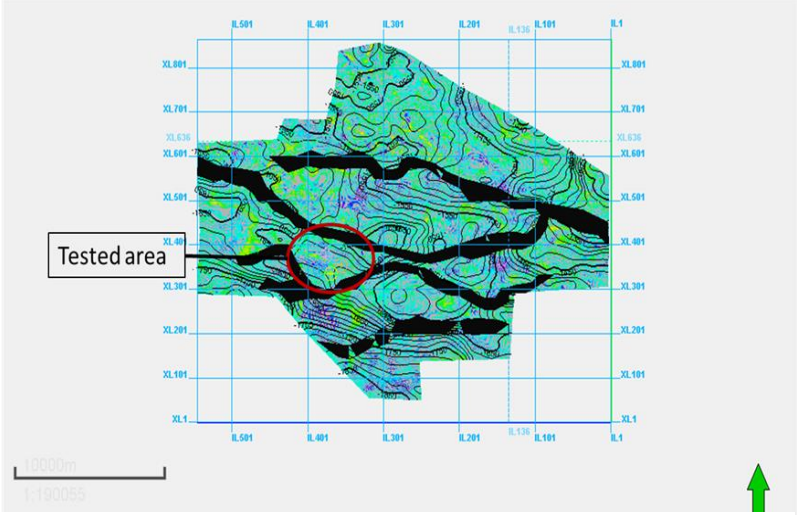

Figure 4.8c: Time map showing maximum amplitude attribute on sand 2.

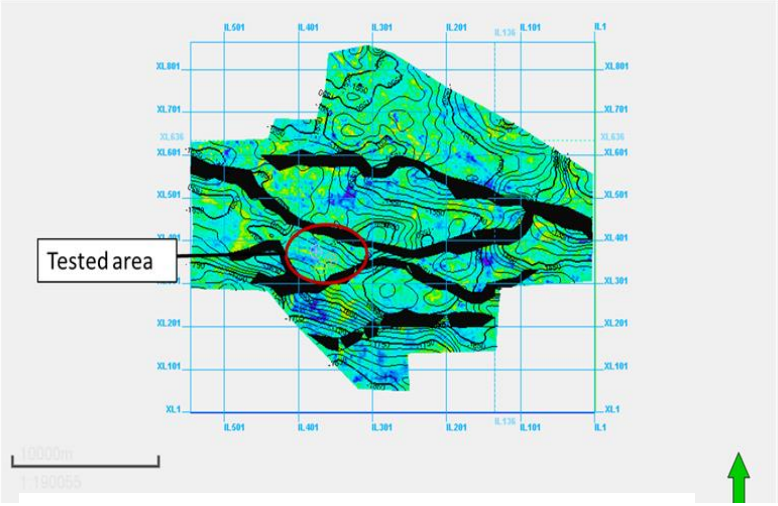

Figure 4.8d: Time map showing sum of amplitude attribute on sand 2.

Sand 3: The time structural map is presented in Figure 4.9a and the depth structural map in Figure 4.9b. Other than the drilled trap, three prospective traps have been identified on the mapped reservoir (Figure 4.9b). The tested trap on this reservoir can be classified as a fault dependent trap. It is noteworthy that hydrocarbon accumulation was not observed on the wells drilled within this trap. The dry hole encountered may be associated to the possibility that the fault may not be sealing and might have resulted in further migration of hydrocarbon away from this trap. Seismic attribute analysis such as RMS amplitude, Maximum amplitude, Sum of energy and sum of amplitude (Figure 4.10a –Figure 4.10d) which was extracted from the reservoir surface has equally not display significant amplitude anomalies. Similarly, none of the prospects have shown significant amplitude anomalies from the seismic attribute analysis.

Nevertheless, Prospect 1 is ranked the highest prospect as it is a fault assisted closure and at a lesser risk of hydrocarbon accumulation when the faults are non-sealing. Prospect 2 and 3 are fault dependent traps and the accumulation of hydrocarbon within this reservoir is therefore dependent on the sealing or non-sealing status of the fault.

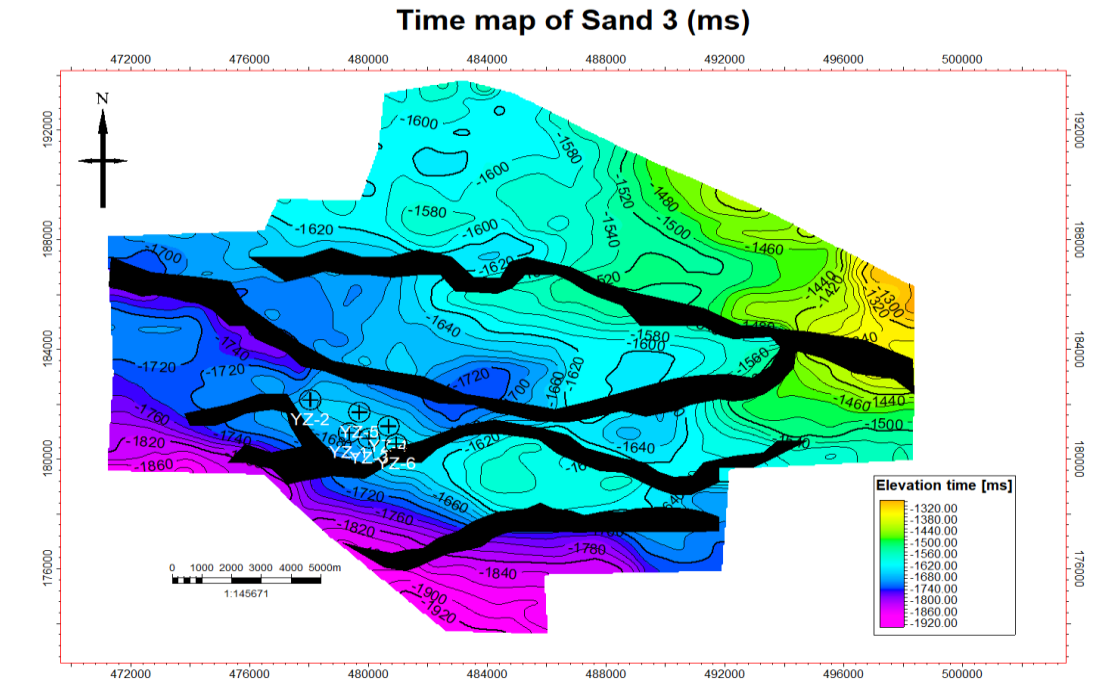

Figure 4.9a: Time structure map for sand 3.

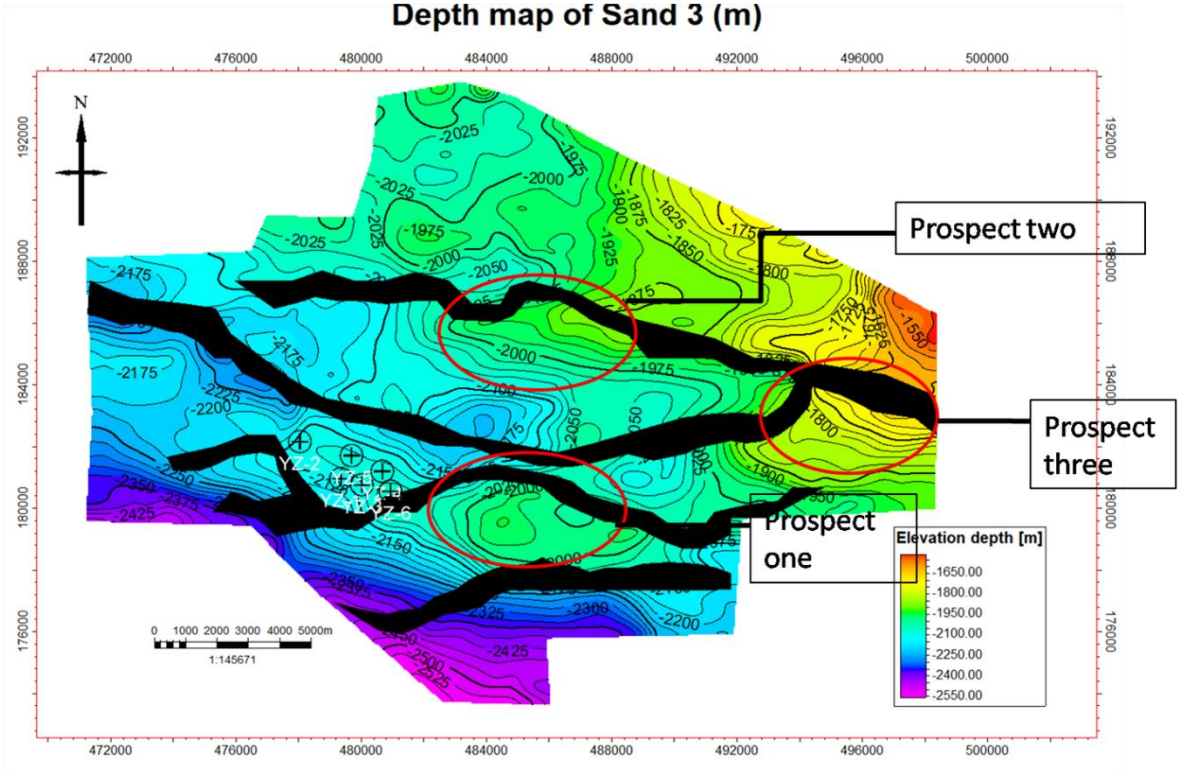

Figure 4.9b: Depth structure map for sand 3 showing the various prospects in YZ field.

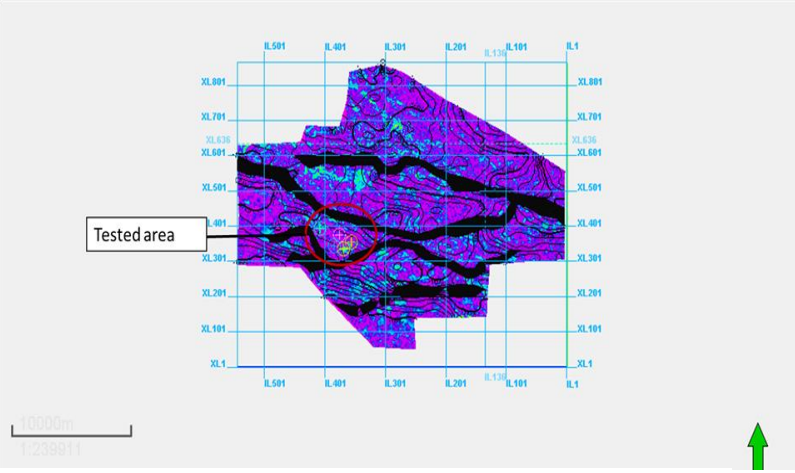

Figure 4.10a: Time map showing RMS amplitude seismic attribute on sand 3.

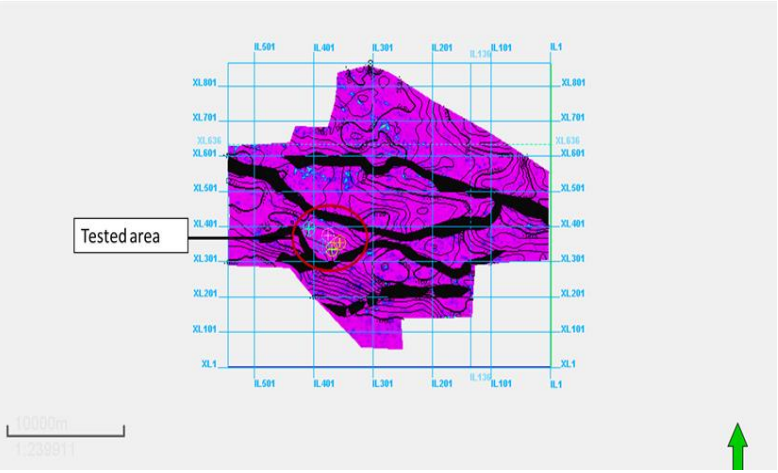

Figure 4.10b: Time map showing sum of energy attribute on sand 3.

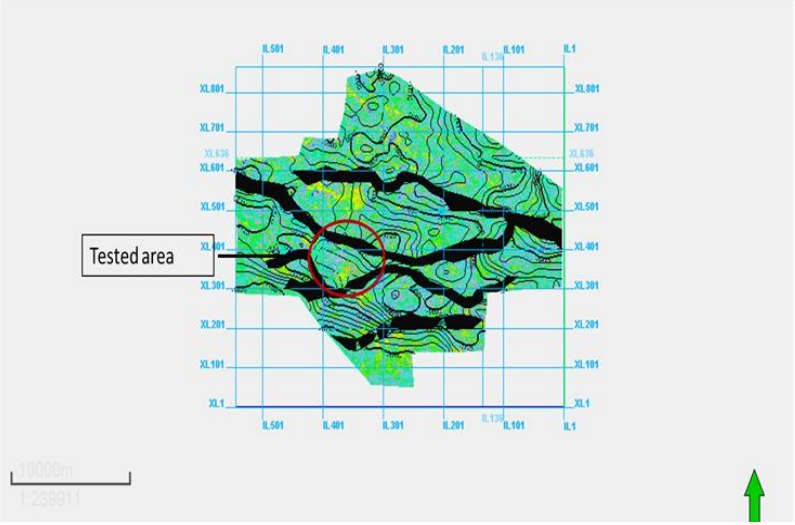

Figure 4.10c: Time map showing maximum amplitude attribute on sand 3.

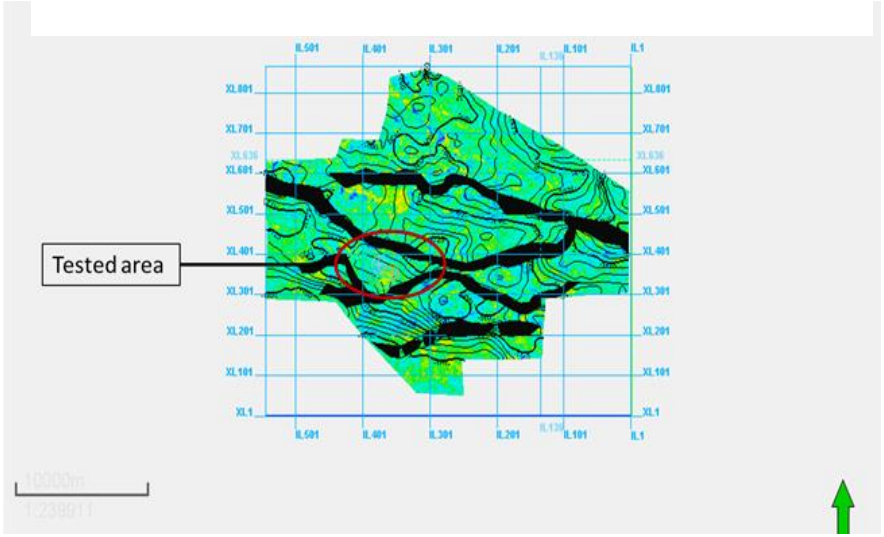

Figure 4.10d: Time map showing sum of amplitude attribute on sand 3.

Sand 4: The time structural map is presented in Figure 4.11a and the depth structural map in Figure 4.11b. Unlike other surfaces, the NE section of Sand 4 could not be mapped due to extremely chaotic seismic reflections (Figure 4.11a). The chaotic reflections exhibited by these seismic reflections could be due to shale diaperism.

Four prospective traps have been delineated on the mapped reservoir (Figure 4.11b). The tested trap on this reservoir can be classified as a fault dependent trap. All the prospects on this reservoir are similarly fault dependent traps and the accumulation of hydrocarbon within this reservoir is therefore dependent on the sealing or non-sealing status of the fault.

Seismic attribute analysis such as RMS amplitude, Maximum amplitude, Sum of energy and sum of amplitude (Figure 4.12a –Figure 4.12d) which was extracted from the reservoir surface has shown significant amplitude anomalies.

However, the prospects within Sand 4 does not exhibit amplitude anomaly and may have higher risk of discovering substantial hydrocarbon accumulation (Figure 4.12a- Figure 4.12d). The prospects are ranked based on their sizes. Prospect 1 is ranked the highest, followed by Prospect 3a/3b and Prospect 2.

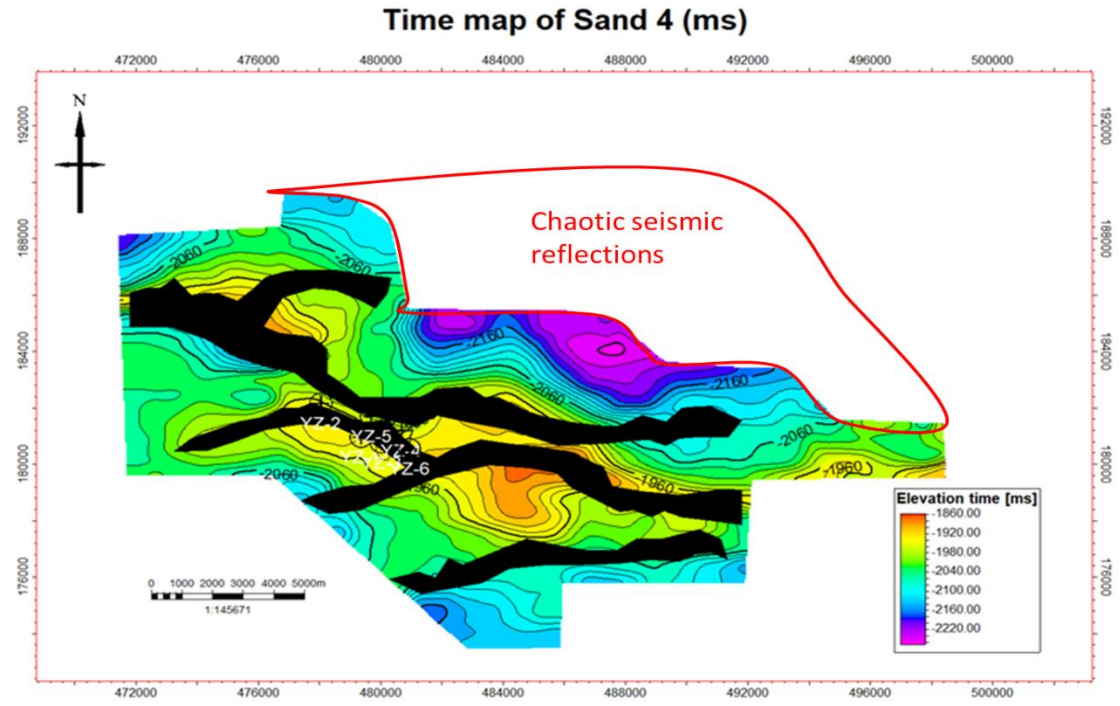

Figure 4.11a: Time structure map for sand 4 showing the area with chaotic seismic reflections.

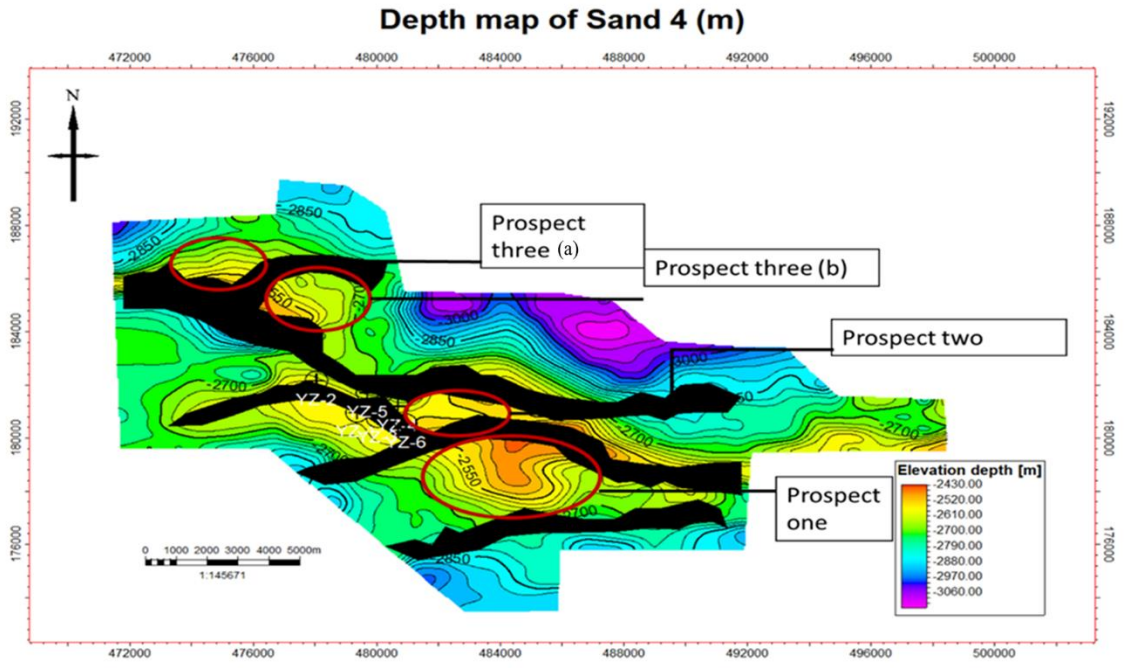

Figure 4.11b: Depth structure map for sand 4 showing the various prospects in YZ field.

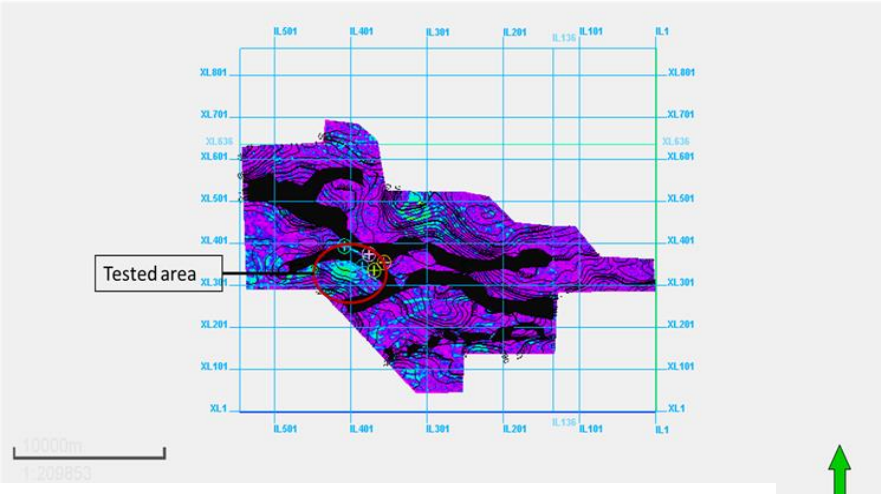

Figure 4.12a: Time map showing RMS amplitude seismic attribute on sand 4.

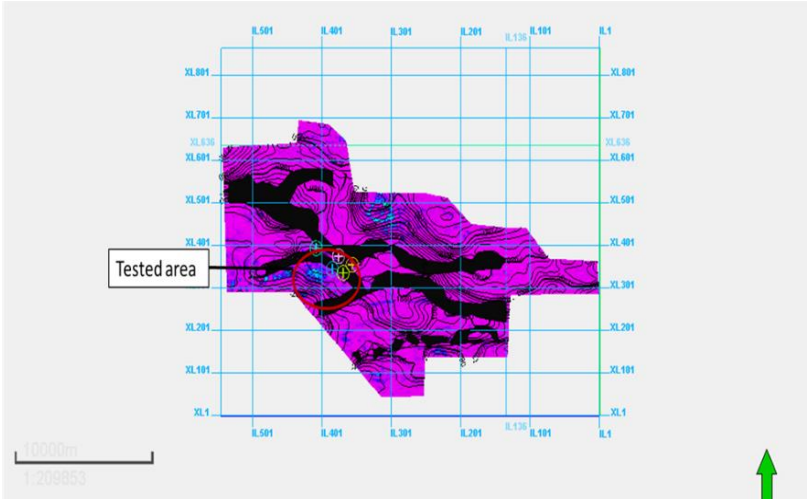

Figure 4.12b: Time map showing sum of energy attribute on sand 4.

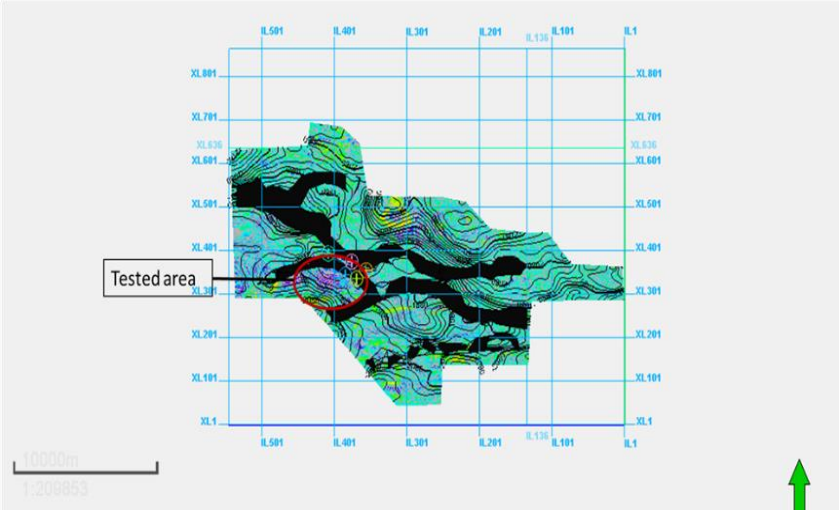

Figure 4.12c: Time map showing maximum amplitude
a

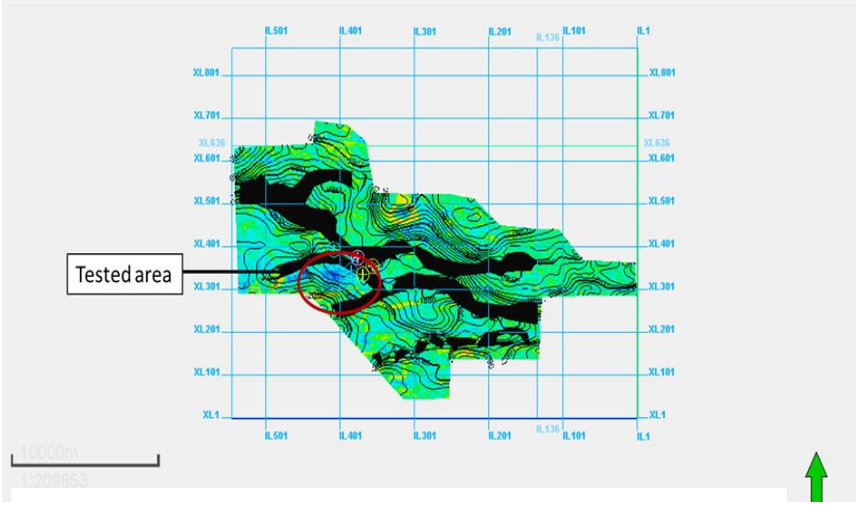

Figure 4.12d: Time map showing sum of amplitude attribute on sand 2.

4.3 VOLUMETRIC ESTIMATIONS OF HYDROCARBON IN PLACE

Volumetric and area estimates of the prospects for sand 1, 2, 3 and 4 was calculated and presented in table 4.1. The total hydrocarbon in place for YZ field is 427,648,602stb.

Sand 1: From the estimated petrophysical properties for sand 1 the expected range for the volume of hydrocarbon in place for the identified prospects ranges from 14,489,265.3stb-66,684,092stb.

The total prospective hydrocarbon in place for this reservoir is 156,119,278stb for all the prospects.

Sand 2: After relevant petrophysical analysis was conducted it was discovered that sand 2 contains dominantly gas and the volume of the hydrocarbon gas in place (GIIP) ranges from 8,592,312 scf to 38,457,838scf. The total hydrocarbon gas in place for this reservoir is 100,203,044scf.

Sand 3: Wells logs encountering sand 3 did not identify any hydrocarbon. However volumetric estimations were calculated for the sand 3 prospects from the estimated petrophysical properties for sand 3 the expected range for the volume of hydrocarbon in place for the identified prospects ranges from 3,062,490stb- 4,654,836stb. The total prospective hydrocarbon in place for this reservoir is 11,022,330stb for all the prospects.

Sand 4: From the petrophysical analysis, this reservoir contains both gas and oil the range of the volume of oil is about 6,503,725stb- 15,007,804stb and the volume of gas ranges from 16,360,138 scf-57,049,834 scf. The total gas in place for this reservoir is 126,916,646scf while the total oil in place is 33,387,305stb.

Table 4.1: Volumetric estimations of the various prospects for each map

		TESTED	PROSPECT ONE	PROSPECT TWO	PROSPECT THREE	PROSPECT FOUR	GRAND TOTAL (stb/scf
Sand 1	Area (m^2)	-	11,639,682	21,950,273	13,030,122	4,769,403.3	-
	STOIIP (stb)	-	35,360,909.8	66,684,091.9	39,585,013.5	14,489,265.3	156,119,278
	GIIP (scf)	-	-	-	-	-	-
Sand 2	Area (m^2)	5,032,756.7	17,520,710	22,525,827	13,612,419	-	-
	STOIIP (stb)	-	-	-	-	-	-
	GIIP (scf)	8,592,312.5	29,912,714.86	38,457,838.76	23,240,177.37	-	100,203,044
Sand 3	Area (m^2)	-	13,976,733	19,685,118	12,951,149	-	-
	STOIIP (stb)	-	3,305,004.131	4,654,835.741	3,062,489.707	-	11,022,330
	GIIP (scf)	-	-	-	-	-	-

Sand 4	Area (m^2)	6,733,694.7	15,538,476	7,839,741.9	4,455,957.2	-	-
	STOIIP (stb)	6,503,725	15,007,804.62	7,571,998.355	4,303,776.964	-	33,387,305
	GIIP (scf)	24,722,899	57,049,834.73	28,783,773.88	16,360,138.65	-	126,916,646

CHAPTER FIVE

5.0 CONCLUSION AND RECOMMENDATION

5.1 Conclusion

Well log analysis and 3D seismic data interpretation of YZ field, Niger Delta was carried out for hydrocarbon characterization and additional prospect identification. To this end, the 3D migrated seismic data and the six composite well logs were loaded into the Petrel software. It was observed that all the wells were drilled around the south western part of the 3D seismic data and a large expanse of the 3D seismic data have not been penetrated by wells.

The well logs were correlated in the North to South direction and five reservoirs namely Sand 1, Sand 2, Sand 3, Sand 4 and Sand 5 were identified based on the low gamma ray readings. The pay thickness ranges from 3 to 39m across the reservoirs. The net to gross of the reservoirs ranges from 76 to 97% and effective porosity ranges from 18 to 22.2%. Petrophysical analysis have shown that the hydrocarbon type in Sand 2 is predominantly gas while Sand 4 is partly oil and gas. Hydrocarbon type in Sand 5 is predominantly oil. The hydrocarbon saturation ranges from 58 to 76 %. On the other hand, Sand 1 and Sand 3 has indicated no accumulation of hydrocarbon within the tested trap.

Synthetic seismogram was generated from the sonic and density logs in the wells to aid mapping of the reservoir tops across the 3D seismic data coverage. The synthetic seismogram was compared with the actual seismic data which had a good peak to peak and trough to tough tie with the seismic data.

Faults were delineated and mapped on the 3D seismic data by identifying abrupt terminations of seismic reflections after this was conducted, it was observed that four major growth faults are present in YZ field while other faults are either synthetic or antithetic to the major faults. Four horizons corresponding to the top of Sand 1 to 4 in the well log analysis were mapped across the 3D migrated seismic data. The mapped horizons were gridded to generate a time map which was converted to depth map by an appropriate velocity model. The structural maps, reveals structural highs and closures that are observed as fault assisted and dependent traps. The six wells are observed to penetrate fault dependent (Sand 1, 2 and 4) and assisted closures (Sand 3) on the

structural maps. Four to five additional prospects that have not been penetrated by the wells were observed. Seismic attributes analysis including RMS, maximum amplitude, sum of energy, sum of amplitude were extracted from the time map to enhance interpretation. Although, the deep resistivity log in Sand 1 for the tested fault dependent trap is dry, positive amplitude anomalies have indicated possible accumulation on Prospect 1 which is also a fault assisted trap. The attribute analysis has shown high anomalies on some of the prospects which is supportive of possible accumulation of hydrocarbon. The identified prospects were ranked partly based on type of closure (fault assisted versus fault dependent), attribute support and volume estimates.

Volumetric estimations were calculated for the tested trap and the additional prospects on the mapped surfaces. The volumetric estimates of STOIIP in the additional prospects of Sand 1 ranges from 14,489,265.3 to 66,684,091.9stb. Sand 2 contains dominantly gas and the volume of the stock-tank-gas-initially-in-place (STGIIP) ranges from 8,592,312 to 38,457,838scf. The volumetric estimates for oil in place in Sand 3, ranges from 3,062,489 to 4,654,835 stb. The stock-tank-oil-initially-in-place for Sand 4 is 6,503,725 to 15,007,804 stb and the GIIP ranges from 16,360,138 to 57,049,834 scf. In summary, additional STOIIP for YZ field is 194,025,188 stb and GIIP for YZ is 193,804,479 scf.

5.2 Recommendation

From the integration of the petrophysical analysis of the available well logs and 3D seismic interpretation of YZ field, it is recommended that further wells should be drilled to test the identified prospects. A directional well is recommended to test Prospect 1 across Sand 1 to 5; partly because it is fault assisted traps and expresses seismic attribute anomalies across most of the surfaces.

References

Aizebeokhai AP, and Olayinka I. Structural and stratigraphic mapping of Emi field, Offshore Niger Delta. Journal of Geology and Mining Research. 2011;3(2):25-38.

Asubiojo, TM; Okunuwadje, SE 2016, Petrophysical Evaluation of Reservoir Sand Bodies in Kwe Field Onshore Eastern Niger Delta, J. Appl. Sci. Environ. Manage Vol. 20 (2) 383 – 393

Asquith, G. and Gibson, C. (1982). Basic Well Log Analysis for Geologists. *AAPG*, Tulsa, OK.

Avbovbo, A.A. (1978). Tertiary Lithostratigraphy of Niger Delta. American Association of Petroleum Geologists Bulletin, Vol. 62:295- 300

Beka, F.T., and Oti, M.N., 1995, The distal offshore Niger Delta—Frontier prospects of a mature petroleum province, *in* Oti, M.N., and Postma, G., eds., Geology of deltas: Rotterdam, A.A. Balkema, p. 237–241.

Cannon, S. (2015). Petrophysics: a practical guide. John Wiley & Sons, 2015.

Doust, Harry, and Omatsola, Ebi, 1990, Niger Delta, *in* Edwards, J.D., and Santogrossi, P.A., eds., divergent/passive margin basins, American Association of Petroleum Geologists Memoir 48: Tulsa, American Association of Petroleum Geologists, p. 201–238.

Edwards, J.D., and Santogrossi, P.A., 1990, Summary and conclusions, *in* Edwards, J.D., and Santogrossi, P.A., eds., Divergent/passive margin basins: American Association of Petroleum Geologists Memoir 48, p. 239–248.

Ejedavwe, J., Fatumbi, A. Ladipo, K., & Stone, K. (2002) "Pan-Nigeria exploration well look-back (Post- Drill Well Analysis). *Shell Petroleum Development Company of Nigeria Exploration Report.*

Ejedawe, J.E, Coker S.J.L., Lambert-Aikhionbare, D.O., Alofe, K.B, Adoh, F.O. (1984). Evolution of Oil Generating Window and Gas Occurrence in Tertiary Niger Delta Basin. AAPG Bull. 68:1744-1751.

Ekweozor, C.M., and Okoye, N.V., 1980, Petroleum source-bed evaluation of Tertiary Niger Delta: American Association of Petroleum Geologists Bulletin, v. 64, p. 1251–1259.

Emina R, Obiadi II* and Obiadi CM. 2016 Evaluation and Prospect Identification in the Olive Field, Niger Delta Basin, Nigeria. J Pet Environ Biotechno

Evamy, B.D., Haremboure, J., Kamerling, P., Knaap, W.A., Molloy, F.A., and Rowlands, P.H., 1978, Hydrocarbon habitat of Tertiary Niger Delta: American Association of Petroleum Geologists Bulletin, v. 62, p. 277–298.

Frost, B.R., 1997, A Cretaceous Niger Delta petroleum system, *in* Extended abstracts, American Association of Petroleum Geologists Bulletin/Brazilian Association of Petroleum Geologists Hedberg Research Symposium, Petroleum System of the South Atlantic Margin, November 16–19, 1997, Rio de Janeiro, Brazil.

Gomes, J. S., Alves, F. B. 2007, O Universo da Indústria Petrolífera – Da Pesquisa à Refinação. Fundação Calouste Gulbenkian, 647 pp.

Haack, R.C., Sundararaman, P., Diedjomahor, J.O., Xiao, H., Gant, N.J., May, E.D., and Kelsch, K., 2000, Niger Delta petroleum systems, Nigeria, *in* Mello, M.R., and Katz, B.J., eds., Petroleum systems of South Atlantic margins: American Association of Petroleum Geologists Memoir 73, p. 213–231.

Journel, A.G. (1995). Geology and Reservoir Geology. Stochastic Modelling and Geostatistics. In: Yarus, J.M., Chambers, R.L. (eds) AAPG Computer Applications in Geology. 3:19–20. Tulsa, Oklahoma.

Kaplan, A., Lusser, C.U., and Norton, I.O., 1994, Tectonic map of the world, panel 10: Tulsa, American Association of Petroleum Geologists, scale 1:10,000,000.

Kulke, H., 1995, Nigeria, *in* Kulke, H., ed., Regional petroleum geology of the world. Part II—Africa, America, Australia and Antarctica: Berlin, Gebrüder Borntraeger, p. 143–172.

Leonardo A. and Guerra R.P 2009, Seismic Attributes in Hydrocarbon Reservoirs Characterization. Departamento de Geociências, Universidade de Aveiro, 2009

Michele L. W. Tuttle, Ronald R. Charpentier, and Michael E.Brownfield. 1999. Assessment of undiscovered Petroleum in the Tertiary Niger Delta (Akata-Agbada) Petroleum System (No. 719201), Niger Delta Province, Nigeria, Cameroon, and Equatorial Guinea, Africa. USGS, p 45.

Nwajide, C. S. (2013). Geology of Nigeria's sedimentary basins. CSS Bookshop Limited, 3013.

Olawale, O.O., Ajayi, F.S. and Akeye, N.A.2017. Evaluation of Petrophysical Properties for Reservoir Characterization of AK Field, Onshore Eastern Niger Delta, Southern Nigeria. Journal of Mining and Geology Vol. 53(1) 2017. pp. 67 – 77

Obiekezie T.N and Bassey E. E. 2015. 3D Structural Analysis of Otu Field, Niger Delta, Nigeria. pp 114-126,

Richard, C. (2008). The Future of Seismic Attributes. Online Webinar. http://www.rocksolidimages.com/pdf/The_Future_of_Seismic_Attributes.pdf

Schlumberger (1989). Log Interpretation, Principle and Application. *Schlumberger Wireline and Testing*, Houston Texas, pp. 21-89

Shannon, P.M., and Naylor N., 1989, Petroleum basin studies: London, Graham and Trotman Limited, p. 153–169.

Short, K.C., and Stäublee, A.J., 1967, Outline of geology of Niger Delta: American Association of Petroleum Geologists Bulletin, v. 51, p. 761–779

Stacher, P., 1995, Present understanding of the Niger Delta hydrocarbon habitat, *in* Oti, M.N., and Postma, G., eds., Geology of deltas: Rotterdam, A.A. Balkema, p. 257–267.

Taner, M. T., Schuelke, J. S., O'Doherty, R., Baysal, E. (1994). Seismic attributes revisited. 64th Annual International Meeting, SEG, Expanded Abstracts, 1104 – 1106.

Telford, W. M.; Geldart, L. P.; Sheriff, R. E. (1990). Applied Geophysicis. Cambridge University Press. 2nd Edition, 136 – 280.

Tuttle, M. L.W, Charpentier, R.R, Brownfield, M. E. (1999). The Niger Delta Basin Petroleum System: Niger Delta Province, Nigeria, Cameroon, and Equatorial Guinea, Africa; *Open-File Report 99-50-H, United States Geological Survey World Energy Report*, 4.

Weber, K.J., and Daukoru, E.M., 1975, Petroleum geology of the Niger Delta—World Petroleum Congress, 9th, v. 2, Geology, Proceedings: London, Applied Science Publishers, Ltd., p. 210–221.

Whiteman, A., 1982, Nigeria—Its petroleum geology, resources and potential: London, Graham and Trotman, 394 p.